

SQT

DOE/NASA/0115 80-1
NASA CR-159841
BALES-McCOIN 80-BMT-002

DESIGN STUDY OF CONTINUOUSLY VARIABLE ROLLER CONE TRACTION CVT FOR ELECTRIC VEHICLES

(NASA-CR-159841) DESIGN STUDY OF A CONTINUOUSLY VARIABLE ROLLER CONE TRACTION CVT FOR ELECTRIC VEHICLES Final Report (Bales-McCoin Tractionmatic, Inc.) 197 p Unclass
HC A09/HF A01 CSCL 13I G3/37 08024

D.K. McCain and R.D. Walker
Bales-McCoin Tractionmatic, Inc.
El Paso, Texas

September 1980



Prepared for
NATIONAL AERONAUTICS AND SPACE ADMINISTRATION
Lewis Research Center
Cleveland, Ohio 44135
Under Contract DEN 3-115

for
U.S. DEPARTMENT OF ENERGY
Electric and Hybrid Vehicle Division
Office of Transportation Programs



DOE/NASA/0115-80/1
NASA CR-159841
80-BMT-002

DESIGN STUDY OF A CONTINUOUSLY VARIABLE
CONE - ROLLER TRACTION TRANSMISSION
FOR ELECTRIC VEHICLES

Dan K. McCain and Richard D. Walker, Authors

Bales-McCoin, Inc.
9032 Roseway
El Paso, Texas

September 1980

Prepared for:

National Aeronautics and Space Administration
Lewis Research Center
Cleveland, Ohio 44135

Under Contract DEN 3-115

For:

US DEPARTMENT OF ENERGY
Electric and Hybrid Vehicle Division
Office of Transportation Programs
Washington, D.C. 20545

1. Report No. NASA CR-159841	2. Government Accession No.	3. Recipient's Catalog No.
4. Title and Subtitle Design Study of a Continuously Variable Cone/Roller Traction Transmission for Electric Vehicles		5. Report Date September 1980
7. Author(s) Dan K. McCain, Richard D. Walker		6. Performing Organization Code
9. Performing Organization Name and Address Bales-McCoin Tractionmatic, Inc. 9032 Roseway El Paso, Texas 79907		8. Performing Organization Report No. 80-BMT-002
12. Sponsoring Agency Name and Address U.S. Department of Energy Office of Transportation Programs Washington, D.C. 20645		10. Work Unit No.
		11. Contract or Grant No. DEN 3-115
		13. Type of Report and Period Covered Contractor Report
		14. Sponsoring Agency Code DOE/NASA/5115-80/1
15. Supplementary Notes Final Report Prepared Under Interagency Agreement EC-77-A-31-1044. Project Manager, S. Loeventhal, Bearing, Gearing, and Transmission. Section, NASA Lewis Research Center, Cleveland, Ohio 44135		
16. Abstract <p>This report presents the results of design studies of continuously variable ratio transmissions (CVT) featuring cone and roller traction elements and computerized controls.</p> <p>Based on the design and analysis results obtained, the CVT as presented herein meets or exceeds all requirements set forth in the design criteria. Further, a scalability analysis indicates the basic concept to be applicable to lower and higher power units, with upward scaling for increased power being more readily accomplished.</p>		
17. Key Words (Suggested by Author(s)) Electric Vehicle, Continuously Variable Transmission (CVT)- Roller-Cone Traction Drives		18. Distribution Statement Unclassified - unlimited STAR category 37 DOE category UC-96
19. Security Classif. (of this report) Unclassified	20. Security Classif. (of this page) Unclassified	21. No. of Pages 189
22. Price*		

* For sale by the National Technical Information Service, Springfield, Virginia 22161

TABLE OF CONTENTS

	<u>Page</u>
EXECUTIVE SUMMARY	1
INTRODUCTION.	3
PROGRAM SCOPE AND APPROACH.	4
TASK I - Design Study.	8
TASK II - Design Requirements, Design Criteria Identification of Required Technology	9
TASK III - Suitability for Alternate Appli- cations	11
TASK IV - Design and Technology Assessment Report.	12
DISCUSSION	
Transmission Description	13
Materials.	23
Lubrication System	24
Traction Control System.	24
Control System Component Description	25
ANALYTICAL RESULTS	
Efficiency	29
Cost	50
Weight	50
Noise.	55
Reliability.	55
Maintainability.	56
Scalability.	61

TABLE OF CONTENTS (CONTINUED)

	<u>Page</u>
Alternate Electric Drive	61
Alternate Hybrid-Electric Drive.	62
Potential Problem Areas.	63
TECHNOLOGY ASSESSMENT	66
CONCLUSIONS AND RECOMMENDATIONS	67
LIST OF REFERENCES.	69
APPENDIX.	70
LISTINGS	
Figures.	III
Tables	V
References	69
Appendices	70
Symbols.	188

LIST OF FIGURES

<u>Figure No.</u>	<u>Figure Title</u>	<u>Page</u>
1.	CVT with Flywheel and Electric Motor .	5
2.	CVT with Electric Drive Only	6
3.	CVT with Hybrid, I.C. Engine and Electric Motor	7
4.	Photograph of Key Components in a Computer Traction Control, Roller- Cone CVT	16
5.	Schematic Diagram of a Roller-Cone Regenerative CVT Configuration	17
6.	A Regenerative CVT Configuration	18
7.	High Reduction (CVT/IVT) Torque Multiplication Limits with Slip. Study Design Range Overplotted	19
8.	Slip Control Block Diagram	22
9.	Typical Traction Force VS Slip Curve .	27
10.	Typical Traction Force VS Slip Curve Family	28
11-15.	Net CVT Efficiency 7.5 KW (10HP) to 75 KW (100HP) VS Output Speed for the Input Speed Spectrum	34-38
16.	Ratio of Recirculating HP to Output HP VS Total CVT Ratio.	39
17-21.	Efficiency VS Ratio of Recirculating HP to Output HP and Total CVT Ratio for 7.5 KW (10HP) to 75 KW (100HP) Respectively	40-44
22.	Volmetric Plot of Peak Traction Coefficient Over the Operating Spec- trum for the Regenerative CVT Geometry	49

<u>Figure No.</u>	<u>Figure Title</u>	<u>Page</u>
23	Composite Traction Life VS Output Speed.	58
24	Cone Power VS Output Speed	59
<u>APPENDIX:</u> 25	Alternate Roller Carrier and Shifting Mechanism.	73
26	Revised Cone Mount and Loading System	74
27	Regenerative CVT with Forward Output Rotation	77
28	Radial Load Distribution in Regenerative CVT	78
29	Multispeed CVT Function Diagram.	81
30	Volumetric Efficiency; Regenerative CVT VS Multispeeding - Typical	82
31	Multispeed CVT Functional Layout	83
32	Basic Slip Control Diagram	85
33	Alternate Analog Divider Diagram	90
34	Typical Traction Curve (Traction Force VS Slip)	93
35	Typical Traction Curve (Normal Force VS Slip)	95
36	Typical Traction Curve Control Spike (Δ Slip/ Δ Normal Force).	96
37	Optimized Traction Computer Diagram.	97
38	Control Response to Error.	98
39	Dither and Control Response VS Time.	102
40	Encoder Aperature Duty Cycle Correction	106

LIST OF TABLES

<u>Table No.</u>	<u>Table Title</u>	<u>Page</u>
1.	Regenerative Total Power Loss.	30
2.	Regenerative Net Efficiency.	32
3.	Regenerative Loss Source Summary	45
4.	Incremental Roller Position.	47
5.	Cone Diameter, Traction Ratio, and Cone Speed to RPMn VS RPMo	48
6.	Cost	51
7.	Transmission Weight, Itemized.	52
8.	Bearing Life	57
9.	Gear Stresses.	60
 Appendix:		
10.	Transmission Ratio	114
11.	Input Planetary Gear Data.	115
12.	Input Planetary RPM/Flywheel RPMn.	118
13.	Output Planetary Gear Data	119
14.	Output Planet RPM VS RPMs.	120
15.	Output Planet Power.	124
16.	Spiral Bevel Gear Data	126
17.	Helical Idler Gear Data.	128
18.	Cone Torque.	135
19.	Single Cone HP	137
20.	Cone HP (4 Cones).	139

<u>Table No.</u>	<u>Table Title</u>	<u>Page</u>
21.	Cone Normal Load (LB).	141
22.	Cone Bearing Loss (4 Cones).	143
23.	Spin Velocity (RAD/SEC).	145
24.	J_6 , Dimensionless Spin Torque.	146
25.	Traction Power Loss (4 Contacts)	149
26.	Contact Ellipse Dimensions	151
27.	"g".	153
28.	J_7/J_4 Loss Factor.	162
29.	J_1 , Dimensionless Slip Factor.	163
30.	J_3 , Dimensionless Spin Factor.	164
31.	$g^3/(W_n)^{1/3}$	166
32.	Flywheel to RPM _g	168

EXECUTIVE SUMMARY

This report presents the results of design studies of continuously variable ratio transmissions (CVT) featuring cone and roller traction elements and computerized controls.

This work was part of the Electric and Hybrid Vehicle Program of the U.S. Department of Energy. It was performed under contract DEN 3-115 and managed by the Bearing, Gearing, and Transmission Section of the NASA Lewis Research Center.

A computer controlled traction drive CVT embodying traction cones and rollers in a regenerative path epicyclic gear differential was designed and analyzed.

Detailed assessment of cone-roller Traction CVT suitability to the electrical vehicle application was made. Vehicle configurations included: 1) flywheel energy storage system driving through the CVT to an electric motor into the vehicle differential; 2) electric motor driving through the CVT into the differential; and 3) hybrid I.C. engine driving through the CVT with CVT and electric motor input into the differential. (See Figures 1 through 3, pages 5 through 7).

The computer controlled regenerative traction unit controls the speed of the ring gear in the epicyclic gear differential. The traction unit consists of a crowned roller and four cones. The roller, driven by the center shaft through a recirculating ball spline, drives the traction cones. The center shaft also drives the sun gear of the epicyclic gear differential (Figure 4, 5 and 6, pages 16, 17 and 18.)

Speed variation of the output shaft is accomplished by moving the traction roller axially along the cones, thus varying the cone rotational speed and, in turn, varying the ring gear speed relative to the sun gear speed.

Power from a flywheel is transmitted through an input epicyclic reduction stage to the center shaft. The ring gear of the input reduction unit is controlled by a modulating clutch. The clutch allows de-coupling of the flywheel at flywheel speeds below minimum (less than 14000 RPM), to de-couple the flywheel at output shaft speeds below 850 RPM and reverse output speeds.

The computer control system maintains optimum traction, speed, and power for all operating conditions via traction slip monitoring and slip control feedback. Continuous sampling of system parameters (cone and roller speed, zero

slip ratio setting, cone piston pressure, input speed, accelerator pedal position, brake pedal pressure, provides continuous control system updating. Optimum traction control provides maximum component life, minimum power drain from the batteries, and maximum vehicle range and performance.

Study results indicate an overall operating efficiency of the regenerative CVT as 91.5% for the mean power condition, 16KW (22HP) and 3,000 Rpm output. Calculated efficiency ranged from 92.1% at 15KW (20HP), 14,000 Rpm in, 3,000 Rpm out, to 76.64% at wheel slip "Torque Limit" of 39.8KW (53.4 HP) with 28,000 Rpm input and 850 Rpm output. (See Appendix B, page 79).

Based on the design and analysis results obtained, the computer controlled traction CVT's as presented herein meets or exceeds all requirements set forth in the design criteria. Further, a scalability analysis indicates the basic concept to be applicable to lower and higher power units, with upward scaling for increased power designs being more readily accomplished.

The present study specifically addresses:

- Efficiency
- Size and weight
- Reliability
- Noise
- Controls
- Maintainability
- Cost

of a traction regenerative configuration. The objective of this study is to design a traction CVT which meets or exceeds all the design specifications and operating requirements established in the contract. Analytical substantiation of traction elements, bearings, and gear stresses and life will also be investigated for the design. Structural alternatives are presented for prospective problem areas and trade-off considerations made.

- Weight: Approximately 34 Kg (75 lbs) for 75 KW (100 HP)
- Production Cost: Estimated at \$330.00

INTRODUCTION

As a fuel efficient alternative to the reciprocating engine driven vehicle, the electric vehicle (E.V.) has been recognized and is being developed. Considerable E.V. investigations have been performed through analysis, subsystem development testing, and vehicle service evaluation. Combinations of hybrid power plant, energy storage flywheel, variable ratio transmission, and vehicle/motor control systems are being investigated for the purpose of devising a viable electric vehicle.

The purpose of the present study is to contribute to the mechanical transmission subsystem technology for the electric vehicle. The study covers analysis and design of a continuously variable traction transmission (CVT) which accepts input from an energy storage flywheel and provides variable speed drive continuity to the electric motor. Two alternative approaches which utilize the CVT are pure electric and hybrid reciprocating/electric drives.

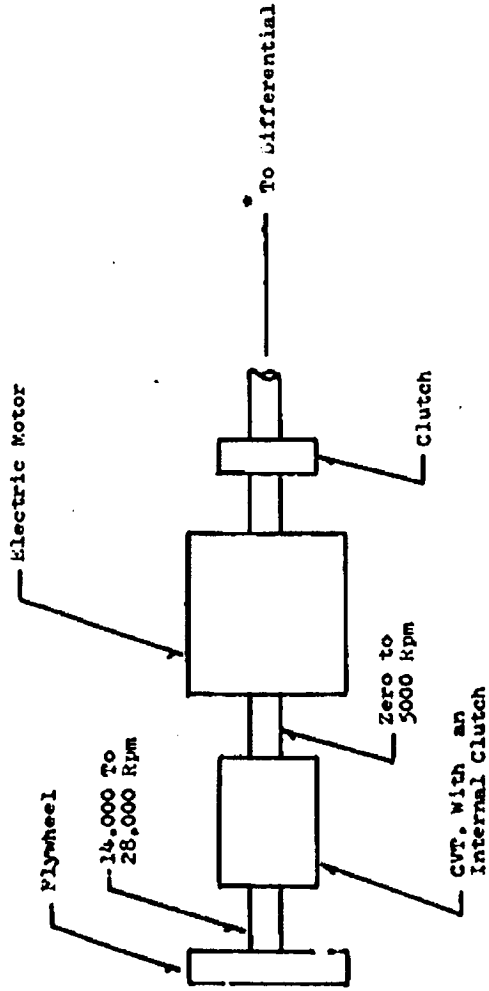
>> It has long been recognized that the E.V. could most effectively utilize the CVT to achieve maximum performance. The innate ability of the CVT to allow the drive motor to operate at optimum speed and minimize battery drain strongly suggests justification for intensive study and development of the CVT. A government sponsored study concluded that the CVT with flywheel was necessary to make the electric postal jeep meet minimum satisfactory performance. Without the CVT the vehicle could not perform satisfactorily for most terrains.

PROGRAM SCOPE

The scope of the program encompasses the design of CVT of reasonable size, weight, and cost to provide an effective and reliable means of controlling and utilizing power augmentation of an energy storage flywheel in an electric vehicle. The CVT must accept power output from the flywheel at any speed between 14,000 RPM and 28,000 RPM and provide output shaft power at any speed between 850 RPM and 5,000 RPM. De-coupling must be accomplished for output shaft speeds below 850 RPM, and reverse. An alternative to de-coupling is a CVT design which provides neutral and reverse (effectively an IVT, infinitely variable transmission), Figure 1, page 5.

Alternative applications are the pure electric and hybrid electric vehicles as depicted in Figures 2 and 3, pages 6 and 7, respectively.

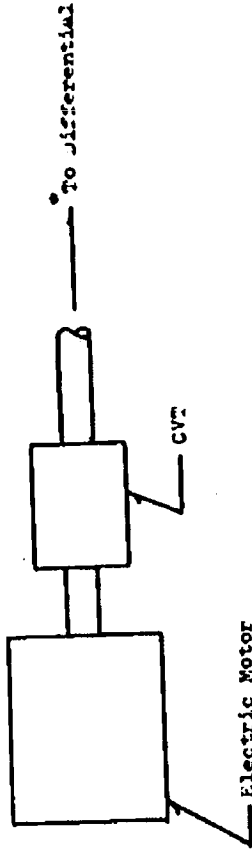
**SCHEMATIC OF CVT DRIVETRAIN, UTILIZING
FLYWHEEL AND ELECTRIC MOTOR**



Torsional dampening as required

Figure 1:

SCHEMATIC OF ELECTRICALLY DRIVEN CVT DRIVE TRAIN



torsional dampening as
required

Figure 2:

SCHEMATIC OF I.C. ENGINE/ELECTRIC MOTOR DRIVEN
(HYBRID) CVT DRIVETRAIN

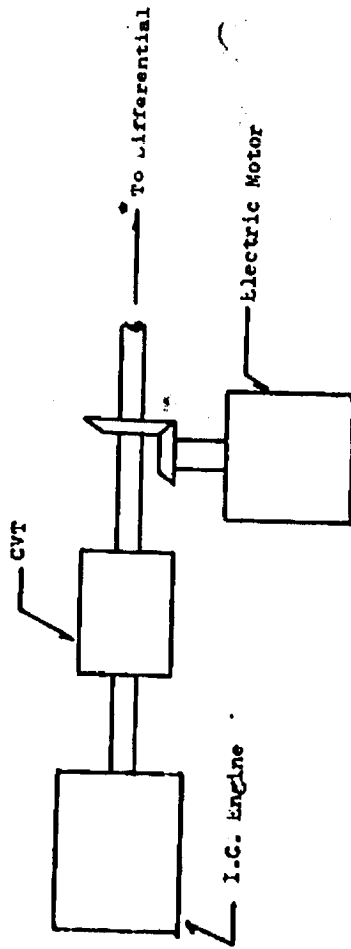


Figure 3:

Torsional dampening as required

APPROACH

The approach taken herein was to perform the design study through iterative layouts concurrent with an assessment of possible technology advancements required to support the design. The study was implemented through the following statement of work.

A. Task 1 - Design Study of a CVT for Flywheel Application

A. Conduct an engineering design study and perform the necessary analysis to determine the optimum arrangement of a continuously variable speed transmission (CVT) to couple the high speed output shaft of an energy storage flywheel to the drive train of an electric vehicle as shown in Figure 1, page 5. The CVT shall be comprised of the variable speed element together with any ancillary mechanical components, such as couplings, clutches or gear sets, which are required to satisfy the requirements specified below.

DESIGN REQUIREMENTS

The following design requirements, based on a representative vehicle having a curb weight of 1700 Kilograms (3750 pounds), shall apply:

1. The speed ratio of the CVT shall be continuously controllable over the following range of input and output speeds:

High speed (flywheel output shaft), 14,000 to 28,000 RPM.

Low speed (differential input shaft), zero to 5000 RPM.

If it is impractical to design the proposed CVT to be continuously controllable down to zero output speed, then the CVT shall be designed to be continuously controllable down to a minimum speed not to exceed 850 RPM and a variable speed clutch element shall be incorporated to regulate differential input speed to zero.

2. The CVT shall provide forward vehicle speed only, since reverse may be accomplished by reversing electric motor rotation, unless reverse can be accomplished within the CVT without additional complexity.

3. Disengagement of the flywheel from the drive train shall be accomplished with the CVT or with a clutch, if required.

4. The CVT shall be capable of withstanding all sudden shock loads and sudden torque conditions that may be expected in typical automotive applications.

5. The CVT shall be capable of bi-directional power flow at the above power ratings for regenerative braking and for charging of the flywheel with the electric motor.

The operating power and life requirements for the transmission as stipulated are:

1. Mean output power = 16 KW (22 HP)
2. Mean output speed = 3,000 RPM
3. Mean input speed = 21,000 RPM
4. Life at mean conditions = 2,600 hours at 90% survivability.
5. Maximum output speed = 5,000 RPM
6. Maximum input speed = 28,000 RPM
7. Minimum output speed = 850 RPM (clutched to zero)
8. Minimum input speed = 14,000 RPM

In addition, the following operating parameters are considered:

1. Maximum useable energy from flywheel = 1.8 MJ (1.5 KWH)
2. Maximum CVT transient power output = 75 KW (100 HP) for 5 sec.
3. Maximum CVT torque output at wheel slip = 450 N-m (330 ft. lb.)
4. Maximum time from maximum to minimum reduction ratio, or vice versa, 2 seconds.

DESIGN CRITERIA

The design of the CVT and associated drive system components, shall be on the basis of the following criteria in order of overall importance:

1. Efficiency - The transmission shall have high efficiency over its entire operating spectrum. Special attention shall

be given to maximizing transmission efficiency under those operating conditions in which the transmission spends most of its operating time.

2. Cost - The future production cost of the transmission, on a large scale basis (100,000 units per year), shall be an early consideration. The use of special manufacturing processes and materials shall be avoided. Design techniques, as well as drive system components such as bearings, gears, and seals, shall be typical of, and consistent with, automotive practice.

3. Size and Weight - The overall size and weight of the CVT, including suitable controls and all ancillary mechanical components, shall not be significantly greater than present automotive transmission of equal horsepower capacity.

4. Reliability - The transmission, including all support systems (i.e., cooling and controls), shall be designed to operate a minimum of 2600 hours at the conditions specified in the design requirements.

5. Noise - An important consideration in the early stages of design shall be to eliminate potential noise generating sources and to contain (within the transmission housing) that noise which is unavoidably generated.

6. Controls - The control system used to operate the transmission drive system shall be stable, reliable and responsive. The system shall provide driver "feel" response similar to that of a standard passenger vehicle, equipped with an internal combustion engine and standard automatic transmission. The control system selected shall closely simulate the full-scale system required for actual vehicle application.

7. Maintainability - The transmission shall be designed with maintainability equal to, or better than, the maintainability of present-day automotive automatic transmission. All internal components which require normal maintenance and/or occasional replacement shall be made readily accessible.

8. Task II - Identification of Required Technology Advancements

Identify all technology advancements required to develop the selected CVT to the point of satisfying the design requirements and criteria of Task I.

Define the nature of the required advancements, define the difficulty of the problems, and estimate the means and

effort required to solve the problems. Areas of technology considered shall include, but shall not be limited to, materials, lubricants, bearings, seals, gears, controls, and other subsystems or modules required.

C. Task III - Determination of CVT Concept Suitability for Alternate Electric and Hybrid Vehicle Applications

Determine the suitability of the concept of the CVT designed in Task I for the alternate electric and hybrid vehicle applications specified below. This task shall be limited to the identification of: (1) the differences in arrangement, size, ratio, or other design variables, and (2) any additional new technology required to apply the CVT concept to each alternate application. Perform only the preliminary design analysis necessary to identify in a broad, general sense, the above differences and not perform specific design analyses or prepare layout drawings for these alternate applications.

Electric Vehicle Powered by Electric Motor Only

Determine the suitability of the CVT concept of Task I to match an electric motor to the drive train of an electric vehicle (without flywheel energy storage) as shown in Figure 2, page 6.

Design Requirements

1. The speed ratio of the CVT shall be continuously controllable over the following range of input and output speeds:

High speed (motor output shaft), zero to 6000 RPM

Low speed (differential input shaft), zero to 3000 RPM

2. All other requirements shall apply except for those specifically referring to the flywheel storage device which are deleted for this application.

Design Criteria

All criteria stated in Task I shall apply to this alternate application.

Hybrid Electric Vehicle With An Internal Combustion Engine

Determine the suitability of the CVT concept of Task I

to match an internal combustion engine to the drive train of a hybrid electric vehicle as shown in Figure 3, page 7.

Design Requirements

1. The speed ratio of the CVT shall be continuously controllable such that the output speed shall range from zero to 3000 RPM with the input speed and power requirements according to the specified engine operating schedule.
2. The CVT shall provide forward, reverse, neutral, and at-rest vehicle operation with single lever operation.
3. All other requirements, as stated in Task I, shall apply, except those specifically referring to the flywheel storage device which are deleted from this application.

Scalability of Selected CVT With Flywheel Energy Storage for Alternate Maximum Output Torques

Determine the suitability of the CVT concept of Task I with flywheel energy storage for scaling to alternate maximum output torques. The design requirements and criteria shall be the same as specified in Task I except that the following alternate maximum output torques at wheel slip shall be considered. Low speed (differential input) shall be zero to 5000 RPM and the CVT input speeds shall be 14,000 to 28,000 RPM in all cases.

CASE	VEHICLE WEIGHT	MAXIMUM CVT OUTPUT (DIFFERENTIAL INPUT) TORQUE
1	790 kg (1750 lbs.)	210 N-m (155 lb-ft)
2	10,000 (22,000 lbs.)	2,600 N-m (1900 lb-ft)

D. Task IV - Design and Technology Assessment Report

Submit a design report of the CVT concept together with supporting data and analysis. Sufficient detail and analysis shall be provided to verify that the design is credible and capable of meeting the required design specifications and criteria.

An estimation of the steady state efficiencies at 7.5, 15, 30, 52, and 75 KW; output speed range of zero to 5000 RPM for input speeds of 14,000, 21,000, and 28,000 RPM.

DISCUSSION

Transmission Description

The transmission is a continuously variable (CVT) regenerative traction drive gearbox (Figure 5, page 17). Power flows through the input planetary assembly to the splined throughshaft. The power is transmitted to the traction cone by the roller together with part of the power which is transmitted regeneratively from the sun gear of the output planetary assembly back to the roller shaft. The cones drive the ring gear of the output planetary assembly through a spiral bevel-helical gear. The purpose of the regenerative power loop is to expand the basic cone speed ratio.

It may be seen in Figure 6, page 18, that if the output carrier shaft is restrained, rotating the input roller shaft turns the planetary sun gear. With the carrier stationary, the sun causes counter rotation of the planet idlers and couples that rotation to the ring gear. The ring gear motion then turns the cones via the idler, so as to cause it to counter rotate against the roller. It may be seen therefore that roller and cone diameters may be selected so that the system simply rotates without driving the carrier. This point occurs when the ring and sun gear have velocities that are equal in magnitude but opposite in their direction and is equivalent to neutral or an infinite (input/output) Rpm ratio. Moving the roller from this neutral position upsets the peripheral velocity balances in the system and causes carrier output motion or traction in the contact to occur.

Moving the roller toward the minor diameter of the cone would cause the cone Rpm to increase to maintain the same peripheral velocity as the roller. The increased cone Rpm is transmitted to the ring gear and thereby causes the carrier to be driven in a reverse direction in respect to the input. The transmission studied, as shown in Figure 5, page 17, is of this type by has gear and traction component diameters selected to preclude the output from reaching neutral at the largest cone diameter.

If a restraint, such as an external load, is applied to the carrier output shaft, it will tend to decrease in Rpm. The ring gear and hence the cone Rpm would also tend to decrease. - The cone Rpm decrease produces shear (slip) in the fluid film between the traction conjunction and the resulting shear force creates a torque load. The amount of torque load varies with the amount of shear (slip), temperature, contact geometry and peripheral velocity but in the design studied the maximum power transfer (optimum slip) ranged from 0.8% to 2.0% over the range of design variables. Due to the output planetary expansion of cone ratio, the effect of slip is also expanded and appears as speed droop in the output shaft. Speed droop for the design ranged from 1.75% to 3.25% for 0.8% to 2.0% slip respectively.

It is clear from Figure 6, page 18, that a transmission with any desired input to output ratio range can be designed using any given cone geometry, by selecting the appropriate roller-cone diameters. This feature is used in the current design to expand the approximate traction cone-roller ratio range of 3.5/1 to produce the required overall transmission ratio range of about 12/1.

Transmissions which go to zero (neutral) as described are called "Infinitely Variable Transmissions (IVT)." Even though the design presented is not an IVT, it employs the same regenerative principles to expand the basic cone ratio and therefore must be evaluated as a limited range IVT. Specifically, regenerative gearing used in IVT's or in this case a high reduction ratio "Continuously Variable Transmission (CVT)", produces magnification of power internally and this must be considered in the design. This is reflected in the data and may be seen by noting that for 75 KW (100 HP) output the total cone-roller traction power varies from 95 KW (127 HP) to 316 KW (424 HP) in this design. (A magnification "m" value of 1.27 to 4.24).

The overall efficiency of the transmission is impacted by any change in internal power. When internal power rises above output power, efficiency is decreased because the internal percentage power loss of components are applied against larger amounts of horsepower.

Also any increase in internal horsepower increases the heat load that must be dissipated by the oil cooler. So there is a compound effect to efficiency loss by using regeneration to expand basic cone ratio.

Regeneration may be viewed as "recycling" and therefore power must make multiple passes through the same contacts or components, which logically holds that net efficiency must also be decreased in direct relation to the amount of regeneration in the system for any given operating point. So this effect varies as the system operating ratio is varied.

These features, inherent in any regenerative design, make it imperative that a judgement be made between the losses generated in the traction contact by the basic cone design, chosen to produce a variable speed component, versus the amount of regeneration used to expand the cone ratio, and must further be weighed against other means of expanding overall transmission ratio (See Appendix B, page 79).

Torque capacity of an IVT or high reduction CVT that employs regeneration, is a function of the gearing used and the traction coefficient. The traction coefficient is a function of the fluid selected, temperature, Rpm, surface finish and component geometry used. The normal load applied (pressure) between the traction components, in conjunction with the traction coefficient, results in the production of the specific torque generated.

The design takes advantage of a thin fluid film which separates the traction elements and the fact that the fluid viscosity and resistance to shear (slip) rises rapidly under high pressure (contact Hertz stress in the conjunction). The transmittal of power through a fluid film requires that some shearing action (strain) in the fluid occur.

Figure 7, page 19, is a plot of torque multiplication and speed ratio of an IVT without the input planetary reduction (Figure 6, page 18) versus output speed and for the operating range of the current design, percent speed is carrier Rpm/Sun gear Rpm. The graph reflects that the current design is well above the point where torque capacity is lost. Torque capacity to input/output ratio in a CVT, unlike gears, is limited by the tractive force produced at specific shear velocities in the fluid film separating the variable speed components. High Overall reduction ratios are produced in regenerative CVT's by decreasing differential velocities across planetary components. When the percentage differential velocity in the planetary gears becomes smaller than the "optimum" percent shear (slip) velocity for peak torque transfer by the fluid film then the capacity to transmit torque decreases. This feature allows the traction conjunction to effectively become a variable taut-band fluid coupling which in the normal operating ranges varies from fractions of a percent slip to around 2% but rapidly goes to 100% at neutral. In comparison a fluid torque converter will typically vary from 10% to 50% in the operating range with variation in load and still applies some minimum torque load when the output shaft is stopped with low Rpm to the input.

Pressure Modulating
Valve (PVC)

100 Aperture
Encoder 1000

Ball Spline

Ball Nut

Encoder
Head Head

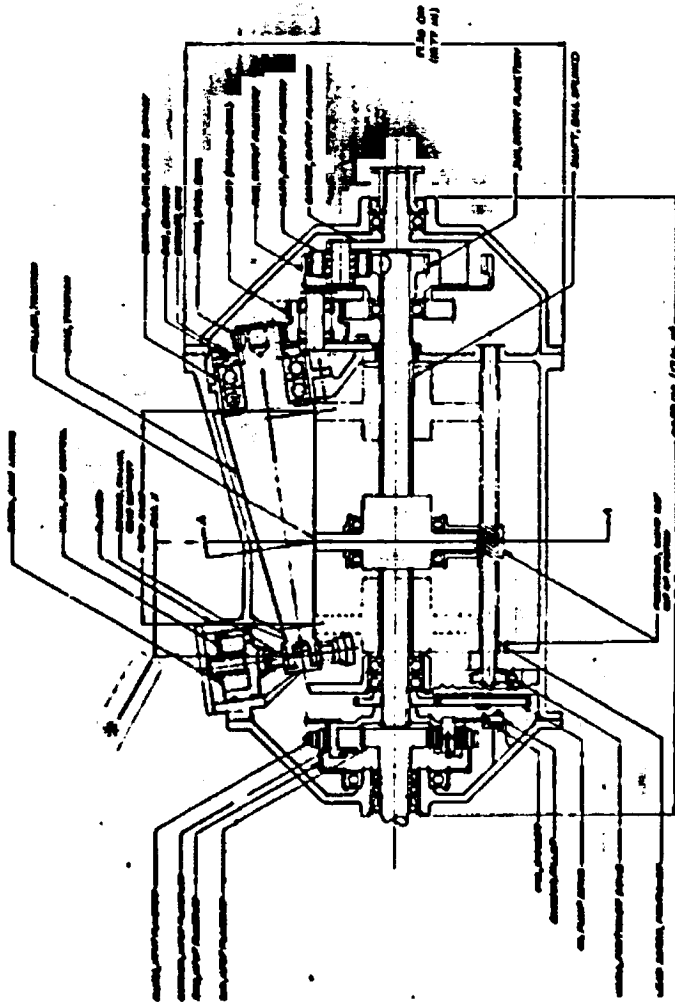
Roller
(TR1)

Loading
Piston

Figure 4

Photograph of Key Components of a Roller-Guns Traction Car

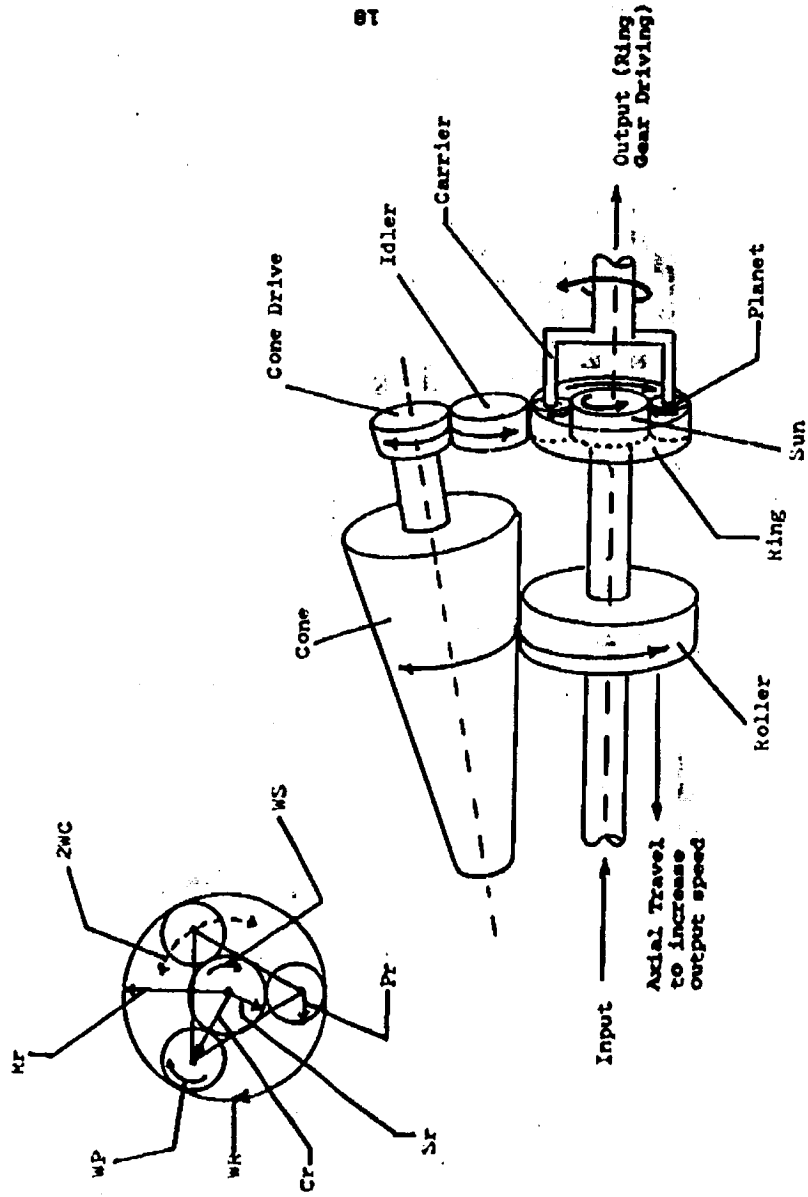
16



PRODUCTION PART NO.	107 8477 000
DESCRIPTION	VALVE-CONTROL TRANSDUCER
QUANTITY	1
DATE	
BY	
CHECKED	
APPROVED	

ALL DIMENSIONS IN INCHES
 DIM. X. OR (IN)

Figure 5: 17



Regenerative CVT
(Less Input Reduction)

Figure 6.

X Ratio (Rpm In/Rpm Out) = Normal Torque Multiplication of gears.

• Torque Multiplication Computed, Traction IVT.

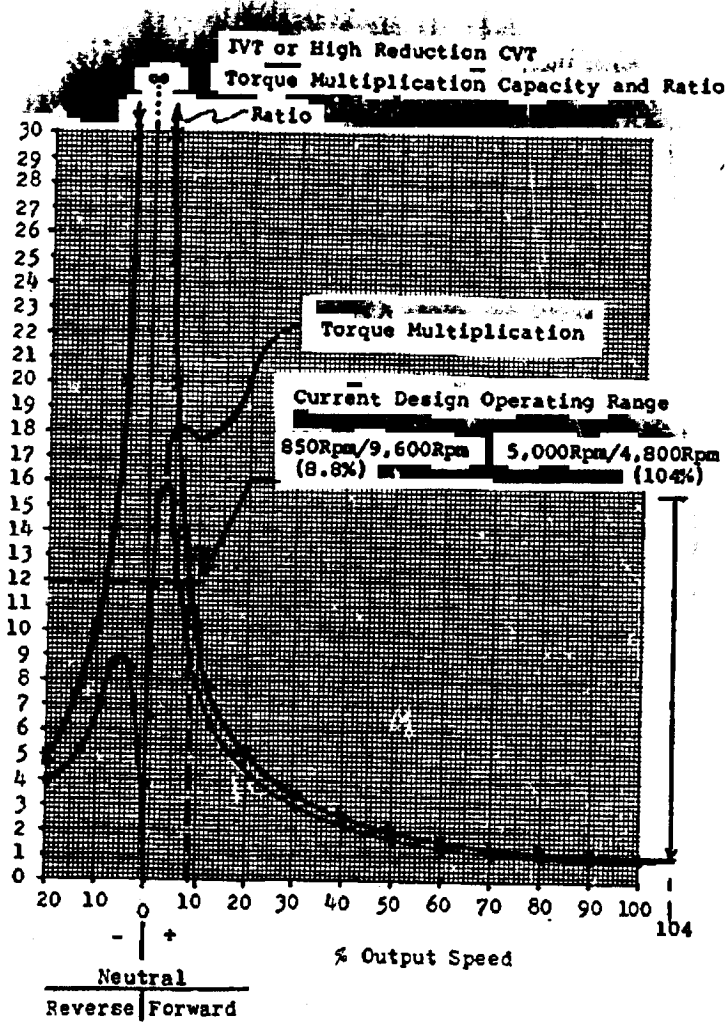


Figure 7:

The transmission ratio variation is accomplished by moving the traction roller along, and parallel to, the traction cones, thereby varying the rolling radius of the cones. The speed of the output ring gear is therefore varied, which, in turn, proportionally varies the output shaft.

Traction forces are generated between the roller and cones through a normal force applied at the small end of the cone. The force is supplied by a hydraulic piston which houses a cone support bearing. The magnitude of the normal force is determined by the transmission output torque requirement, traction coefficient (μ), ratio expansion and operating slip.

Pressure modulation to the hydraulic cylinder (which furnishes the cone force) is provided by a signal from the computer control system. (See control system description, page 25).

Referring to Figure 5, page 17, output from the flywheel powers the sun gear of the input planetary assembly. The ring gear is clutched by a band brake to engage or disengage the flywheel. The input planetary carrier is attached to the splined through-shaft, as is the oil pump drive gear.

The through-shaft is the inner race of a recirculating ball spline which drives the traction roller, while allowing relatively free axial motion of the roller to accomplish ratio change. The through-shaft also supports, and is driven by, the output sun gear. Four traction cones, driven at high speed by the roller, transmit power to the spiral bevel-helical cluster gears which, in turn, drive the output ring gear.

Spiral bevel gears on the idler are necessary to turn the 9.24° shaft angle of the cones to the centerline of the gearbox. The helical gear teeth have a helix angle which produces an opposite and equal axial force to the spiral bevel gear axial load. This enables the use of cylindrical roller bearings since no thrust exists. The use of helical gears also reduces noise generation. The action of helical and spiral bevel gears with adequate spiral or helix angles is much smoother than straight spur gears; hence, the operating noise levels are relatively much lower.

The output planetary carrier is the transmission output member. With the inputs of the through-shaft to the sun gear and the cones to the ring gear a variable ratio is accomplished to the carrier (output shaft). For normal input speed range of 14,000 to 28,000 RPM of the flywheel, the output speed range is from 850 RPM to 5,000 RPM.

The output shaft is de-clutched from the flywheel by the input planetary band clutch when zero output speed is required. De-clutching is necessary to enable the drive motor to reverse direction and drive the vehicle in reverse. The clutch also allows the electric motor to propel the vehicle when the flywheel is not charged.

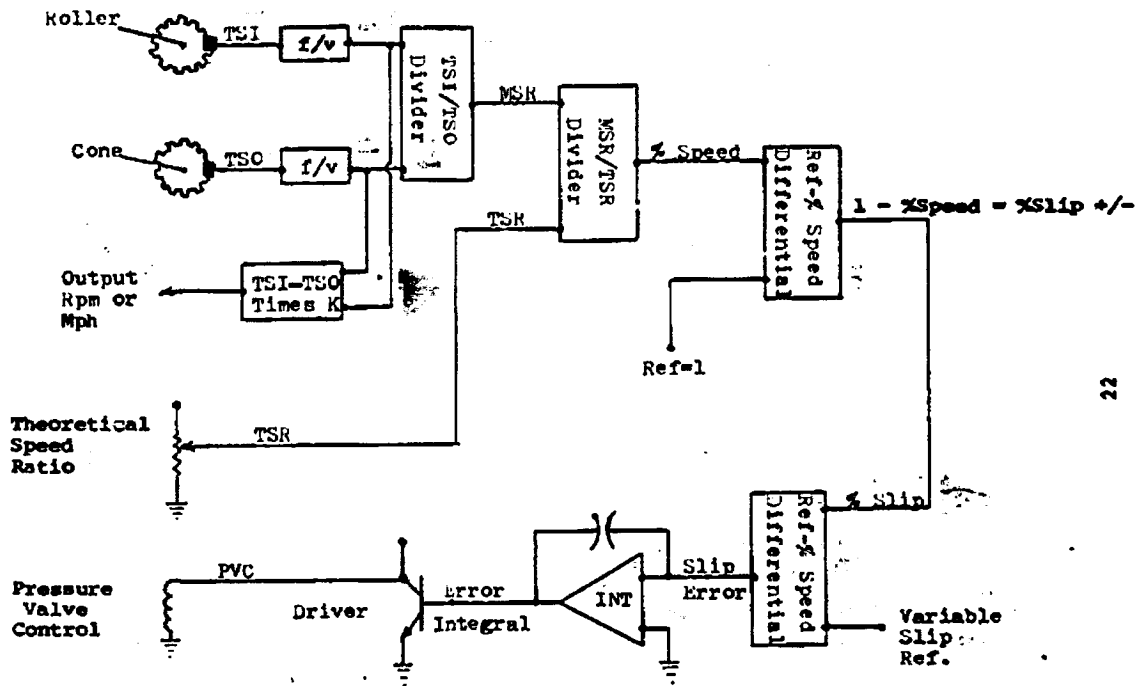
A toothed disc is mounted on the cone (or to reduce its speed and provide greater circumference it may be located on the ring gear) to provide cone speed information to the controller via a photoelectric or magnetic read head. Pulses or square waves are generated by the encoder read head as the apertures rotate past the device. Spatial timing or frequency to voltage I/O processing converts the encoder signals into speed data. The system is insensitive to absolute accuracy of speed measurement because the technique employs speed ratios. See Figure 8, page 22.

It is the ratio in speed indicated that is important to the system, not the absolute representation of "true" RPM, or "true" ratio. This dramatically reduces the controller design requirements.

Similarly the disc mounted on the input planetary carrier provides roller speed information. From the "relative" cone-roller speed information, cone/roller speed ratio is derived by division producing MSR (Measured Speed Ratio). And as above, the absolute accuracy of the MSR is unimportant. What becomes important is the ability of the controller to predict an equivalent Theoretical Speed Ratio (TSR) with no slip, which is based upon the selected component geometry and the traction conjunction location axially. This is accomplished by attaching a linear transducer between the case and the roller carrier assembly.

TSR positional accuracy in absolute terms is not needed. However, correlation between TSR and the MSR (with no-slip) is most important because deviation between MSR and TSR signals represents "slip" in the traction junction.

Traction component speeds are divided to produce Measured Speed Ratio (MSR), which is then divided by Theoretical Speed Ratio (TSR) to produce a % speed result. $1 - \% \text{ speed}$ becomes % slip and is subtracted from a varying slip reference to produce % slip error. The error is integrated and the driver amplifier modulates the pressure control valve to regulate normal force in a direction to correct for slip error. For a more detailed discussion on the system, and specifically regarding components of producing the variable slip reference, see control system details in the appendix starting on page 84.



Slip Control Block Diagram

Figure 8 :

Transmission output speed is provided by Traction Speed In (TSI) and Traction Speed Out (TSP), in accordance with the planetary power flow formulation and may likewise be converted to road speed by mathematical treatment including rear axle ratio and tire size.

$$\text{Rpm}_o = \text{WC} = \frac{\text{WSSr} - \text{WRRr}}{2 \text{ Cr}} = \frac{\text{TSI}(\text{Sr}) - \text{TSO}(\text{Rr})\text{K}}{2 \text{ Cr}} \quad (1)$$

Where K is the reduction ratio between the cone and ring.

Output speed and road speed are not required for traction control but may be used in the vehicle control system (VCS).

Materials

The materials which comprise the rolling elements are chosen for particular stresses and/or associated failure modes. The prevalent failure mode is rolling-element fatigue for virtually all dynamically loaded roller and gear elements.

All gears in the transmission will be fabricated from surface hardenable steel (eg., SAE 93100, SAE 4620) and finished to automotive tolerances and surface conditions. Operating bending and surface compressive stresses are kept relatively low in order to avoid the traction losses associated with the traction fluid under high compressive contacts (high pressure with sliding). The gears will be relatively fine pitch helical spur designs except for the spiral bevel gears on the cones.

The bearings in the transmission are commercially available, fabricated from vacuum degassed 52100 steel, heat treated to Rc 58-61.

The roller in the transmission is fabricated from vacuum-degassed 52100 steel heat treated to Rc 60-63. The roller outside diameter is finish ground with a 12.7 cm (5 inch) crown radius. Normal bearing steel heat treatment practice is observed in producing the roller.

The cones are fabricated from premium vacuum-processed SAE 9210 steel. They are carburized all over to produce a .10 cm (.040 inch) deep case of Rc 60 hardness. The roller journals, cone surfaces, and spiral bevel gear cone journal diameters are finish ground to a surface finish of approximately 6 RMS.

The housings are cast aluminum. Their simplicity suggests the use of the die casting technique in their production.

Lubrication System

The lubrication system consists of an oil pump, oil filter, pressure modulation valve, pressure reducing valve, and relief valve. The distribution of oil to the pertinent dynamic elements is accomplished by oil transfer tubes, cast passages, and an oil manifold/jet system on the roller positioner.

Oil is pumped from the sump through the filter to the pressure modulator valve. The oil flow is then divided; part flowing to the cone loading cylinders, and part to the lubrication system of the gearbox.

Oil that is directed to the cone loading cylinders is pressure modulated to provide a closely controlled piston load on the cones. The modulating signal is produced through the computer to maintain the required amount of normal force between the rollers and cones to provide optimum slip. A flow control valve in each cylinder allows pressure relief during load relaxation periods.

Oil that flows to the pressure reducing valve is directed to the lubricating jets and passages at 34×10^4 to 48 to 10^4 N/m^2 (50 to 70 psi). Surplus oil then flows through a relief valve to the sump.

The jet system on the roller positioner consists of a manifold which supplies oil to four jets. These jets, in turn, spray oil into the traction conjunction. A telescoping transfer piston attached at one end to the forward bearing support provides oil to the positioner.

Traction Control System

The instantaneous torque capacity of the traction contact depends on the normal load between the roller and cone, the lubrication traction coefficient, peripheral velocity, surface finish, temperature and component geometry. Figure 9, page 27 depicts the relationship existing between roller and cone traction force (proportional to torque) versus slip at constant normal force (proportional to control pressure). At sufficient rolling velocity (V_r), to form and maintain an elastohydrodynamic (EHD) film thickness great enough to separate the contacting elements, the transmitted torque increases rapidly as slip ($V_r - V_c$) increases from zero until a peak is reached. This is the optimum operating slip value for the traction to exhibit maximum torque at the particular normal force. As can be seen the amount of torque that may be generated diminishes

for values of slip greater or lesser than the optimum value. Conversely, in order to generate a predetermined or definite amount of torque, it is necessary to apply the depicted normal force (for fixed rotational speed, temperature, etc.). The depicted normal force is then the minimum necessary to give required transmitted torque. The relationship between traction and various normal forces is shown in Figure 10, page 28. It can be seen from the figures that traction torque capacity diminishes when slip is too high or too low or when normal force is changed while operating at optimum slip conditions. Therefore, if slip can be maintained at the optimum value for any normal force then maximum traction torque will be generated. Extending this rationale to cover a variable torque requirement, if optimum slip can be obtained by varying the normal force then maximum traction may be generated with minimum normal force for all values of required traction torque. Minus (-) slip is defined as insufficient slip (less than optimum) and positive (+) slip as excessive slip for control logic purposes. Referring to Figure 11, it can be seen that 1,112 N (250 lbf) traction may be generated by normal forces of 21,240 N (4,775 lbf) at -2.8% and +6.4% slip. Also by 18,896 N (4,248 lbf) at -3.5% slip and +5.2% slip, or 17,940 N (4,033 lbf) at +/- 4.2% slip. Obviously, any normal force greater than 17,940 N (4,033 lbf) is excessive and if more is actually supplied to the traction components then an insufficient (-) slip condition exists for the 1,112 N (250 lbf) traction requirement. With less normal force, slip becomes excessive. Component life and horsepower capacity suffer for any slip/pressure conditions except optimum.

The computer analyzes the information and outputs control information to the pressure control valve modulating the cone loading hydraulic system. System pressure to the cone loading piston is increased if sensed slip is too high, so that a greater normal force is imposed which will reduce slip to the required value. Conversely, the pressure is decreased, if slip is too low, until slip increases to the required value. The control system assures optimum pressure between roller and cones for all traction loop torque requirements.

Control System Component Description

Components comprising the control system are an analog or micro-processor computer (MPU), two encoder read heads, two toothed discs, two linear transducers, a pressure modulating valve, two pressure transducers, and a positioner drive motor. (One linear transducer is used on the accelerator, one pressure transducer is used on the brakes, and the remainder of components are used for Optimized Traction Control (OTC)). See Figures 32 and 37, pages 85 and 97 in the appendix.

The positioner drive motor reversibly actuates the lead screw on the roller carrier. The vehicle control system (VCS) delivers the required polarity and motor speed information to an amplifier, and then to the drive motor. The positioner is moved at the rate and in the direction dictated by the computer. The motion of the drive motor ceases when the ratio is correct, as determined by the linear actuator attached to the accelerator or pressure on the brake, in comparison to true vehicle speed.

Functionally, when the accelerator is depressed the ratio changes and causes the flywheel to deliver increased power through the CVT and hence to the rear wheels. The actual ratio is determined by instantaneous flywheel speed and output speed requirement. As power is delivered to the CVT the slip condition in the traction cones and roller will change. This change will be manifest as an acceleration between the roller and cones, and electronically is an MSR change without comensurate TSR change.

Typical Traction Force VS Slip Curve

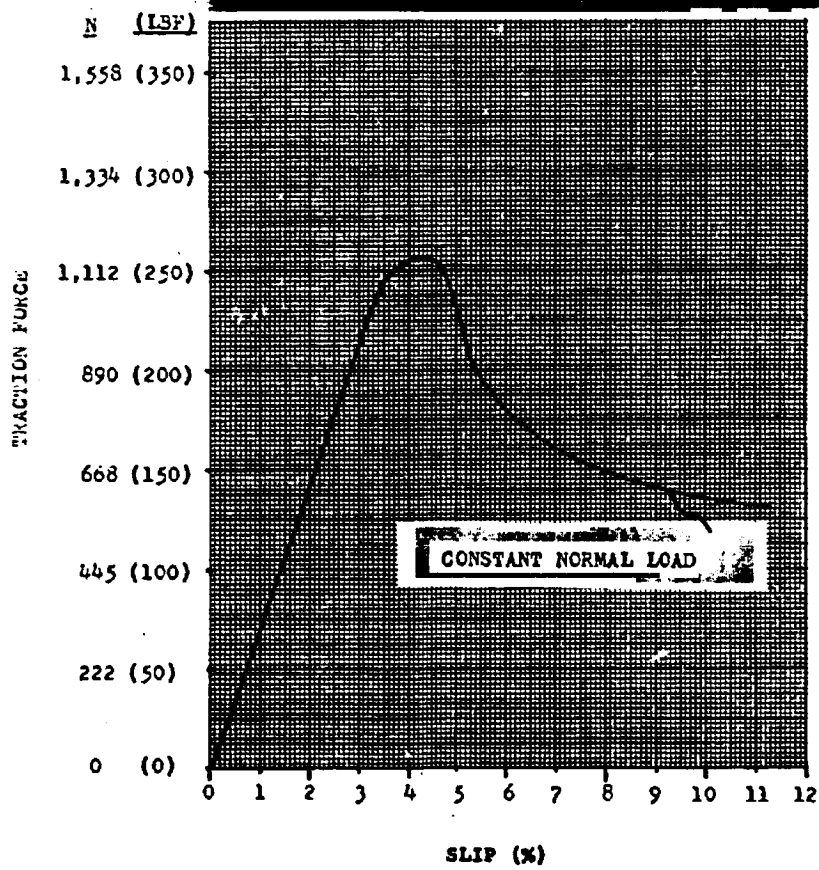


Figure 9:

Typical Traction VS Slip Curve Family

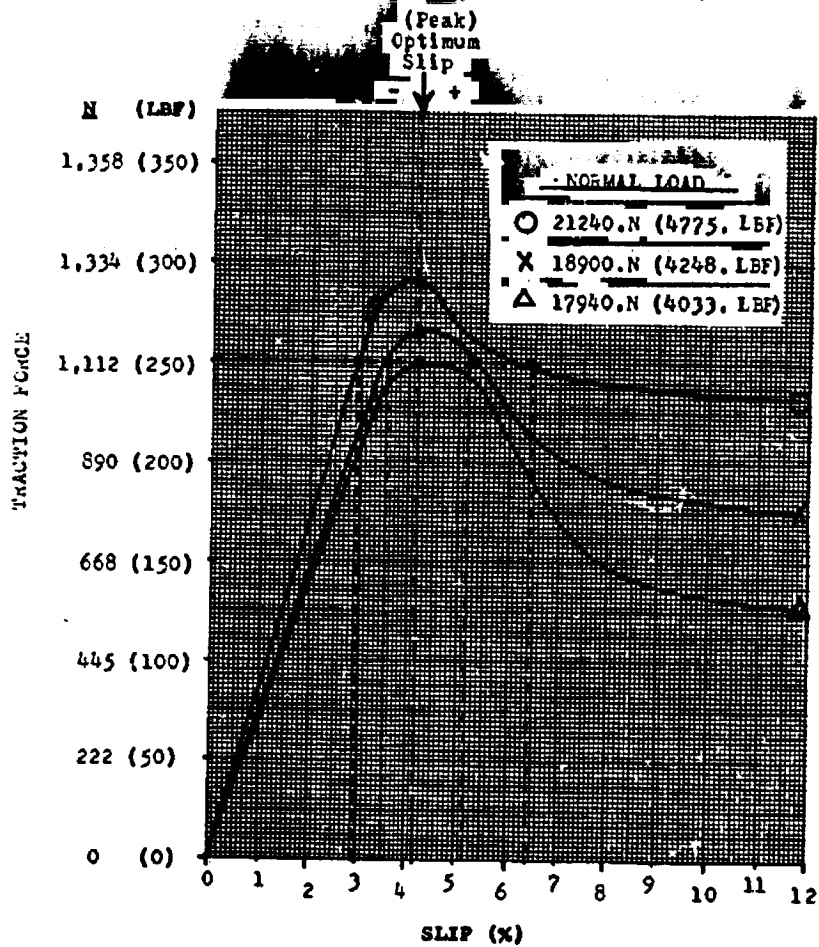


Figure 10 :

ANALYTICAL RESULTS

Efficiency

The overall efficiency of the Transmission is determined by summing the individual component power losses. Each gear and bearing is analyzed and the power losses multiplied by the number of like gears or bearings, then added together. The traction component losses are likewise added to produce the cumulative effect of the four cone/roller contacts. Total power loss for varied input and output speeds the power is shown in Table 1, page 30. Corresponding efficiencies are shown in Table 2, page 32, and Figure 11 through 15, page 34 through 38, respectively.

Figure 16, page 39, graphically expresses the linear relationship between the ratio of recirculating horsepower (m) to total output horsepower, and the total CVT ratio. Figure 17 through 21, page 40 through 44, are plots of total efficiency versus the total CVT ratio and the ratio of recirculating horsepower to total output horsepower.

The bearings are analyzed by a high speed digital computer which calculates bearing lives, operating stresses, and internal loads, kinematics, and friction losses. Bearing friction losses are predicated on a constant coefficient of friction of .075. - This value is reasonably close at very high bearing loads, but the actual friction coefficient at moderate to low loads is much lower. The power loss attributed to the bearings is therefore much lower than is calculated by the computer program. A corresponding increase in efficiency would be reflected through lower power loss if a variable friction coefficient were used.

Gear losses are determined from the gear geometry, ratio, and friction coefficients as presented in Reference 1. Each different gear mesh is analyzed to determine the power loss factor then multiplied by the number of like meshes. Total power loss attributed to the gears is then determined for each power condition by multiplying the gear loss factor by the operating power ($H_p \times m$). The component power loss factors

were assumed to be constant, for a conservative appraisal, and were used as such throughout the analysis. (Table 3, page 45).

REGENERATIVE CVT
TOTAL POWER LOSS
 (INCLUDES GEARS, BEARINGS AND TRACTION ELEMENTS)

<u>7.5 KW (10 HP)</u>	<u>28,000</u>	<u>21,000</u>	<u>14,000</u>
Rpm _o ↓	Rpm _n →		
	KW Loss		
5000	1.00	.93	.91
4000	.92	.95	.83
3000	1.01	.99	.80
1500	1.39	1.24	.95
850	1.97	1.59	1.21
<u>15 KW (20 HP)</u>			
5000	1.89	1.75	1.61
4000	1.73	1.64	1.58
3000	1.92	1.75	1.62
1500	2.86	2.45	1.93
850	4.06	3.31	2.47
<u>30 KW (40 HP)</u>			
5000	3.53	3.62	3.64
4000	3.45	3.43	3.56
3000	3.98	3.70	3.58
1500	6.28	5.35	4.28
850	8.91	7.30	5.31
<u>52 KW (70 HP)</u>			
5000	6.63	7.05	7.88
4000	6.73	6.61	7.40
3000	7.68	7.23	7.46
1500	12.00	10.43	8.69
*(39.8KW) 850 *(53.4 HP)	17.79 (10.3) *	14.62 (7.86) *	10.65 (5.55) *

Table 1: *() Wheel Slip Limit

TOTAL POWER LOSS (REGENERATIVE CVT), continued

<u>75 KW (100 HP)</u>		<u>KW Loss</u>		
5000		9.66	10.52	12.54
4000		9.98	9.98	11.09
3000		11.11	10.54	11.32
*(70.3KW)	1500 *(94.3 HP)	16.73 (16.09)*	14.73 (12.86)*	13.70 (9.76)*
*(39.8KW)	850 *(53.4 HP)	26.46 (12.8)*	21.62 (9.59)*	16.92 (6.85)*

Table 1: *() Wheel Slip Limit
Continued

REGENERATIVE CVT EFFICIENCY

<u>7.5 KW (10 HP)</u>		<u>28,000</u>	<u>21,000</u>	<u>14,000</u>	
Rpm _o	Rpm _n	Percent			
5000		90.0	90.7	90.9	
4000		90.8	90.5	91.7	
3000		89.9	90.1	92.0	
1500		86.1	87.6	90.5	
850		80.3	84.1	87.9	
<u>15 KW (20 HP)</u>					
5000		90.6	91.3	92.0	
4000		91.4	91.8	92.1	
3000		90.4	91.3	91.9	
1500		85.7	87.8	90.4	
850		79.7	83.5	87.7	
<u>30 KW (40 HP)</u>					
5000		91.2	91.0	90.9	
4000		91.4	91.4	91.1	
3000		90.1	90.8	91.1	
1500		84.3	86.6	89.3	
850		77.7	81.8	86.7	
<u>52 KW (70 HP)</u>					
5000		90.5	89.9	88.7	
4000		90.4	90.6	89.4	
3000		89.0	89.7	89.3	
1500		82.9	85.1	87.6	
*(39.8KW)	850	*(53.4 HP)	74.6 (80.72)*	79.1 (85.30)*	84.8 (89.61)*

Table 2: *() Wheel Slip Limit

REGENERATIVE CVT EFFICIENCY (continued)

<u>75 KW (100 HP)</u>	<u>Percent</u>		
5000	90.3	89.5	87.5
4000	90.0	90.0	88.9
3000	88.9	89.5	88.7
* (70.3KW) 1500 *(94.3 HP)	83.3 (86.14) *	85.3 (86.36) *	86.3 (89.65) *
* (39.8KW) 850 *(53.4 HP)	73.5 (76.64) *	78.4 (82.04) *	83.1 (87.17) *

Table 2: *() Wheel Slip Limit

REGENERATIVE CVT

- INPUT SPEED
○ 14,000 RPM
× 21,000 RPM
△ 28,000 RPM

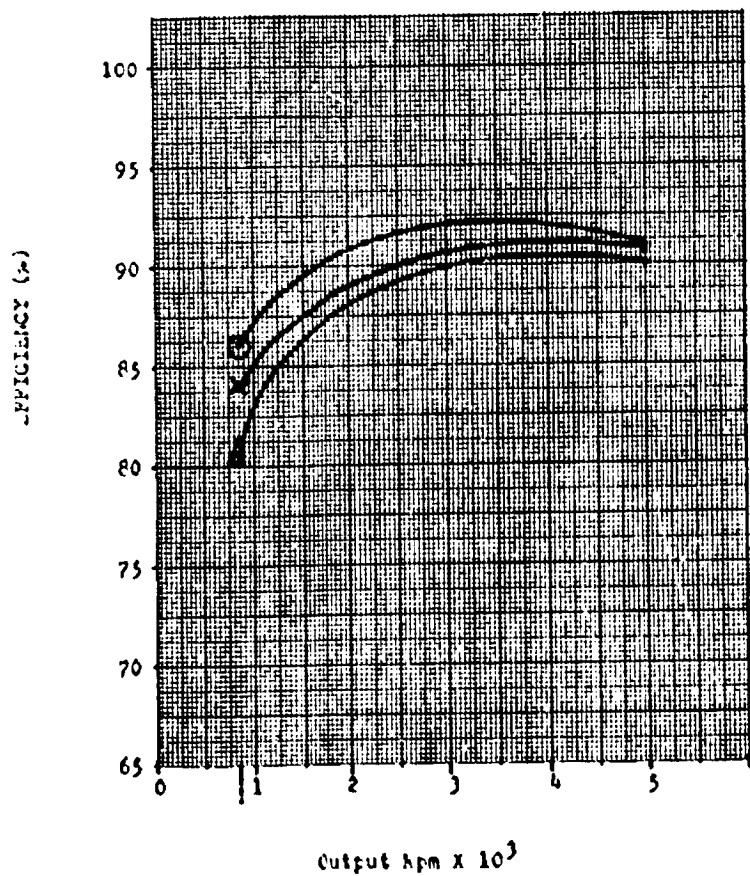


Figure 11: CVT Efficiency At 7.5 K: (10 Hp).

REGENERATIVE CVT

INPUT SPEED

- 14,000 RPM
- X 21,000 RPM
- △ 28,000 RPM

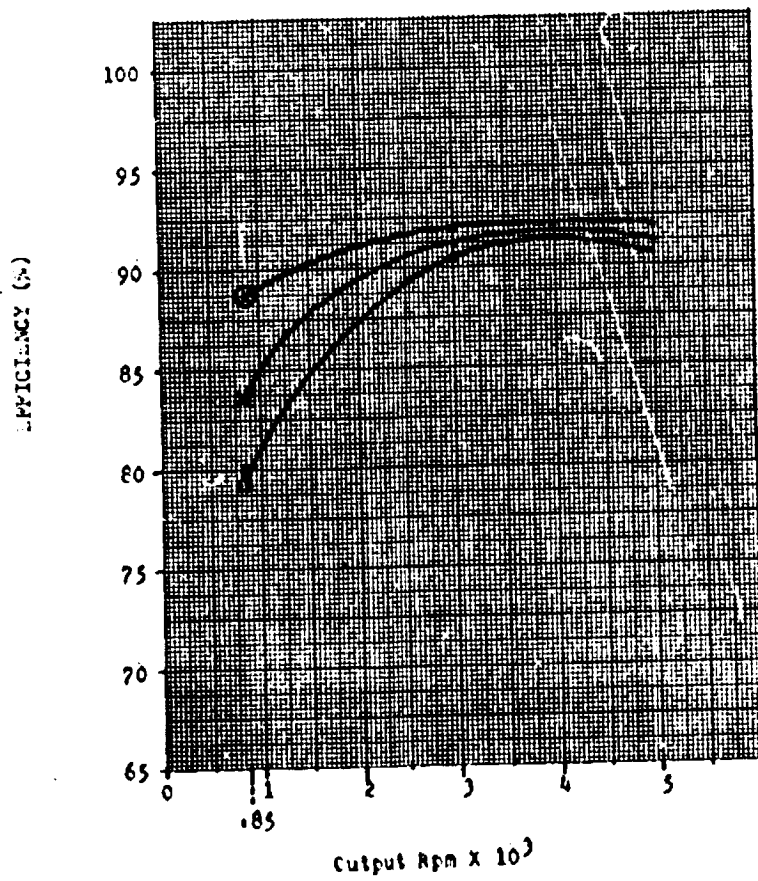


Figure 12: CVT Efficiency At 15 kW (20 Hp).

REGENERATIVE CVT

- INPUT SPEED
○ 14,000 RPM
× 21,000 RPM
△ 28,000 RPM

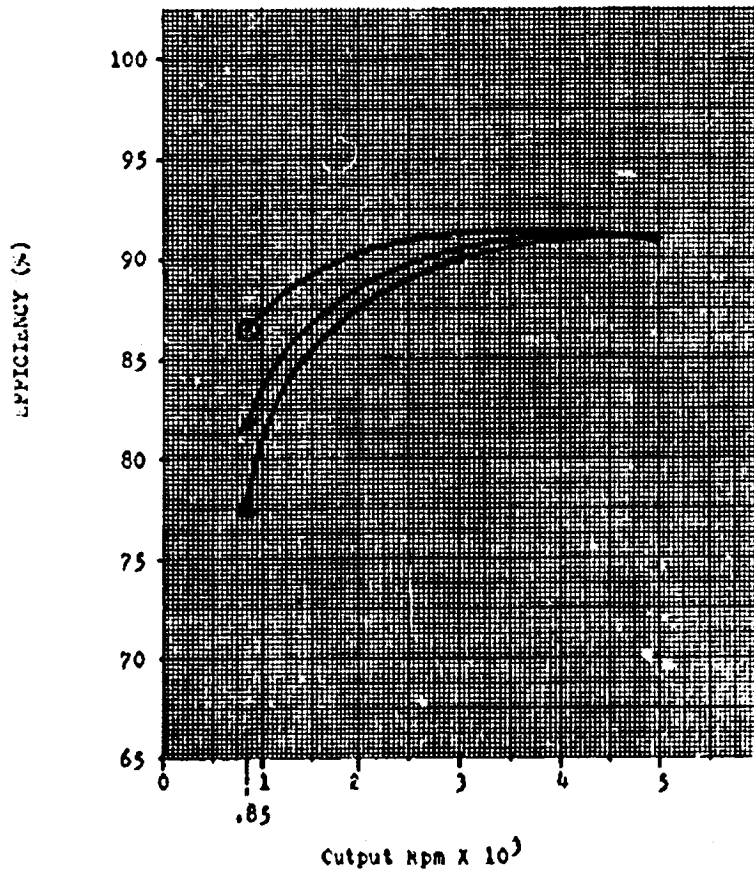


Figure 13: CVT Efficiency At 30 Kw (40 Hp)

REGENERATIVE CVT

INPUT SPEED

○ 14,000 RPM

X 21,000 RPM

△ 28,000 RPM

- - - With Wheel Slip Torque Limited

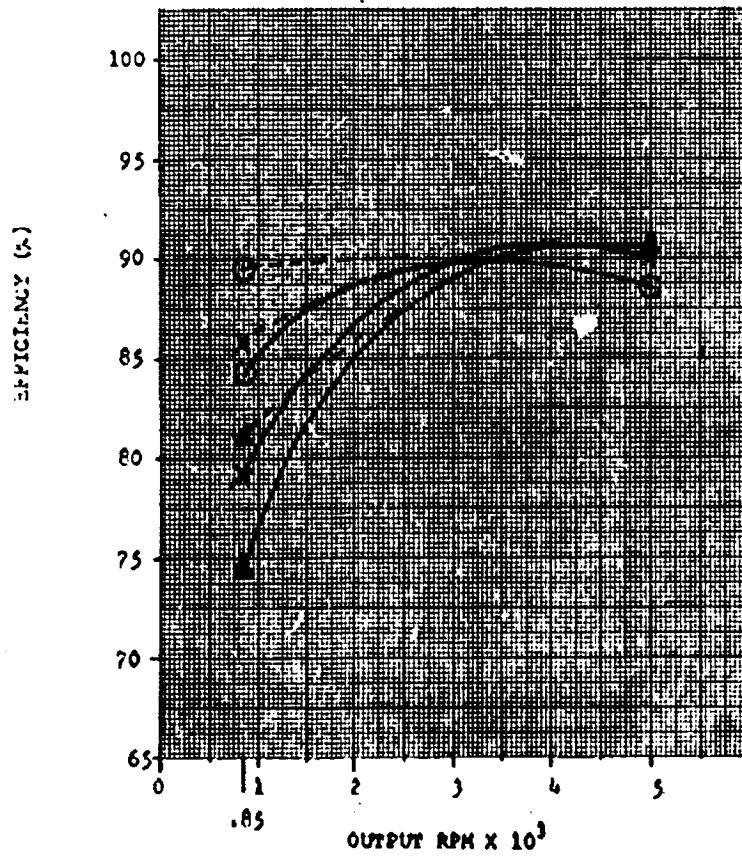


Figure 14: CVT Efficiency at 52 Kw (70 Hp).

REGENERATIVE CVT

INPUT SPEED

- 14,000 RPM
- X 21,000 RPM
- △ 28,000 RPM

--- With wheel Slip Torque Limited.

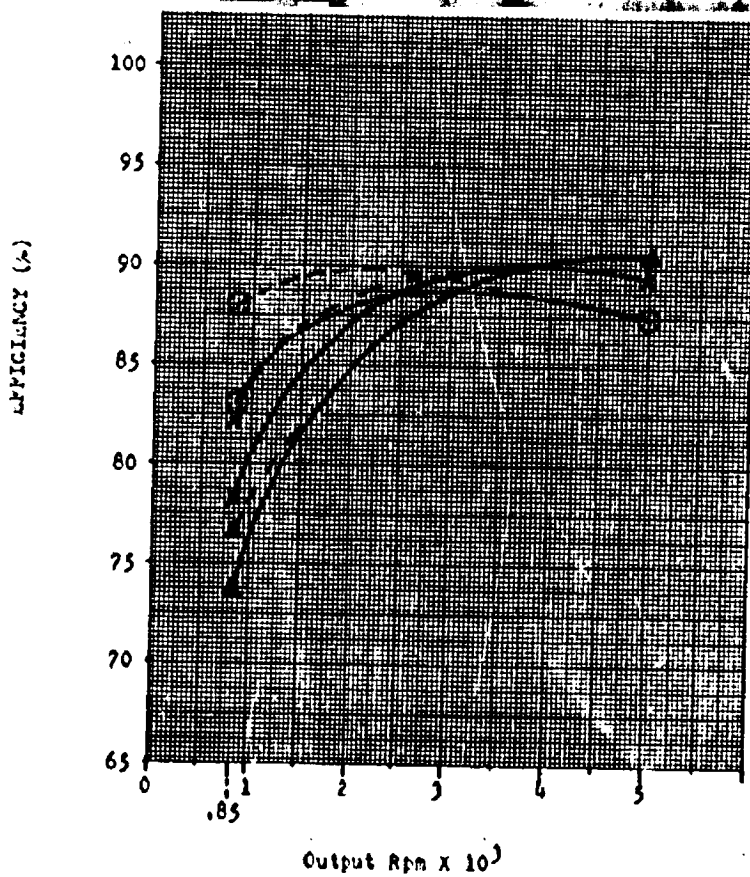


Figure 14 CVT Efficiency At 75 kW (100 Hp).

REGENERATIVE CVT

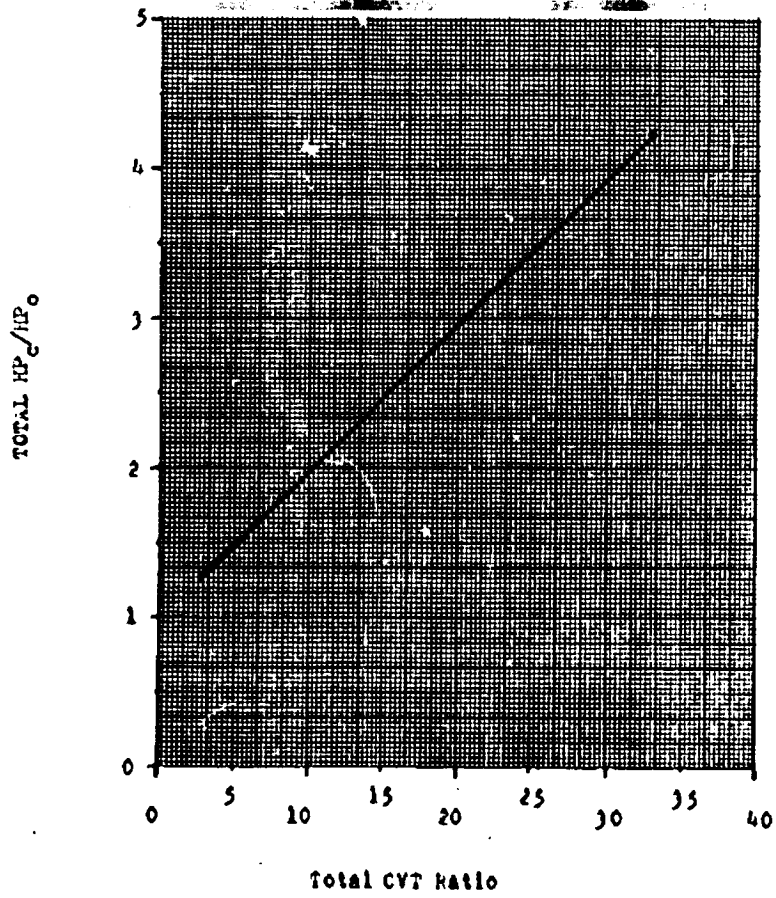


Figure 16: Ratio of Recirculating Hp To Output Hp VS total CVT Ratio

efficiency VS Ratio of Recirculating Hp
To Output Hp and Total CVT Ratio At
7.5 K_v (10 Hp).

FLYWHEEL RPM
INPUT SPEED

- 28,000 RPM
- × 21,000 RPM
- △ 14,000 RPM

REGENERATIVE CVT

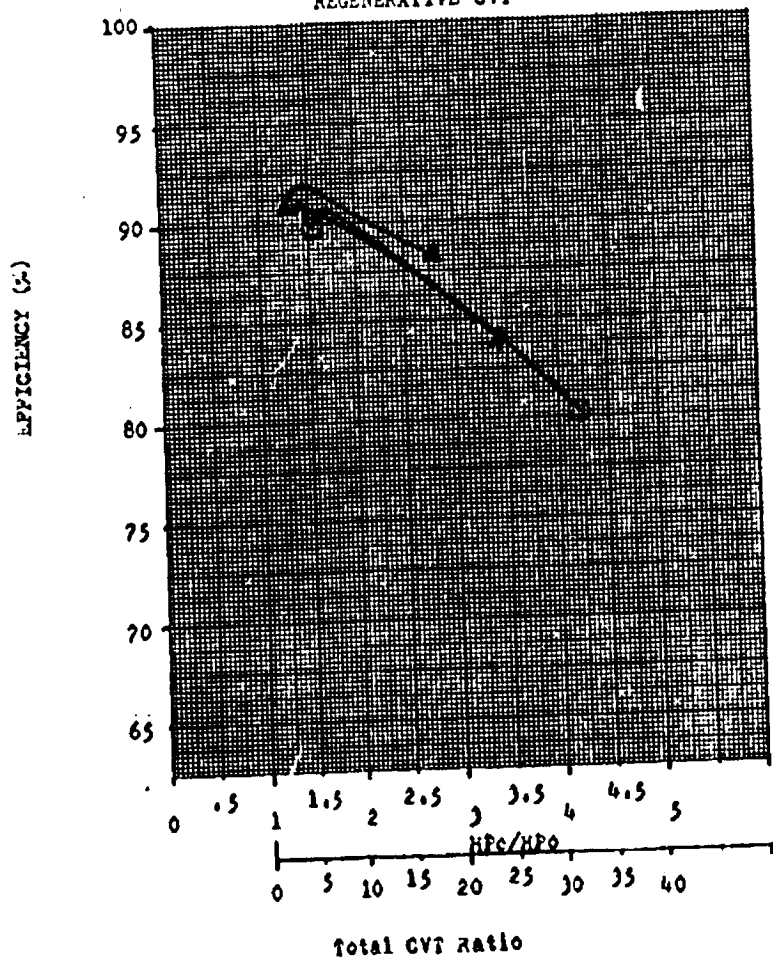


Figure 17:

Efficiency VS Ratio of Recirculating Hp to Output Hp and Total CVT Ratio At 15 Kw (20 Hp).

- FLYWHEEL RPM
- 28,000 RPM
 - × 21,000 RPM
 - △ 14,000 RPM

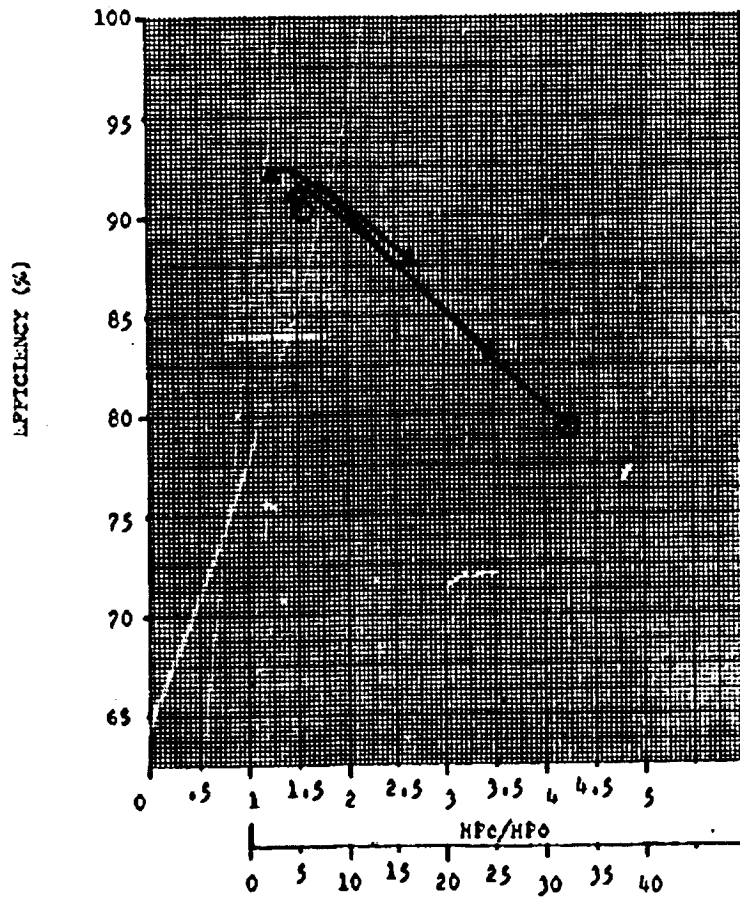


Figure 18:

Total CVT Ratio

Efficiency VS Ratio of Recirculating Hp to Output Hp and Total CVT Ratio At 30 KW (40 Hp).

- FLYWHEEL RPM
- 28,000 RPM
 - × 21,000 RPM
 - △ 14,000 RPM

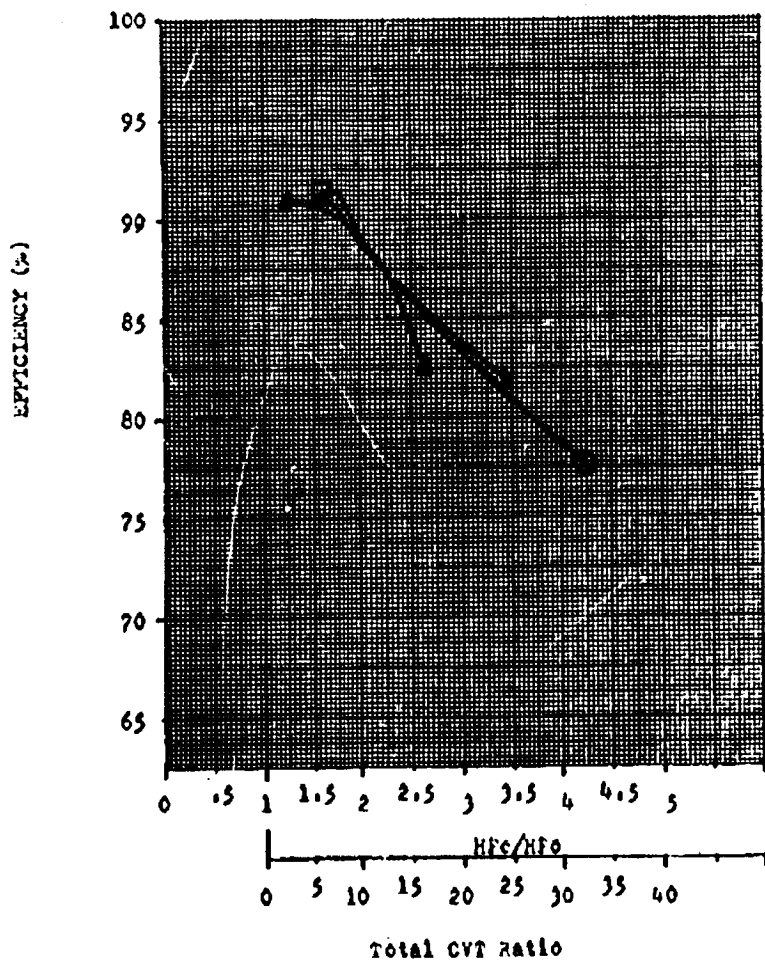


Figure 19:

Efficiency VS Ratio of Recirculating Hp to Output Hp and Total CVT Ratio At 52 KW (70 Hp).

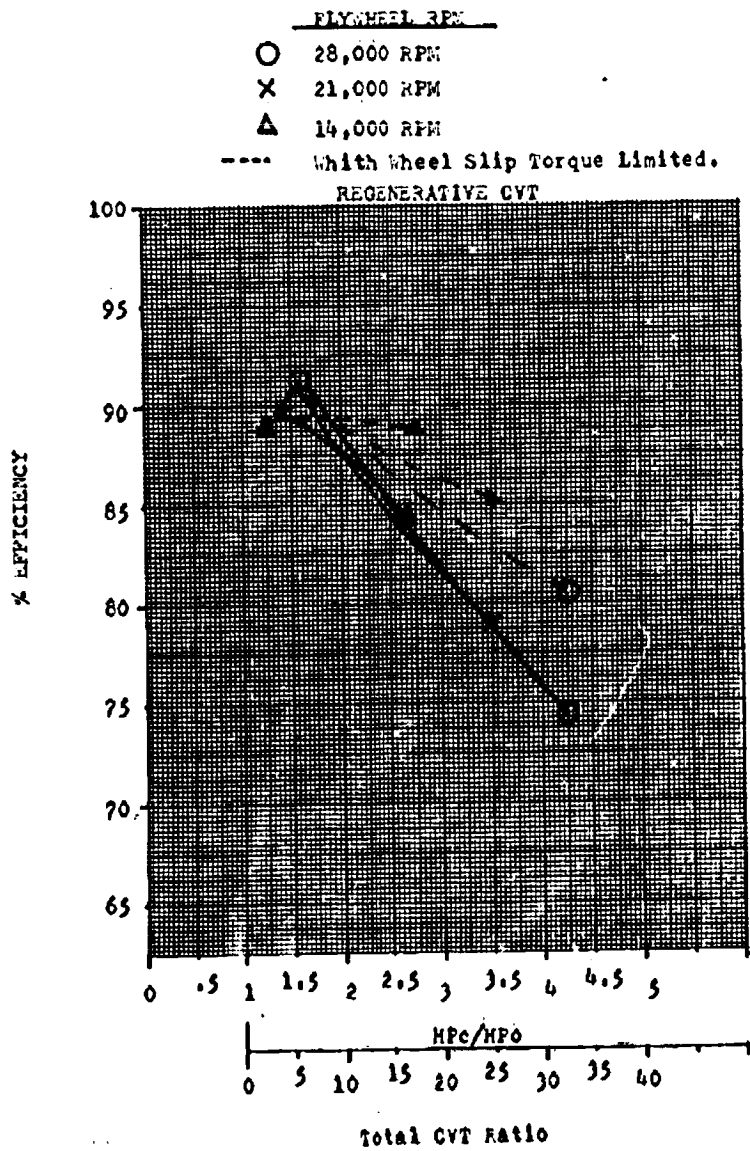


Figure 20 :

Efficiency VS Ratio of Recirculating Hp to Output Hp and Total CVT Ratio At 75 KW (100 Hp).

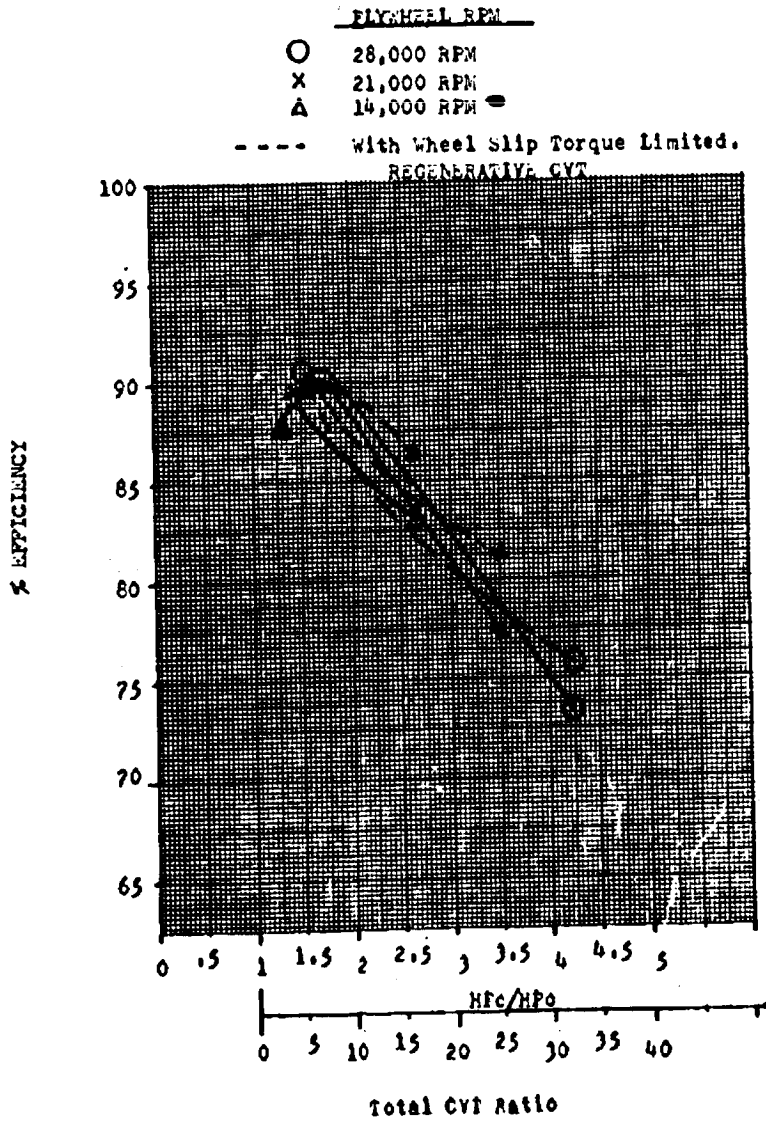


Figure 21:

Regenerative CVT Loss Source

	<u>% Loss Each</u>
Input Planetary	0.65
Spiral Bevel - Idler	0.81
Helical - Idler	0.44
Output Planetary	0.49
9.24° Cone/Roller Junction	1.60
Cone Bearings (3 sets/cone) wide variance with RPM and roller position (radial load distribution).	<u>2.3/8.1</u>
Loss Totals	6.29/12.09

Baseline Efficiency 93.7 to 87.91

The % loss totals are of internal horsepower. "m", and wheel slip limit values producing net output efficiency over the operating spectrum of 76.64% to 92.1%.

Table J:

The traction unit losses are determined by using the method shown in Reference 1 as a guide. An example calculation is shown in the Appendix on page 159. Incremental positions of the roller along the cone (Table 4, page 47) for fixed flywheel Rpm (Rpm_n) to fix output Rpm (Rpm_o).

is used to identify cone diameters at specific transmission ratio points (Table 5, page 48), and from which Traction Ratio and Cone Speed may be equated. These relationships are carried throughout calculations to determine Cone Torque (Table 18, page 135), Cone Normal Load (Table 21, page 141), Single Cone Horsepower (Table 19, page 137), Total Cone Horsepower (Table 20, page 159), and Traction Power Loss (Table 25, page 149) at specific output horsepower levels to quantify efficiency over the operating spectrum under given conditions. Sample calculations of these values are given in the Appendix as listed on page 70.

The contact geometry is calculated (Appendix page 151), then the spin velocity in the contact area is determined (Appendix page 145). Finally, the power loss through the traction unit (J7/J4, reference 1) is determined from tabulated values of slip and spin parameters (Appendix page 163 and 164). The power loss factor is then used to establish power loss in the traction unit for each power spectrum transmitted.

The coefficient of traction was taken to be a constant 0.07 for all calculations. Figure 22, page 49, is a volumetric plot of computer calculated peak traction coefficients over the operating spectrum for the regenerative CVT geometry.

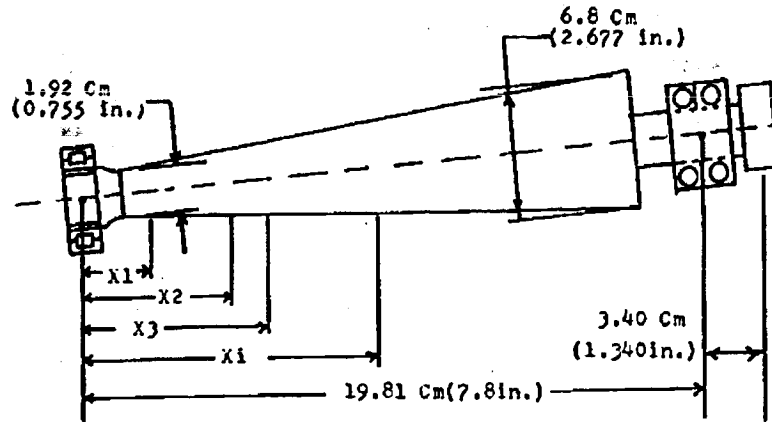
Power loss due to windage of the gears was shown to be negligible. (See Appendix D, page 112). An overall loss factor of 0.037 KW (0.05 HP) was added to account for lightly loaded roller bearing conditions.

Study results indicate an overall operating efficiency of the regenerative CVT as 91.5% for the mean power condition, 16KW (22HP) and 3,000 Rpm output. Calculated efficiency ranged from 92.1% at 15KW (20 HP), 14,000 Rpm in, 3,000 Rpm out, to 76.64% at wheel slip "Torque Limit" of 39.8KW (53.4 HP) with 28,000 Rpm input and 650 Rpm output. Cone speed at the mean condition is approximately 23,480 Rpm; roller speed is 7,200 Rpm. The Roller Rpm equates to the output planetary sun gear (Rpm_s) and is used in certain calculations.

$$Rpm_s = \text{Flywheel Rpm } (Rpm_n) / 2.91666$$

(See Table 32, page 168).

ROLLER
AXIAL LOCATION



Xi, Cm (in.)
AXIAL LOCATION

	RPM _n → 28,000	21,000	14,000
RPM _o ↓			
5000	5.62(2.213)	3.90(1.534)	1.80(0.710)
4000	7.06(2.781)	5.22(2.056)	3.62(1.442)
3000	9.02(3.550)	7.06(2.781)	4.51(1.775)
1500	13.65(5.375)	11.78(4.637)	9.02(3.550)
850	16.87(6.643)	15.34(6.038)	12.85(5.060)

Table 4:

CONE DIAMETER, C_n (in.)

$$D_c = 11.53 \text{ cm}/R_c \text{ (4.65 in.}/R_c) \quad \text{RPM}_s = \text{RPM}_n / 2.91666$$

RPM _n \ RPM _s →	9600	7200	4800
5000 ↓	3.15(1.242)	2.60(1.022)	1.92(0.755)
4000	3.62(1.426)	3.03(1.191)	2.27(0.895)
3000	4.25(1.675)	3.62(1.426)	2.79(1.100)
1500	5.76(2.266)	5.15(2.027)	4.25(1.675)
850	6.80(2.677)	6.30(2.481)	5.50(2.164)

TRACTION RATIO

$$\text{RPM}_n = (.2154 R_c - .2857) \text{RPM}_s \quad \text{RPM}_s = \text{RPM}_n / 2.91666$$

$$R_c = \frac{(\text{RPM}_n)}{(\text{RPM}_s)} + .2857$$

$$\quad \quad \quad .2154$$

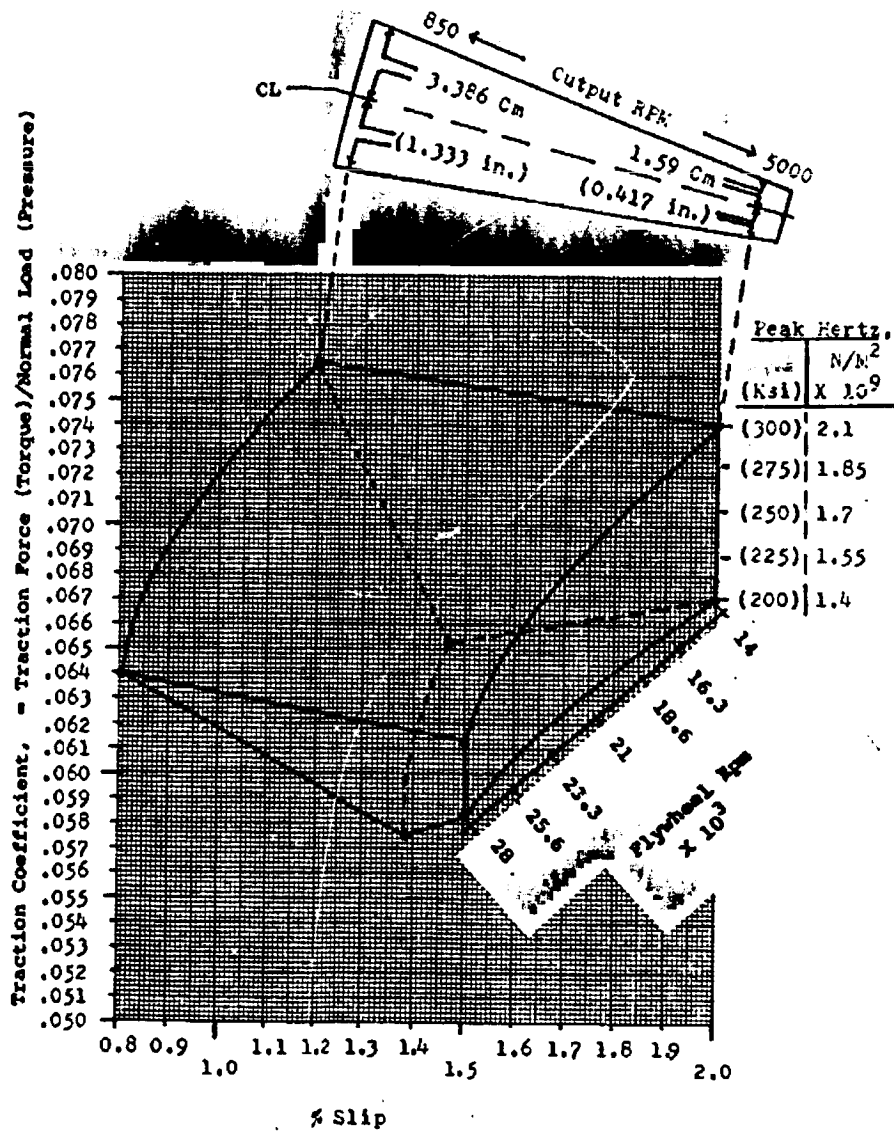
RPM _n \ RPM _s →	9600	7200	4800
5000 ↓	3.744	4.550	6.162
4000	3.261	3.906	5.195
3000	2.777	3.261	4.228
1500	2.052	2.294	2.777
850	1.737	1.874	2.149

CONE SPEED (RPM)

$$\text{RPM}_c = (R_c) (\text{RPM}_s) \quad \text{RPM}_s = \text{RPM}_n / 2.91666$$

RPM _n \ RPM _s →	9600	7200	4800
5000 ↓	35942	32760	29578
4000	31306	28123	24936
3000	26659	23479	20294
1500	19699	16516	13329
850	16675	13493	10315

Table 5:



Volume-graph of Optimum Slip for Santotrac 50 at 70°F over normal operating range. (Current Geometry)

Figure 22:

Cost

A detailed review of all the elements comprising the transmission based on operating parameters and quantity per gearbox and a comparison to standard automotive parts was made. A weight and cost analysis was conducted for 5 makes of passenger car automatic transmissions in use for the past 10 years. Common elements in the CVT uses conventional automotive gears and bearings, planetary assemblies, and housings. The weight and cost analysis (Table 6, page 51) indicates a cost/pound of \$3.20 to \$7.40 for existing automatic transmissions with torque converters. Elements that differ are torque converter, control valve body, disc clutches, and control system in the standard automatic, and in the traction components and control system in the CVT.

The automatic transmission is considerably more complex than the CVT in the areas of number of detail parts, machining requirements, and assembly time, based on 100,000 units of each. The CVT has stringent tolerance and balance requirements on the cones and the finish requirements are on the order of antifricition bearing values.

However, all machining and processing variables necessary to manufacture the cones and rollers are well established. Tooling requirements would be no more restrictive or costly than for bearings or other precision components. Although no actual cost analysis has been possible (as by a bearing manufacturer) the processing techniques (grinding, heat treat, inspection) are well developed. A qualitative statement based on relative similarities between detail parts and processes in the automatic transmission and the CVT then would indicate a close similarity in cost per pound for each on a like production level basis. Based on this premise, it is believed that the CVT cost would be \$330.00, based on a dry weight of 34 KG (75 lbs.).

Weight

A detailed weight analysis of the CVT produced a total weight of 39 KG (85 lbs), Table 7, page 52. The housings are cast aluminum and the planetary carriers as shown are forged aluminum. However, in a value analysis program for the gearbox, the carriers would probably be made from steel stampings with selective welded construction. The weight and cost would be reduced for a high volume production run.

REGENERATIVE CVT
TRANSMISSION COSTS
(RETAIL, AUTOMOTIVE)

<u>TYPE</u>	<u>COST*</u>	<u>WEIGHT*</u>	<u>\$/KG</u>	<u>\$/LB</u>
FORD C-4	\$ 532.85	60.8(134)	\$ 8.76	\$3.98
FORD C-6	\$ 562.85	79.9(176)	\$ 7.04	\$3.20
GM 200	\$ 829.00	50.8(112)	\$16.32	\$7.40
GM 300	\$ 862.00	53.1(117)	\$16.23	\$7.37
GM 350	\$1008.00	65.8(145)	\$15.32	\$6.95
CHRYSLER (TORQUEFLITE)	\$ 650.00	72.2(159)	\$ 9.00	\$4.09

*WITH TORQUE CONVERTER

AVERAGE COST = \$12.11/KG (\$5.50/LB)

RETAIL MARK-UP (ASSUMED) = 20%

MANUFACTURING COST = (.8) (\$12.11) = \$9.69/KG (\$4.40/LB)

QUANTITY PRODUCTION COST OF CVT = \$9.69/KG

FOR 34 KG (75 LB) (MAX), COST = \$330.00

**REGENERATIVE CVT
TRANSMISSION WEIGHT**

<u>ITEM</u>	<u>WEIGHT (LB) KG</u>	<u>QUAN- TITY</u>	<u>TOTAL WEIGHT (LB) KG</u>
INPUT HOUSING	(2.14)0.97	1	(2.14)0.97
MAIN HOUSING	(11.86)5.39	1	(11.86)5.39
OUTPUT HOUSING	(3.39)1.54	1	(3.39)1.54
INPUT SUN GEAR	(.71)0.32	1	(.71)0.32
INPUT RING GEAR	(.89)0.40	1	(.89)0.40
INPUT PLANET	(.07)0.03	3	(.21)0.10
INPUT CARRIER	(.44)0.20	1	(.44)0.20
INPUT PLANET SHAFT	(.03)0.01	3	(.09)0.04
BRAKE	(.28)0.13	1	(.28)0.13
ENCODER DISC	(.21)0.10	1	(.21)0.10
OIL PUMP PINION	(.25)0.11	1	(.25)0.11
OIL PUMP GEAR	(.30)0.14	1	(.30)0.14
PLANETARY KEY	(.004)0.0018	1	(.004)0.0018
LEAD SCREW	(1.72)0.78	1	(1.72)0.78
WORM GEAR	(.05)0.02	1	(.05)0.02
WORM	(.06)0.03	1	(.06)0.03
ROLLER POSITIONER	(.97)0.44	1	(.97)0.44
ROLLER	(3.40)1.55	1	(3.40)1.55
BALL SPINE	(1.96)0.89	1	(1.96)0.89
PISTON	(.17)0.08	4	(.68)0.31
SPRING	(.03)0.01	4	(.12)0.05
SPHERICAL SLEEVE	(.25)0.11	4	(1.00)0.45

Table 7

<u>ITEM</u>	<u>WEIGHT (LB) KG</u>	<u>QUAN- TITY</u>	<u>TOTAL WEIGHT (LB) KG</u>
CONE	(5.05)2.3	4	(20.20)9.18
CONE NUT (ROLLER BRG END)	(.05)0.02	4	(.20)0.09
CONE NUT (DUPLEX BRG END)	(.05)0.02	4	(.20)0.09
DUPLEX LINER	(.60)0.27	4	(2.40)0.11
DUPLEX CLAMP PLATE	(.58)0.26	4	(2.32)1.05
CONE ENCODER	(.09)0.04	1	(.09)0.04
SPIRAL BEVEL PINION	(.12)0.05	4	(.48)0.22
PINION KEY	(.01)0.0045	4	(.04)0.02
IDLER	(.43)0.20	4	(1.72)0.78
IDLER SHAFT	(.09).041	4	(.36) .16
IDLER PLATE (LEFT)	(1.29)0.58	1	(1.29) .58
IDLER PLATE (RIGHT)	(.71)0.32	1	(.71) .32
SPACER, BALL SPLINE SHAFT	(.05)0.22	1	(.05) .22
OUTPUT RING GEAR	(2.04)0.93	1	(2.04) .93
OUTPUT PLANET GEAR	(.29)0.13	4	(1.16) .53
OUTPUT PLANET SHAFT	(.07)0.03	4	(.28) .13
OUTPUT CARRIER	(.70)0.32	1	(.70) .32
OUTPUT SUN GEAR	(.34)0.15	1	(.34)0.15
OUTPUT FLANGE	(.18)0.08	1	(.18)0.08
BEARING, INPUT SUN DUPLEX (6904)	(.16)0.07	1	(.16)0.07
BEARING, INPUT RING BALL (6910)	(.28)0.13	1	(.28)0.13
BEARING, BALL SPLINE DUPLEX (6004)	(.32)0.15	1	(.32)0.15

Table 7 (continued)

<u>ITEM</u>	<u>WEIGHT (LB) KG</u>	<u>QUAN- TITY</u>	<u>TOTAL WEIGHT (LB) KG</u>
BEARING, ROLLER POSITIONER BALL (SPECIAL)	(.24)0.11	2	(.48)0.22
BEARING, OUTPUT RING BALL (6004)	(.16)0.07	1	(.16)0.07
BEARING, OUTPUT BALL (6004)	(.16)0.07	1	(.15)0.07
BEARING, CONE ROLLER (304)	(.38)0.17	4	(1.52)0.69
BEARING, CONE DUPLEX (7206)	(.90)0.41	4	(3.60)1.64
BEARING, INPUT PLANET ROLLER (B-78)	(.02)0.009	3	(.06)0.03
BEARING, BALL SPLINE ROLLER (B-167, IR-128)	(.08)0.04	1	(.08)0.04
BEARING, IDLER ROLLER (MR-100)	(.02)0.009	8	(.16)0.07
BEARING, OUTPUT PLANET ROLLER (MR-100)	(.02)0.009	8	(.16)0.07
OIL PUMP	*(.50)0.23	1	(.50)0.23
OIL	(9.38)4.26	1	(9.38)4.26
MISC. (NUTS, BOLTS, SNAP RINGS, SEALS, ETC.)	*(2.00)0.91	1	(2.00)0.91

*Estimated

TOTAL TRANSMISSION WEIGHT = 38.37KG (84.51LB)
 DRY WEIGHT = 34.11KG (75.13LB)

(DOES NOT INCLUDE CONTROLS, ELECTRONICS, OR FILTER)

Table 7 (Continued)

Noise

Noise generating components in the CVT are gears, hydraulics and windage loss components (wind noise).

The gear teeth in the CVT are helical spur designs and spiral bevel designs which are sized to have a sufficiently large helix (spiral) angle to yield a high (> 2.0) total contact ratio. Helical action at the beginning and end of action of the conjugate teeth is much quieter than for straight spur gears. Gear tooth modifications of lead and profile also are used to assure smooth action. The gear teeth are lightly loaded so modifications will be small. By virtue of the light loads and helical and spiral gear designs the noise generated by the operating gears will be well below the audible range in the vehicle. The windage losses within the CVT are also quite low, hence the noise level will be below the audible level.

The noise effect of bearings and traction components will be much lower than for the gears. Therefore it is expected that the CVT will run quieter than the comparable automatic transmission.

Reliability

The CVT is designed for 2600 hours minimum life at the mean condition of 16 KW (22 HP) out at 3000 RPM output and 21,000 RPM input. The gear stresses at mean and maximum torque are all less than $82.7 \times 10^6 \text{ N/m}^2$ (12,000 psi) and $413.7 \times 10^6 \text{ N/m}^2$ (60,000 psi), respectively, which results in a virtual infinite life for the maximum stressed component. Similarly, the lowest life bearing is the input planetary pinion roller bearing with a life of 22,960 hours at the mean condition (Table 8, page 57). ASME life modification factors for the bearings are shown.

The minimum traction element life is 2920 hours (Appendix, page 134), as determined by the analytical method defined in Reference 3. The life of the traction elements, again, are determined at mean condition: 16 KW (22 HP) out 21,000 RPM in, 3,000 RPM out. Stress calculations are based on an 11.8 cm (4.65 inch) diameter roller, at 7200 RPM, with a 12.7 cm (5 inch) crown radius and 3.6 cm (1.426 inch) diameter cone, with a normal load of 2,217 n (498.5 lbs). Figure 23, page 58, illustrates the dramatic decrease in contact life as the power to the CVT is increased. Hertz stress at the traction contact point at the mean and maximum torque conditions was $1.58 \times 10^9 \text{ N/m}^2$ (230,480 psi) and $2.97 \times 10^9 \text{ N/m}^2$ (432,060 psi), respectively (Appendix LL, page 157).

The respective cone bending stresses were $38.3 \times 10^6 \text{ N/m}^2$ (5560 psi) and $259.0 \times 10^6 \text{ N/m}^2$ (37,330 psi) (Appendix U, page 130). Figure 24, page 59, is single cone HP vs output RPM.

While fatigue life of the dynamic elements is the general criterion for determining gearbox longevity, it is equally necessary to consider wear. The elements which are subjected to relative sliding may produce wear and wear particles which further accelerate the tendency to wear. Gear teeth, bearings, and traction elements are subject to wear, depending on the lubrication regime in which they operate. In all instances the dynamic elements are operating at such a relative velocity as to preclude gross metal to metal contact. Each set of gears in mesh are separated by a film of oil sufficiently thick to virtually eliminate any metallic contact. The same is true of the traction elements where the film thickness is $10.1 \times 10^{-4} \text{ mm}$ (39.6 in.) at the mean power condition (Appendix KK, page 155). The worst condition of power loading, 75 kW (100 HP) at 450 N-m (330 ft-lbs) output results in a film thickness of $7.1 \times 10^{-4} \text{ mm}$ (27.8 in.).

The ratio of film thickness to composite roughness in the traction cone and roller is $h/\sigma = 4.66$ (mean). There will be relatively insignificant wear associated with this condition. Table 9, page 60, reflects gear stresses at maximum and mean power conditions.

Maintainability

Maintenance requirements for the CVT will be minimal. Due to the lack of wear exhibited by the dynamic components in conjunction with the variable load mechanism for the cones against the roller, it is anticipated that the only service required after initial run-in will consist of no more than an oil filter change.

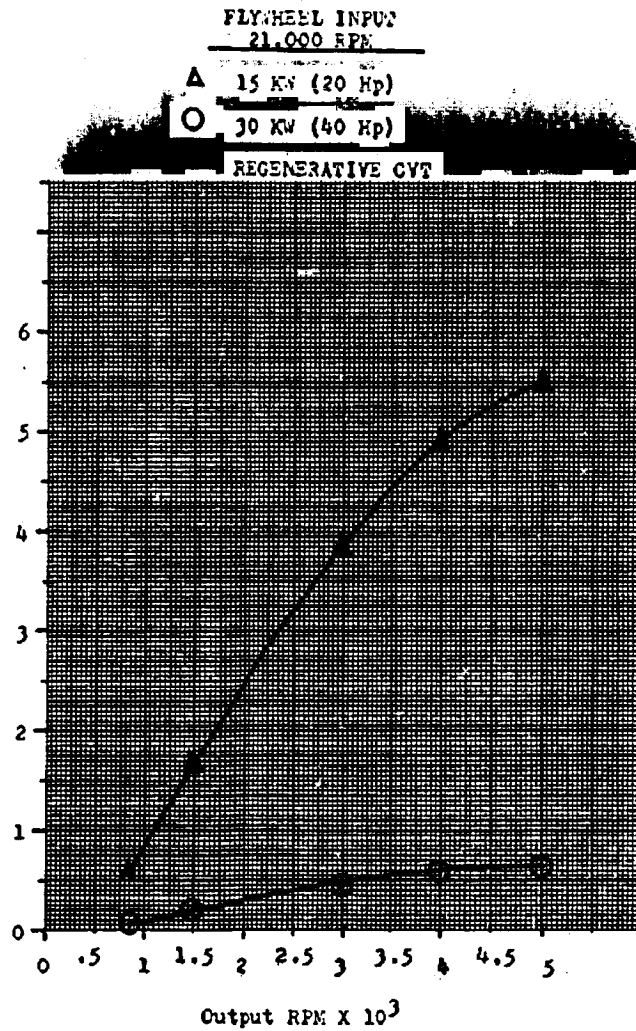
Seal leakage, the major cause of transmission removal, will be minimized. The input seal is a carbon face magnetic seal, operating in a well aligned state, which adequately accepts the speed of the input shaft (up to 28,000 RPM). The output seal is a standard double lip elastomeric seal operating at low rubbing speed also in a well aligned condition. The only other seal is a double lip seal on the positioner motor. This seal is well above the static oil level in the CVT so no leakage is anticipated. This seal will be splash lubricated.

BEARING LIVES AT MEAN CONDITION

BEARING (LOCATION)	ASME LIFE FACTOR (D) (E) (F) (REF. 5)	L ₁₀ (HOURS)
BALL, DUPLEX (INPUT)	--	> 10 ⁶
BALL, INPUT (RING SUPPORT)	--	> 10 ⁶
ROLLER (INPUT PLANETARY)	6	22,960
BALL, DUPLEX (ROLLER SHAFT)	--	> 10 ⁶
ROLLER (CONE SUPPORT)	6	23,480
BALL, DUPLEX (CONE SUPPORT)	6	34,590
BALL, OUTPUT (RING SUPPORT)	--	> 10 ⁶
ROLLER (ROLLER SHAFT)	--	> 10 ⁶
ROLLER (OUTPUT PLANETARY)	--	31,120
BALL (OUTPUT SHAFT)	--	> 10 ⁶

Table 8

COMPOSITE TRACTION CONTACT LIFE (X 10³ HOURS).



Composite Traction Contact Life VS Output Speed.

Figure 23:

7.5KW (10 Hp)	▲	14,000 Rpm In
	○	28,000 Rpm In
30KW (40 Hp)	▼	14,000 Rpm In
	■	28,000 Rpm In
75KW (100 Hp)	×	14,000 Rpm In
	•	28,000 Rpm In

--- Wheel Slip Torque Limited.

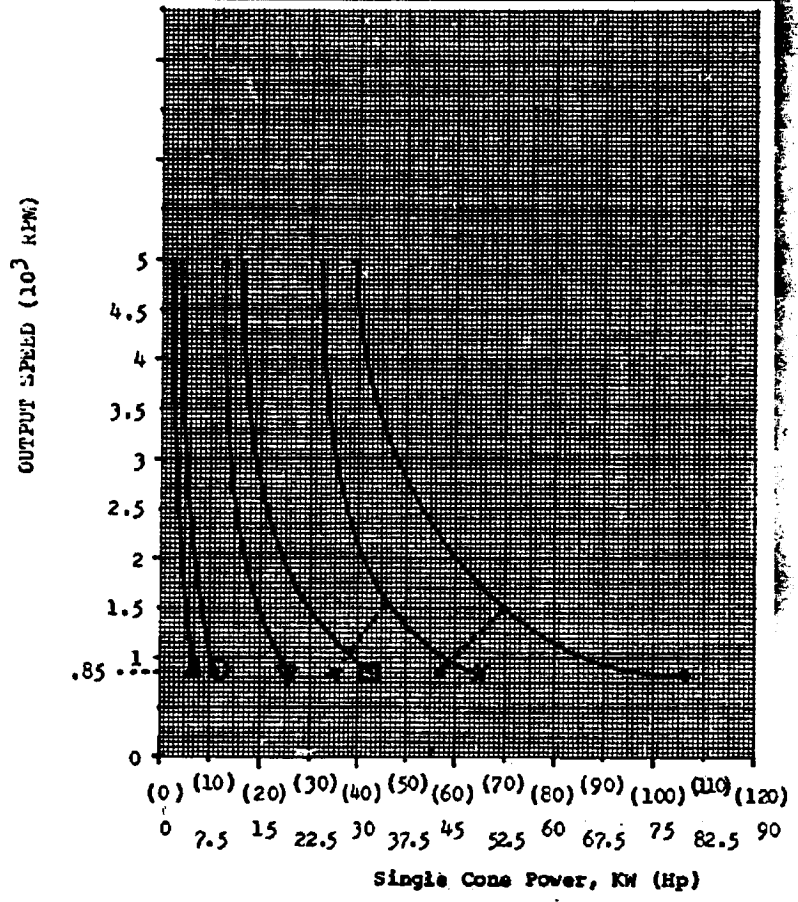


Figure 24 :

Cone Power VS Output Speed

GEAR STRESSES

	BENDING 10^8 N/m^2 (10^3 PSI)		COMPRESSIVE 10^8 N/m^2 (10^3 PSI)	
	MEAN	MAX	MEAN	MAX
INPUT PLANETARY SUN PLANET	.630(9.15) .483(7.01)	3.267(47.42) 2.502(36.32)	6.231(90.44)	14.18(205.79)
SPIRAL BEVEL PINION GEAR	.0096(1.400) .0096(1.400)	.4992(7.240) .4992(7.240)	4.859(70.47)	11.06(160.42)
IDLER HELICAL SUN PLANET	.234(3.400) .194(2.810)	1.213(17.60) 1.005(14.58)	3.191(46.29)	7.264(105.36)
OUTPUT PLANETARY SUN PLANET	.143(2.080) .101(1.460)	.073(10.77) .5198(7.54)	2.490(36.12)	5.669(82.22)

Table 9

Scalability

The design requirement and criteria for scalability are the same as specified previously, with the exception of maximum output torque at wheel slip. The wheel slip torques to be considered are 210 N-m (155 lb ft) and 2690 N-m (1900 lb ft).

In reference 3 it is shown that the life of a traction conjunction varies in proportion to the size to the 8.4 power. That is, the life increases at a very rapid rate with any increases in size. While no actual calculations were performed to verify a similar trend of capacity with size, one set of calculations using a 22.9cm (9.0 in.) diameter roller and a 7.6 cm (3.0 in.) diameter cone was used to determine the capacity of the traction elements. With the surface velocity maintained the same as the baseline unit, 44.5 m/s, and using six cones, the capacity of the traction unit was 810 KW (1086 HP)

based on $13.2 \times 10^8 \text{ N/m}^2$ (192,300 psi) Hertz stress in the conjunction. The rotational speed of roller and cones was reduced to maintain the same surface velocity. The weight of such a unit would vary at a slightly higher rate than the square of the diameters. That is, the weight of an 810 KW

gearbox would vary slightly more than $(9/4.65)^2 = 3.76$ times the 75 KW (100 HP) unit, which was designed for this study.

Downward scalability is more difficult to attain except by reducing the number of traction cones. In the case of the lower horsepower unit the rating was attained by simply reducing the number of cones from 4 to 2. Although for other practical reasons it would be advantageous to redesign the unit and maintain a minimum of 3 cones to maximize inherent component stability and equal distribution of forces and stresses within the system. An attempt to reduce the size resulted in very little actual reduction when faced with maintaining the life based on surface stresses in the traction conjunction.

Alternate Electric Drive

The electric motor input differs very little from the flywheel input in actual function. The use of the CVT, being directly driven by the electric motor and directly driving the differential, will provide the required performance. The only modification to the basic CVT shown in Figure 1 will be ratio changes in the planetary and cluster gear assemblies to produce the required output speed.

This will allow the traction portion of the transmission to remain virtually unchanged for the change in prime mover and operating speeds. The motor is allowed to operate at its optimum speed for the required vehicle drive power. The motor current would be monitored by the computer, with the control effect being to either speed up or slow down the motor, in conjunction with a CVT ratio change, to seek the minimum power drain for all conditions. Parametric sampling by the computer would be exactly as with the flywheel input. The CVT would furnish the optimum performance for the electric motor only when compared to the use of stepping devices or other speed control means to control the motor. In all alternate schemes to provide an adequate vehicle speed for all terrains (i.e., uphill), the motor lugs down or absorbs too high a current drain to function efficiently. The use of the CVT, coupled with the constant monitoring by the computer, eliminates the adverse effects of excess power drain and assures optimum performance, to the extent that a smaller motor could be used in the same vehicle and exceed the operating characteristics of the vehicle without the CVT.

Alternate Hybrid-Electric Drive

A similar situation exists with the internal combustion (I.C.) engine driving into the CVT. I.C. input speed would be required to go through a speed-up planetary assembly to provide proper traction component speeds. The CVT will perform the function of allowing the I.C. engine to operate at its optimum BSFC for all output power requirements. The addition of the electric motor to the output shaft would have no effect on the actual CVT operation. The electric motor, when augmenting I.C. engine power at high power operating regimes, would simply transfer power to the vehicle drive wheels.

As previously described, the output planetary ratio and cone drive idler ratio would necessarily change in order to accomplish the output operating speed range. The ratio could be changed to accomplish the reverse and neutral conditions, as required. However, the efficiency at or near the neutral position suffers due to the regenerated power in the traction loop. As an alternative, the addition of an output planetary with reversing clutches could accomplish the range change without diminishing the efficiency beyond accepted levels. Further, a two or more speed unit with clutches could maintain the high efficiency for most of the speed range with a minimum of additional complexity. While multi-speeding adds some complexity and number of machined elements to the system the effects on overall efficiency increase are dramatic. See Figure 30, page 82.

POTENTIAL PROBLEM AREAS

Certain elements and features of the CVT design present potential problems and require special attention. These are: reaction to the tangential load on the cones (traction force), deflection of the cone and the associated traction contact pattern skew, hydraulic control response (piston motion and time), ratio change rate with the lead screw, binding effect of the axial force on the positioner imposed by the lead screw, piston relaxation time after pressure is reduced, and the accuracy and response time of the encoder/toothed disc monitor system. Addressing each item in sequence:

Reaction to the tangential load on the cones:

The traction force is reacted by the cone mounting bearings which are supported on the aft end by a quill in the transmission housing and on the forward end by the cone loading piston. This piston moves radially in plane with the cone/roller contact. The traction force generated in the traction conjunction causes a side load on the piston, which tends to bind the piston in the cylinder and prevent piston motion. To prevent the piston from actually binding an integral skirt is provided on either side of the piston to accept the side load. Further, the cast material will be a low friction material, such as 4032 aluminum, containing a high percentage of silicon. The magnitude of the side force will be always less than 1780 N (400 lbs) and the relaxation will lag the pressure drop. This always assures a load sufficient to maintain operation on the negative side of the optimum slip point. See page 74 for an alternative design.

Deflection of the Cone:

Bending moments imposed on the cone by the loading system will cause a curved shape of the cone, distorting the contact pattern in the traction conjunction. The roller is crowned with a 12.7cm (5.0 inch) crown radius. The drop from the point of the crown to the edge of the roller is .033 cm (.013 inches) which is much greater than the deflection of the cone for any loading condition. The roller is crowned to prevent edge loading under abnormal conditions and to provide an abbreviated major diameter of the contact ellipse. Crowning eliminates edge loading, provides reasonable contact ellipse dimensions, and reduces spin velocity.

Hydraulic control response:

Response of the hydraulic system to a computer output signal is determined by the modulator valve response time and the compliance in the hydraulic system. The response time will affect the slip rate and corrective traction force generation. If the response time is too great the output torque requirement may cause uncorrectable slip in the traction unit, thereby causing a runaway condition. The modulator valve responds in a matter of 1-5 ms (milliseconds) and the hydraulic system has at least the oil system pressure present at all times. The pressure lines are short with thick wall passages. Therefore, the response time is sufficiently short to allow all corrective motions of the piston to occur. The only feature to possibly cause a lag in the response motion is in the relaxing direction. The side load may be sufficient to prevent immediate reduction of the load thereby maintaining the traction load. See page 74 for an alternative design.

Ratio rate change with the lead screw:

The worm driven lead screw could limit the excursion time of the positioner from one end of the cone to the other end. The requirement to traverse the length of the cone from maximum ratio to minimum ratio, and vice versa, is 2.0 seconds. The lead screw requires 6.5 turns to produce the total excursion. The worm-wheel ratio is 16.5:1 which requires the drive motor to rotate 107 turns to move the positioner from one end of the cone to the other. The average speed of the motor would then be 3210 RPM. The positioner drive motor is 5,000 RPM reversible d.c. motor, which provides adequate margin to accomplish the excursion-time task.

It is recognized that the choice of a worm drive results in considerable loss in the worm-wheel set. The drive motor must therefore be sized to produce the required power for all control response inputs. The axial restraint of the roller at the traction conjunction is an unknown variable which must be evaluated on test; therefore the actual size of drive motor is an empirical factor. The worm-wheel design was done to maintain simplicity in concept and may require a lower power loss design in prototype and production units. See page 73 for an alternative design.

Binding effect of the axial force on the positioner:

Since the positioner lead screw drives the positioner axially at a considerable radial distance from the roller centerline, a bending moment is applied to the lead screw. The lead screw and drive motor may be unable to withstand the

bending moment. The result would be binding in the screw at the positioner. In this event a second screw would be provided diametrically opposite the existing screw. Two screws thus situated would eliminate the imposed bending moment and apply a pure axial load to the positioner. See page 73 for an alternative design.

Piston relaxation time:

As previously described, the relaxation time required for the piston to unload the cone is a function of piston side load and friction. The piston is fitted with a flow control valve which serves a dual purpose: relieving the piston pressure to the lubricating system pressure of $34 \times 10^4 \text{ N/m}^2$ (50 psi) and lubricating the cone support bearing. In the event that the lag time between load and relaxation is greater than the normal loading response time, the load would be maintained at a value in excess of what is required which would prevent excessive slip. However, this is not expected. When the pressure is relieved the load vanishes, thereby relieving the piston side load. Piston return would follow immediately. See page 74.

Accuracy and response time of the encoder/toothed disc monitor system:

This item is addressed in the section "Detail Control System Description", page 84 in the Appendix.

TECHNOLOGY ASSESSMENT

The mechanical transmission design embodies "conventional" automotive detail components; gears, bearings, shafting and housing. The unique elements are the traction components. Uniqueness is only in respect to the use of traction to accomplish variable speed instead of a torque converter and multispeed transmission. The traction roller and cone are fabricated of conventional materials using conventional processing. No new technology is required in their construction.

The traction conjunction physics are similar to gear tooth action or ball bearing action in that rolling and sliding exists in a lubricated conjunction. The use of a traction fluid for a lubricant imparts a greater traction force in the rolling-sliding conjunction than with conventional gear lubricants. Otherwise, the contacts are quite similar.

In the area of the control system, however, it was necessary to explore possible alternatives to the developed system presented herein. The use of electronic components that yield much higher response rates or activity rates was investigated. Alternates to the toothed disc and encoder are programmed magnetic film deposit with read head, digital signal generator and read head, and analog permanent magnet generator systems. While these components do not of themselves represent new technology, their use in the control system would require some development and test in order to be feasible.

CONCLUSIONS AND RECOMMENDATIONS

The design study has resulted in a computer controlled, continuously variable, transmission featuring multiple traction contracts, in a regenerative power. The traction elements are a crowned roller and four (4) cones in the regenerative design. The cones are aligned so that the cone axis is displaced at one half the cone angle from the transmission centerline. This puts the inner surfaces of the cones parallel to the roller axis. The roller is moved axially on a recirculating ball spline to affect a ratio change. Power is transmitted through the traction elements to an output planetary differential ring gear while feedback power is transmitted through the sun gear of the output planetary differential roller shaft. Traction ratio changes cause the output shaft speed to change.

The CVT designs presented herein result in lightweight, highly efficient, cost effective transmissions to be used in an electric vehicle. The designs enable the use of a power storage flywheel in conjunction with an electric motor, with an electric motor. Slight modification to the basic design provides immediate adaptability.

The computer control system provides exact ratio and speed changes to match the storage flywheel speed to the vehicle driveshaft speed. Power may be taken from the flywheel to propel the vehicle or it may be restored to the flywheel through braking. The flywheel may also be charged by the electric motor.

Study results indicate an overall operating efficiency of the regenerative CVT as 91.5% for the mean power condition, 16KW (22 HP) and 3,000 Rpm output. Calculated efficiency ranged from 92.1% at 15KW (20 HP), 14,000 Rpm in, 3,000 Rpm out, to 76.64% at wheel slip "Torque Limit" of 39.8KW (53.4 HP) with 28,000 Rpm input and 850 Rpm output.

The low weight and cost of a computer controlled traction CVT, coupled with its high efficiency, make it a viable transmission system for an electric vehicle. Those elements which represent relatively high risk areas have been addressed in detail. Any questions or potential shortcomings of the design capability at this point would be addressed during test and demonstration.

It is recommended that a follow-on program to conduct a detail design, fabrication and test program be conducted on the basic regenerative CVT or hybrid multispeed shown herein. Integration of the CVT with the computer control system into the electric vehicle would compliment the optimum propulsion system for the E.V.

List of References

1. Tevaarwerk, Joseph L., Traction Drive Performance Prediction for the Johnson and Tevaarwerk Traction Model. NASA Technical Paper 1430, October 1979.
2. Dudley, D.W. et al; Gear Handbook, McGraw Hill, First Edition, 1962.
3. Rohn, D.A., Loewenthal, S.H., Coy, J.J., Simplified Fatigue Life Analysis for Traction Drive Contacts. ASME Trans. Journal of Mechanical Design. Vol. 103, Apr. 1981, pp. 430-439.
4. Modern Methods of Gear Manufacture, National Broach and Machine Division/Lear Seigler Inc., Copyright 1972.
5. Bamberger, E.N. et al.; Life Adjustment Factors for Ball and Roller Bearings. ASME Design Guide. Copyright ASME 1971.
6. Jones, A.B., Analysis of Stresses and Deflections, New Departure, Division of GM Copyright 1946.
7. Daniels, B.K., Non-Newtonian Thermo-Viscoelastic EHD Traction from Combined Slip and Spin. Preprint No. 78-LC-2A-2 ASLE Preprint.
8. Daniels, B.K., Traction Contact Optimization. Preprint No. 79-LC-1A-1 ASLE Preprint.

APPENDIX LISTING

<u>Appendices</u>	<u>Page</u>
A. Structural Alternatives.	72
B. Multispeed Impact on Design & Performance. . .	79
C. Control System Detail.	84
D. Gear Windage Power Loss.	112
E. Bearing Lubrication Factor	113
F. Transmission Ratio Analysis.	114
G. Input Planetary Gear Data.	115
H. Input Planetary Sun Loss Factor.	116
I. Input Planetary Ring Loss Factor	117
J. Input Planetary Assembly Power Derivation. . .	118
K. Output Planetary Gear Data	119
L. Output Planet Speed Derivation	120
M. Output Planetary Sun-Planet Power Derivation	121
N. Output Planetary Ring-Planet Power Loss Factor.	122
O. Output Planetary Assembly Power Derivation	123
P. Output planet Power Derivation	124
Q. Spiral Bevel Gear Data	126
R. Spiral Bevel Gear Power Loss Factor.	127
S. Helical Idler Gear Data.	128
T. Helical Idler Gear Power Loss Factor	129
U. Cone Bending Stress.	130
V. Cone Horse Power Derivation.	131

APPENDIX LISTING
(Continued)

<u>Appendices</u>	<u>Page</u>
W. Traction Cone Life.	132
X. Traction Roller Life.	133
Y. Traction Composite Life	134
Z. Cone Torque	135
AA. Single Cone Horsepower.	137
BB. Total Cone Power (4 Cones).	139
CC. Cone Normal Load.	141
DD. Cone Bearing Loss (4 Cones)	143
EE. Spin Velocity Derivation.	145
FF. J_6 , Dimensionless Spin Torque Factor.	146
GG. Traction Load Determination	147
HH. Traction Power Loss (4 Contact)	149
II. Contact Ellipse Dimensions.	151
JJ. "g"	153
KK. Elastohydrodynamic Film Thickness at the Traction Contact	155
LL. Traction Contact Stress	157
MM. Traction Loss Calculation	159
NN. J_7/J_4 , Loss Factor.	162
OO. J_1 , Dimensionless Slip Factor	163
PP. J_3 , Dimensionless Spin Factor	164
QQ. $O^3/(Wn)^{1/3}$	166
RR. RPM_f /Flywheel RPM_n	168
SS. Bearing and Gearing Computer Data	169
TT. Symbols	188

APPENDIX A

STRUCTURAL ALTERNATIVES

Based on the detailed analysis of the current design the following considerations are made as means to improve design if required to resolve cited prospective problem areas.

1. Weight may be decreased and cost reduced by converting to a three cone system. An approximate 4% increase in cone radius provides the added power capacity for the regenerative design and no change is required for 3 cones in a multispeed arrangement. The restraints being compressive stress and cone bearing performance.

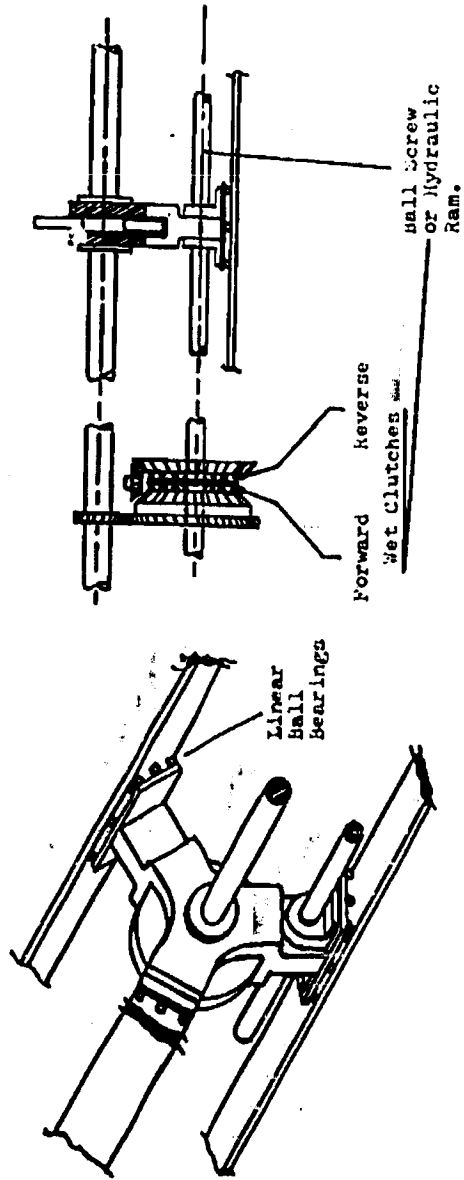
2. Change the shifting mechanism to a ball screw powered by a reversible-modulating wet clutch, driven by the input roller shaft. Or use a hydraulic cylinder to provide a less strenuous, rapid shift capability, and to eliminate bending loads on a screw. Strengthen the roller carrier by using a lightweight webbed assembly to provide continuous, uniform thrust on the roller carrier bearings, or include two or more screws.

"Gibs and ways" may be substituted for the linear ball bearings at the pads. Figure 25, page 73.

3. Convert the piston loading and cone mounting to a configuration as depicted in Figure 26, page 74. The self-aligning Spherical Liners insure proper bearing normal forces under even slight cone deflection or bending. The bearing liner receptacles being fabricated into the case for rigidity, (in lieu of one end being subject to deflection of the piston in the cylinder and cone loads inducing side forces on the control piston).

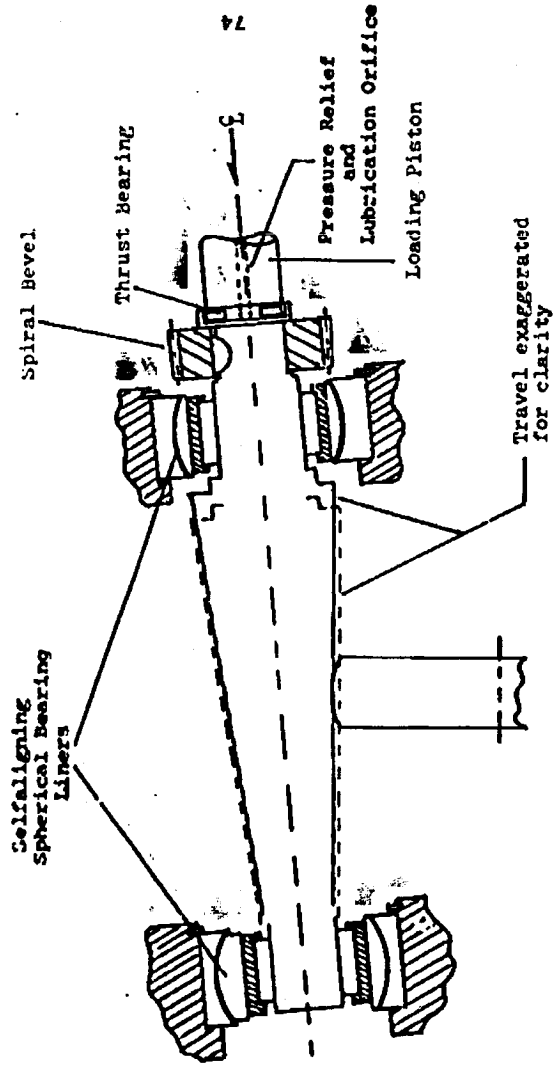
The gear end spherical liners were selected slightly larger in diameter to permit the cone to pass through the liner receptacle on assembly. The cone is merely passed through the hole and the lower journal slid into its bearing. The liner and gear end bearing properly centering the cone. The cone is free to move axially in its bearings and follows its center line angle toward the transmission center line until it contacts the roller.

The cone will contact the roller at a specific cone diameter depending on roller location on assembly.



Alternate Roller Carrier
And Shifting Mechanism(s)

Figure 25 .



Pictorial of End Loaded Cone Mount

Figure 26.

The spiral bevel gear shoulder should be accurately located a given distance from the large cone shoulder or a "finish to fit" sleeve used to space the gear properly along a keyed output shaft for correct gear mesh at cone contact with the roller.

The technique provides simpler assembly with assured alignment and greater all around rigidity.

In addition the spiral bevel angle can be designed to provide thrust in the contact loading direction as a function of traction force (torque). One of the major complications to the optimized control system was the external load induced slip changes and response required to accommodate shock loads. Spiral bevel gear thrust with torque, insures that a rapid rise in external load, is countered with immediate rise in contact normal force. The load transient cannot induce slip without increased torque automatically providing increased normal load because of the traction force to slip relationship on the rising slope of the curve.

The spiral bevel angle should be selected carefully so as to place its response just slightly less than the corresponding A TCP/A CS slope selected for computer operations. (A slight "inadequacy" to maintain traction for the traction coefficient of the best fluid considered for use). Regular oil would then rely more heavily upon the computer to maintain proper traction.

The computer burden would be acutely reduced and its ability to respond greatly enhanced.

One added notation (and benefit) is the angle of the pressure piston. It is not perpendicular to the normal force but has a mechanical advantage of $1/\tan\theta$. For the current cone design $1/\tan\theta = (\theta=9.24^\circ) = 6.147/1$. And the 5.5° cone has a 10.4/1 advantage. The required control pressure is reduced commensurately, bringing pressures into the range of the lubrication system. This eliminates the requirement for a high pressure system. Also the piston is free floating (restrained from rotating) and suffers no effects from cone forces due to load. Only minor travel is required for loading and unloading which is accommodated within normal gear backlash at the spiral bevel. A piston stop should limit the relaxation travel to restrain gear backlash to its maximum allowable value during initial startups, even though there is a spring in the cylinder to maintain minimum pressure.

Slip in the junction insures proper load sharing between the cones.

A small orifice through the piston injects lubrication to the lightly loaded thrust bearing separating the cone and piston.

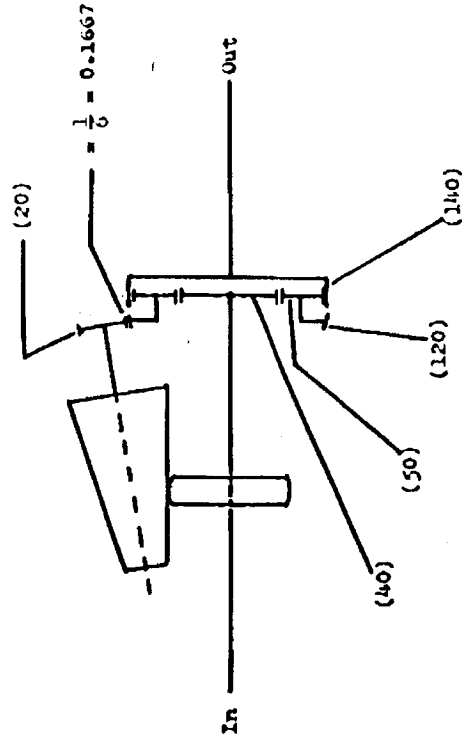
A spring in the piston cylinder provides a minimum load to preclude bearing skidding under light loads and insures initial traction hence spiral gear reaction for baseline loading with limited response then needed from the computer.

4. Change power flow to provide conventional output shaft rotation using the same cone design and the same output speeds. (Figure 27, page 77). Stresses are the same as before because ratio expansion is the same. It requires a slightly larger planetary. Ring 140 teeth, sun 40 and planets 50 teeth, in comparison to the original of 100, 40 and 30 teeth respectively.

The increased size, however, is offset by the elimination of the spiral bevel-helical idler gears. The new spiral bevel junction is larger in pitch diameter (20/120) and should prove more efficient. However, just removing the idler gears and bearings saves 1-3% over the operating range.

5. The predominant loss is (at the highest reduction ratio) in the duplex cone bearings. Power loss curves closely resemble the bearing radial load curve. Figure 28, page 78 shows load distribution to the cone bearings, for the regenerative CVT. They share average loads equally but, 91% of the lightest load being carried by the piston bearing ($m = 1.27 \times .91 = 1.15$), and the duplex bearing must carry 85% of the highest loads, ($m = 4.14 \times .85 = 3.6$). The duplex bearings then have a peak service factor 3.13 times as large as the piston bearings, ($\div 2 = 1.565$). Cone bearing radial load distribution is enhanced by widening the support bearing stance. This becomes readily acceptable in the multispeed configuration where internal horsepower is reduced to a fraction of regenerative CVT horsepower over the operating range. This reduces cone bearing loss sensitivity to roller axial location and maintains a more stable loss/HP in the bearing area.

Forward Speed Regenerative CVT



() Number of Teeth

Kinematic Diagram
(Less Input Reduction)

Figure 27.

- 14,000 RPM In
- × 21,000 RPM In
- ▲ 28,000 RPM In

Cone Bearing Radial Load Distribution Over the Operating Range at 75KW (100 HP) Output.

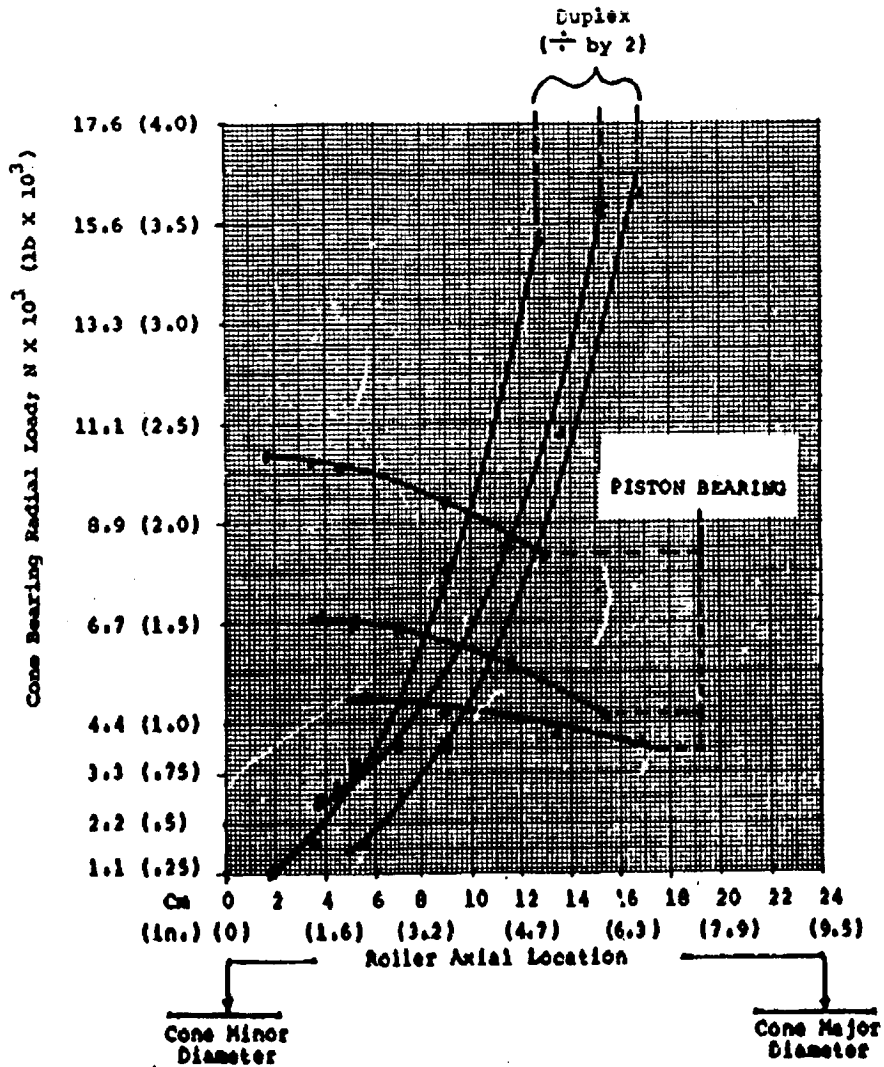


Figure 28:

APPENDIX B

MULTISPEEDING IMPACT ON DESIGN AND PERFORMANCE

Multispeeding step gear transmissions are common in the industry but multispeeding in conjunction with a limited range CVT is of current consideration. First, one primary feature of a CVT, the simplicity, may be lost by multispeeding. Second, the drivability must be carefully considered. Other considerations are cost, size, weight, control, efficiency and service life.

Size and weight appear to be reasonable with the overall design envelope being conducive to retrofit if desired. Cost, control, drivability and survivability all seem reasonable if the method of multispeeding is carefully considered. The efficiency and survivability of the traction components is greatly improved by multispeeding.

Control and drivability are best achieved by clutching the existing planetary to redirect powerflow to change range. Clutching the existing planetary also minimizes the number of parts added to the system, which is helpful from the size, weight, cost vantage point.

The addition of clutcher should not be detrimental to survivability since clutching is designed to occur at points on the cone-roller junction wherein there is minimum or no speed differential at closing.

Figure 29, page 81, reflects the desired principle of the clutched planetary, power flow change, for achieving range changes. Ultimate efficiency is obtained by providing two direct cone drive ranges wherein power regeneration is avoided and in between these two ranges providing a regenerative power flow through the planetary to reverse the cone function so that a range change may be made without having to relocate the roller as part of the shift. While this has been successfully done on paper it does require a complex clutching arrangement and another approach is indicated where acceptable to the specific application. The clutching complexity is not intolerable and it does provide very low stress, light weight design of the traction components and operate continually at high efficiency.

A simpler approach, shown in Figure 31, page 83, is to use a lockable torque converter to provide neutral and high initial reduction ratios, for range 1. The roller is located at the minor diameter of the cone and remains there until some minimum design speed is achieved. The torque converter provides a smooth increase in speed to the point that the CVT may come into use. This provides the same minimal stress designs as before but with only about half as many clutches and components.

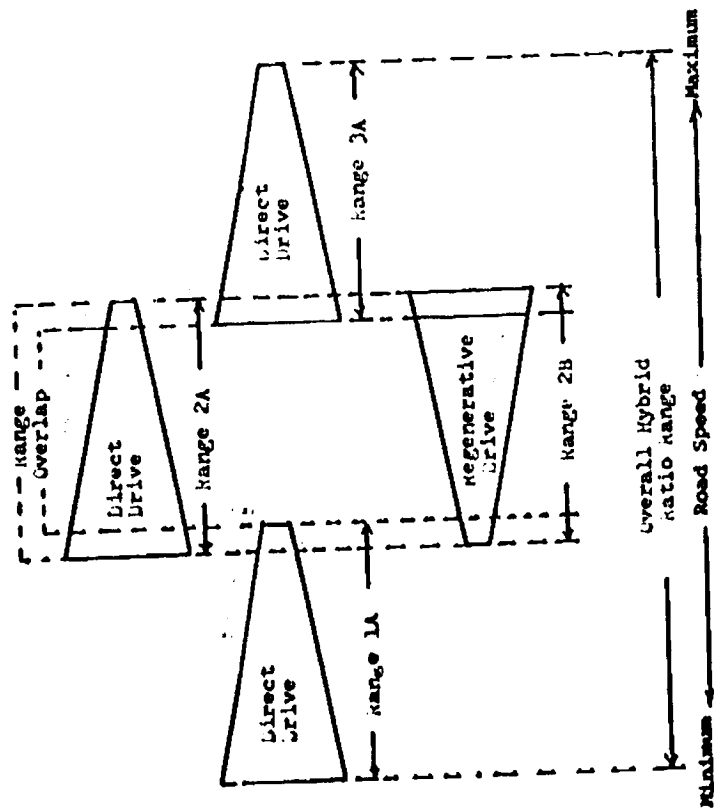
Range 1 is with clutches "b" and "c" engaged and the torque converter in service. When the minimum speed (with some range overlap) is achieved, the torque converter begins to lock up. During this transition the roller only moves to maintain a surge free shift, by compensating the traction ratio downward to offset for the elimination of slip within the torque converter. This is a relatively minor roller motion and while longer than other shifts in the multispeed design, it is no longer than the shift of a conventional automatic transmission; plus does not induce the surge or shock of a conventional shift incurred by the step change between ranges.

The power flow in range 2 is through the input spiral bevel gear driving the cones, through the traction junction to the roller. With clutches "b" and "c" engaged and the torque converter locked, the output (sun gear) is forced to co-rotate with the roller and no relative gear motion is involved. As the roller is moved toward the major cone diameter the roller speed is increased and hence the output speed increases.

When the roller approaches the major cone diameter a point is reached where the roller Rpm exactly matches the input spiral bevel gear and clutch "a" may be closed without a closing speed differential. Clutch "c" is opened and power flow is now split with part flowing from the input spiral bevel gear driving the cones and part through clutch "a" driving the planetary carrier. The part flowing through the cones drives the roller which now only drives the planetary ring gear. As the roller is relocated toward the minor cone diameter the ring gear is slowed and it may be seen that power flowing through the planetary carrier induces a step up speed to the output sun gear. The split power mode provides range 3.

A range 4 may be used in some applications; which is direct motor drive accomplished by positioning the roller so that the input spiral bevel speed matches the roller speed, then engaging all clutches and locking the torque converter. By leaving the roller in this position the output speed is a direct function of motor speed and no traction contact losses or gear losses are generated; this could provide a useful openroad range.

To overcome the inherent thrust developed on the cones by the cone angle, in combination with torque and pressure, and to provide an excess of mechanical spiral bevel gear thrust loading with torque at the cones, the spiral angle would run from 15° to 25° as a function of other design variables and the fluid used. The computer then "unloads" the traction contact to optimize the power capacity and efficiency. Piston control pressures required in the structure are reduced to normal lubrication oil pressures thereby eliminating the high pressure oil system and further provides a failsafe control since the transmission will work without the benefit of optimization through unloading pressure.



Multispeed Function Diagram

Figure 29:

RPM HP
Flywheel/Power
Conditions

- A - 14,000/10
- B - 21,000/40
- C - 28,000/100*

▲ Regenerative CVT as Studied

● Typical Multispeed Design (See Fig. 31, pg 83)

Volumetric Efficiency
Over the Operating Spectrum
of 7.5 Kw(10 HP) to 75 Kw(100 HP
or wheelslip Limit)

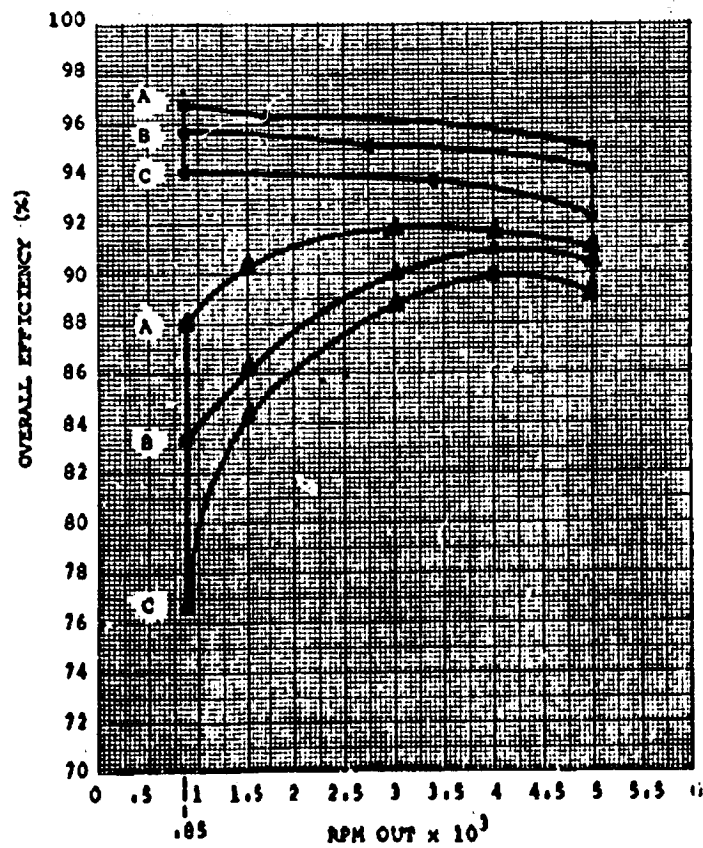
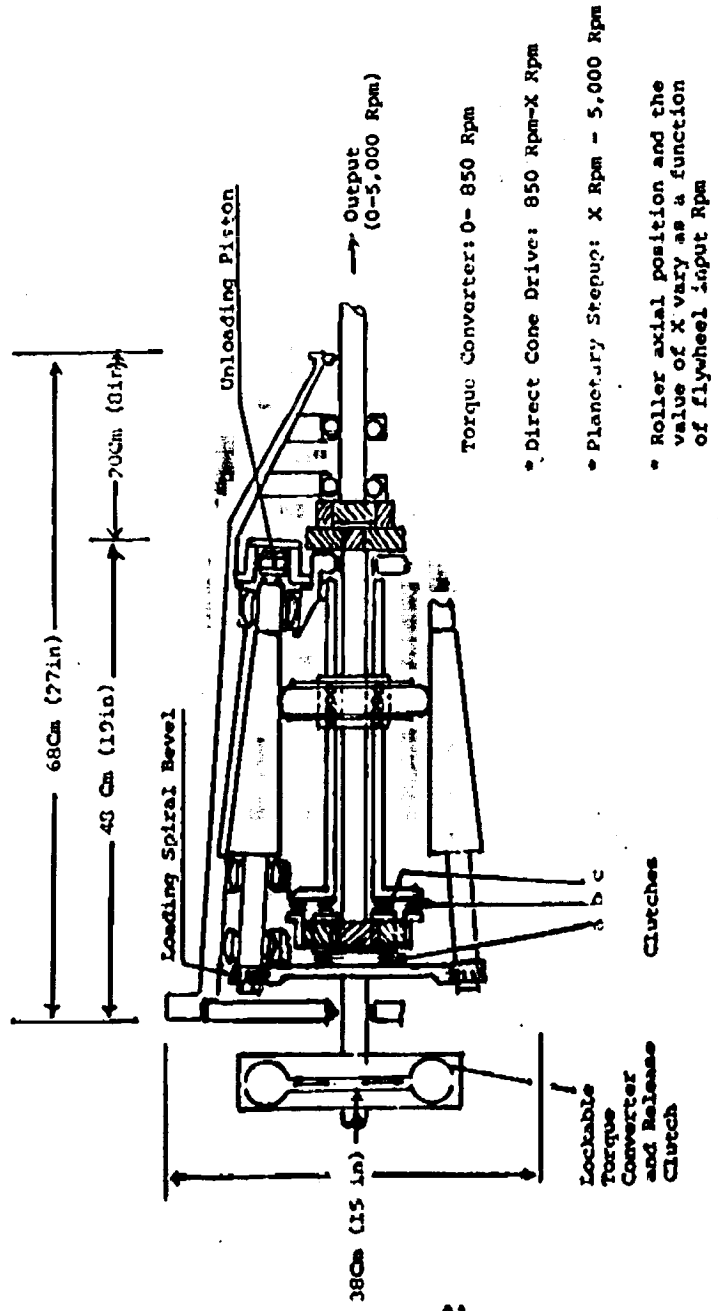


Figure 101



- Torque Converter: 0- 850 Rpm
- Direct Cone Drive: 850 Rpm-X Rpm
- Planetary Stepup: X Rpm - 5,000 Rpm
- Roller axial position and the value of X vary as a function of flywheel input Rpm

Figure: 31 Multispeed/CVT Functional Layout

APPENDIX C

CONTROL SYSTEM DETAIL

Referring to the analog flow diagram Figure 32, page 85 basic automatic slip control is achieved as herein described.

TSI; Traction Speed In (Roller) and Traction Speed Out (Cone); TSO, are either in the form of a voltage proportional to Speed (if permanent magnet generators are used) or pulses from an encoder are converted by a frequency to voltage converter (f/v).

At this point either TSI or TSO is applied to a high quality operational amplifier (OP amp) such as MC1741CL with the other signal being applied to a transconductance quadrant multiplier, for example, a MC1495L. The output of the MC1741CL is also applied to the MC1495L. The response of this loop is to multiply TSO output by TSI and this product is applied to the MC1741CL terminal as negative feedback. In this fashion the MC1495L multiplier in combination with the MC1741CL forms a divider with a net resulting output of

$$V_y = \frac{-10V_z}{V_x} = \text{MSR (Measured Speed Ratio)}.$$

MSR and TSR are then applied to the inputs of another divider network with the resulting output being MSR/TSR or vice versa. Either arrangement produces a final output that represents % speed.

For example if -10V out equals 100% (no-slip), then 95% would be -9.5V out. If the reciprocal mathematics were used, 95% speed would produce an output of -10.5V. In each case 5% slip produces 0.5V change in the processor output.

It may be seen that passing % speed into an "offset null" (OSN) shifting amplifier and adjusting 10V input to equal 0V out, the 0.5V change with 5% slip will produce +/- 0.5V output. (This step is not necessary as will be shown.) However to continue the slip control theme, traction physics is indifferent to slip +/- condition. Slip +/- should not be confused with +/- slip used previously. +/- slip denotes the quantity of slip as insufficient or excessive. Slip +/- is a function of the roller having a higher or lower peripheral velocity than the cone (leading or lagging). Such transitions can occur when the cone-roller junction goes from a retarding force to a driving force or during acceleration to braking transitions.

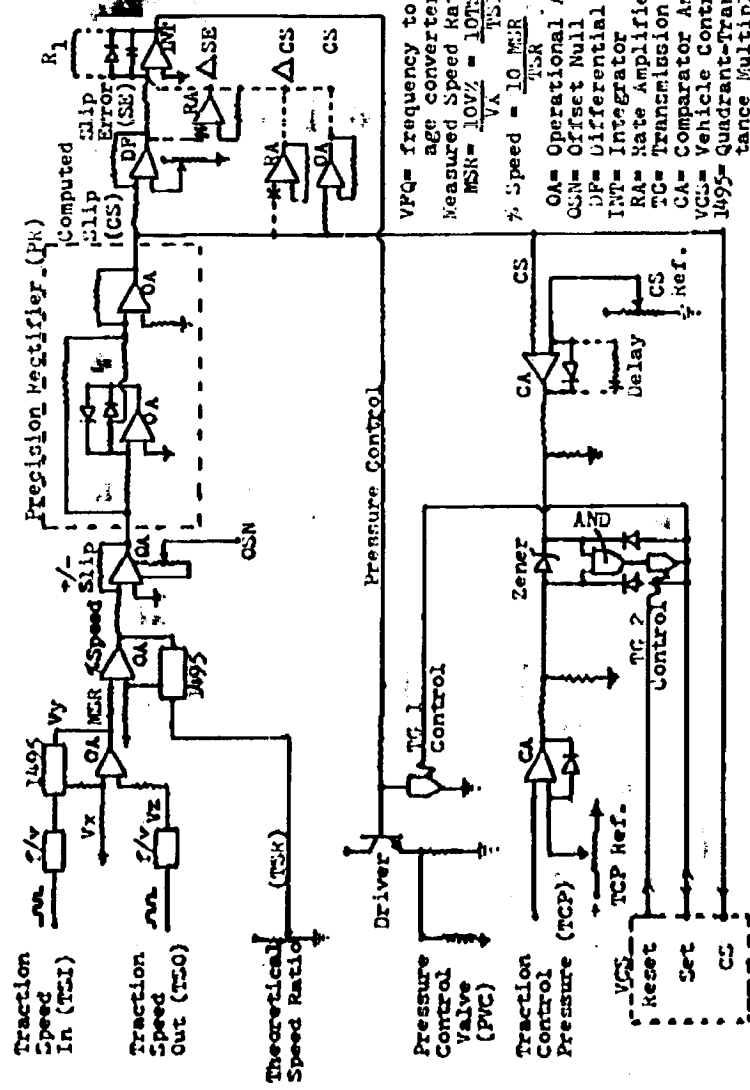


Figure 32. Basic Slip Control Schematic

Since traction is a function of +/- slip and is indifferent to whether the slip is in relation to the roller leading or lagging the cone (slip +/-). The (OSN) slip amplifier output is applied to a precision rectifier (PR) constructed of two Operational Amplifiers (OA). This insures detection and linear amplification of very small signals. (Caution: simple diode rectifiers cannot be used without very high gain of the slip signal because the diode PN junction has a low voltage breakover region where current flow is a non-linear function to voltage.) The P.R. arrangement is very important since our system is analyzing low slip values, near zero voltage output. The alternative of making 1% equal 2V means high gain and is prone to produce oscillation, drift and instabilities that are generally to be avoided. And even at 1% = 2V, the PN junction of some diodes are very non-linear from 0-0.4V which is 0.2% slip equivalent range that would become non-linear.

The output from the P.R. is computed slip (CS) and is applied to differential amplifier (DF). The other DF input is a slip reference voltage (RS). It doesn't matter if the - (inverting) or + (non-inverting) terminals are used. Whichever signal is applied to the - terminal is subtracted from the + signal and the output is proportional to the difference in the two respective inputs. The choice of + or - inputs for a particular signal must agree with final drive supply voltage and the proper response on demand.

The output swings +/- in proportion to the difference between CS and RS depending on which is larger and which terminals have been selected.

The DF output is slip error (SE) and is applied to an integrator, which is an OA with capacitive feedback coupling. The output goes up with even the slightest input current. The output rise is coupled to the - terminal and tries to suppress the rising output, but as the capacitor charges, the negative feedback current diminishes. With less feedback the output continues to rise. When the capacitor receives a full charge the output will be at maximum voltage. In this manner even 0.1% error continues to demand more and more corrective action until error is zero.

The diode is used to preclude the integrator from saturating in the opposite voltage. If slip were less than reference the integrator unwinds from its saturated pressure demand condition and would begin returning to zero. If the diode is not used the amplifier would go past zero and saturate at - voltage supply instead of plus volts supply. With a single ended +12v supply to the driver transistor the only ill effect would be time loss in response to error requiring renewed pressure demand.

The output from the integrator drives a power transistor in the emitter-follower mode to operate the pressure control valve (PVC) which ultimately causes a pressure change, and slip correction.

The capacitive effects of the integrator make its response slower than the detection and computation of error. R_1 added to the feedback loop of the integrator provides a more practical integrator which is much more stable. It provides "proportional band" control where demand for pressure is in response to error magnitude, supplemented by increased demand as long as error exists.

Examples of other control modifier signals (optional) are shown attached by broken lines.

The - terminal of OA's are electronically held to ground potential (not grounded but held to zero volts) by internal circuit. The OA functions are based on currents flowing in the system to hold the - terminal at zero. This is a very important feature in that several inputs may be tied to the - terminal simultaneously by input resistors. With the common side (- terminal) at ground potential each input remains effectively isolated. Their input currents produce a collective output or forms a summing function: $(A + B)$.

The rate amplifier(s), (RA), with capacitive inputs contribute demand proportional to rate of change (\dot{a}). Two are shown: \dot{a} SE or Rate of Slip Error change and \dot{a} CS, Rate of Computed Slip change. These subcircuits contribute stability to the overall control by altering the demand response under certain conditions. As the rate of error change gets larger an even greater correction demand is made to get the situation under control.

Another modifier shown is CS, which simply provides some baseline pressure demand proportional to slip.

Obviously the combination of modifiers is virtually unlimited. For example, the peak traction point changes with temperature (oil viscosity) such that a temperature modifier would appear advisable. Traction, hence optimum slip varies with peripheral velocity (film thickness) of the components and a speed modifier should be added using TSI or TSO signals. The traction contact patch geometry changes over the ratio range settings hence a TSM modifier may be added. Even pressure (normal load) changes the contact patch and optimum slip and a Traction Control Pressure (ICP) modifier could be included.

Many of the traction variables will necessarily need to be determined empirically and the decision regarding control modifier circuits made as a function of cause-effect.

One other logic loop is shown which involves two comparator amplifiers (CA), and AND Gate, and Two Transmission Gates (TG). (TG's are electronic switches, controlled by the signal line shown on the side).

The CA's will saturate + anytime their + input exceeds the level set on the - input, and are clamped to zero anytime the + input is below the - input reference, by the negative feedback diodes.

One CA is monitoring slip and its reference would be set just above an empirically derived worst case (normal) operating condition. The resistor and capacitor shown in broken lines would provide an appropriate time delay, sensitive to the magnitude of the signals. A small transient would be given longer to be corrected than a large transient. If slip remains above normal limits this CA will go from zero to maximum voltage. Logically the output is viewed as a "1" or "0" in binary terms (on or off, respectively). The "1" or "0" output is applied to one input of the AND Gate.

The other CA operates in the same manner and is monitoring Traction Control Pressure (TCP). This is the actual pressure, not demand for pressure. Its reference is set just below the maximum control pressure available as dictated by the high pressure supply manifold adjustment.

The logic is that if slip is becoming excessive and maximum control capability is being approached, an unsafe operating condition is about to occur; a problem that must be corrected. The AND Gate will see both conditions and transmit a "1" output which opens transmission Gate 1 dropping pressure to zero and an auxiliary signal is sent to the Vehicle Control System (VCS) to shift the roller in a tracking mode to bring slip to zero and keep it there.

Diodes from the AND Gate output form a latch by supplying false "high slip" and "control capacity reached" inputs. The latch is reset by the Vehicle Control System opening TG 2 breaking the false signal supply.

A zener diode cross-couples the "high slip" CA output to the TCP limit input to the AND Gate. The purpose is that a faulty relief valve, scoured pump, faulty pressure control valve, plugged filter and many other problems could cause actual control pressure available to be less than normal, causing an inability to increase pressure on demand. In this case the high slip output would reach the zener breakover point and shut the system down by slipping.

An alternative to zener diode protection would be another pressure transducer on the high pressure supply manifold to vary the TCP reference but that adds cost and still would not protect against PCV failure or plugged filter problems.

Whereas the zener diode effectively determines the controls are not getting the job done and shuts the system down.

In this sense TCP need not be considered at all but its inclusion provides an early warning when the problem is vehicle overload or some problem other than hydraulic controls are creating the high slip condition.

Note that CS also is sent to the VCS system. This will be discussed in the VCS presentation.

Previously I mentioned that the OSN sequence was not necessary. This is because % speed is just as effective as % slip in control of the system. To eliminate that step the OSN becomes a DF with a % speed reference in lieu of a % slip reference. If % speed is correct (equal to reference) the output is automatically zero and if % speed is greater or smaller than the reference the output swings + or - accordingly. Through the PR an error signal is then applied directly to the integrator.

If we supply a 95% speed reference we are by negative logic demanding 5% slip. The system can not tell the difference in terms of error and ultimate control.

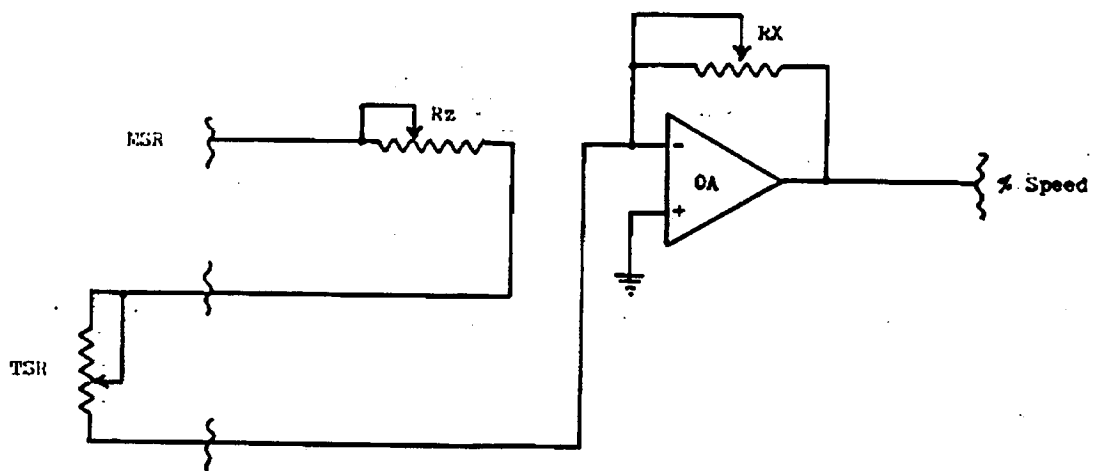
One last point regarding the basic presentation. Transconductance multiplier circuits are quite delicate to calibrate and used as feedback modifiers to achieve division, become 100-fold greater a problem at small signal levels. Cascading two such networks presents undesirable calibration problems. This has been overcome by using TSR directly as a gain control resistor around the % speed amplifier, in lieu of the second MC1495L.

As shown in Figure 33, page 90, the gain of the % speed amplifier is expressed as:

$$\text{Gain} = \frac{R_x}{\text{TSR} + R_z}$$

Since $\text{TSR} = \text{MSR}$ (without slip) R_x and R_z are adjusted to provide a constant % speed output for all TSR ratio settings if no slip is present.

For example, if the roller speed were 5,000 Rpm and the cone speed varies from 10,000 Rpm to 30,000 Rpm, then TSR



% Speed Optional
 Divider Structure
 (from Figure 32, page 85)

Figure 33

produces roller-cone ratios of 6/1 to 2/1; a cone speed variance of 3/1.

The conversion from true 6/2 ratio to 3/1 is accomplished by a scale adjustment at the CR, MSR divider and is not critical in that once set, a given ratio becomes 4v, 6v, 7.2v, or any relative value. The important point becomes matching the span of CR ratios (MSR without slip) output by calibration of TSR, Rx and Rz and not the absolute value or accuracy of ratio calculation.

If TSR travel with roller position varies in resistance from 10K ohms to 700Ω; for example, Rz and Rx values for proper performance may be found by:

$$1. \quad \frac{\text{TSR}}{10K\Omega} = 1/1$$

$$2. \quad 700\Omega = .7K = 3/1$$

$$\frac{Rx}{\Delta \text{TSR} + Rz} = 1$$

$$\frac{Rx}{\text{TSR}_2 + Rz} = 3$$

$$Rx_1 = 3 (.7K + Rz) = 2.1K + 3Rz$$

$$\text{and:} \quad \frac{Rx}{\text{TSR}_1 + Rz} = 1$$

$$Rx_2 = 10K + Rz$$

$$\text{Since:} \quad Rx_1 = Rx_2$$

$$\text{Therefore:} \quad 10K + Rz = 2.1K + 3Rz$$

$$10K = 2.1K = 3Rz - Rz$$

$$7.9K = 2Rz$$

$$\frac{7.9K}{2} = Rz$$

$$Rz = 3.95K$$

Hence: $R_x = 10K + R_z = 10K + 3.95K = 13.95K$
 and $R_x = 2.1K + 3R_z = 2.1K + 3(3.95K) = 2.1K + 11.85K = 13.95K$

Likewise:

$$\frac{13.95K}{10K + 3.95K} = 1$$

and

$$\frac{13.95K}{.7K + 3.95K} = \frac{13.95K}{4.65K} = 3$$

Results:

$$R_x = 13.95K$$

$$R_z = 3.95K$$

For different ratio ranges or different values of TSR resistance over the ratio range these values will vary. But as outlined here for a given "no-slip" MSR, the % speed amplifier output will always remain constant as the transmission is shifted. If MSR is offset by virtue of the presence of slip, % speed output will change. To achieve this the TSR leads are reversed so that when MSR = 3/1; TSR = 1/1 and when MSR = 1/1; TSR = 3/1, thereby providing the constant % speed output with no actual slip.

Optimized Traction Control (OTC):

In lieu of simple slip control which must be tuned to empirical parameters and for maximum effect or benefit must use additional sensing (such as temperature) another technique may be used.

That technique involves recognition that every traction fluid or oil has a peak traction point. This point (in terms of slip) varies from one fluid to another, temperature, peripheral velocity, one transmission design geometry to another, and even at different ratio settings within a given transmission design. See Figure 34, page 93.

The control system just discussed can be calibrated to a specific transmission design. But to function over a wide range of environmental changes required added components to modify its response to such variables and would not work properly if a different fluid were substituted.

○ Points of Equal Traction Force (Torque)

┘ = Optimum Slip Points

Effects of Temperature, Speed, Geometry and Alternate Fluids on the Traction Optimum Slip Value.

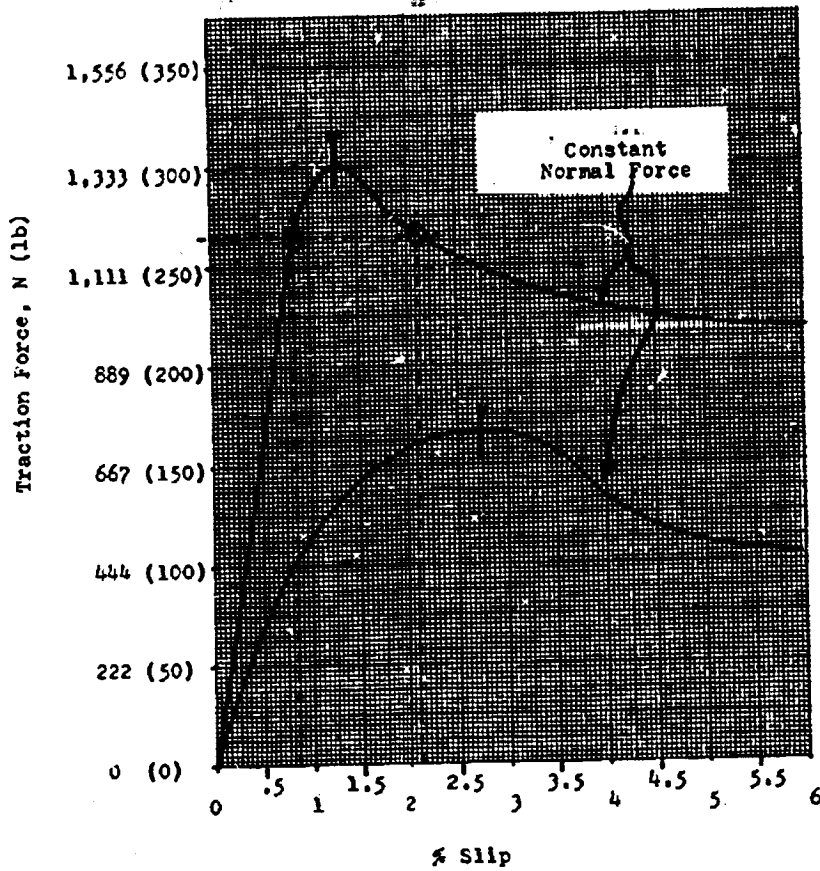


Figure 34: Typical Traction Curve (Constant Normal Force-Pressure).

The fact that every fluid has a peak, and variables only move the peak slip value, permits us to develop a controller that can be attached to any traction drive, using any fluid, in any workable environment, without the necessity of specific calibration, and will have much less sensitivity to calibration drift in the slip computer section.

It is shown in Figure 35 and 36, pages 95, and 96, respectively that regardless of the absolute slip magnitude for peak traction, the rate of slip change to rate of pressure change ($\Delta CS / \Delta TCP$) = . . .

THIS STATEMENT HOLDS TRUE FOR EVERY FLUID, EVERY KNOWN TRACTION DEVICE, AT ALL SPEEDS, TEMPERATURES OR RATIOS.

With that in mind we can start with CS and TCP signals of Figure 32, page 85, and develop the Optimized Traction Control (OTC) system, Figure 37, page 97.

CS and TCP signals are converted into +/- ACS and +/- ATCP. These rate signals in turn are then applied to a PR resulting in ΔCS and ΔTCP signals. The previously described divider network then has an output that is proportional to $\Delta TCP / \Delta CS$ which is a representation of slope. Slope identifies where on the traction curve the system is operating.

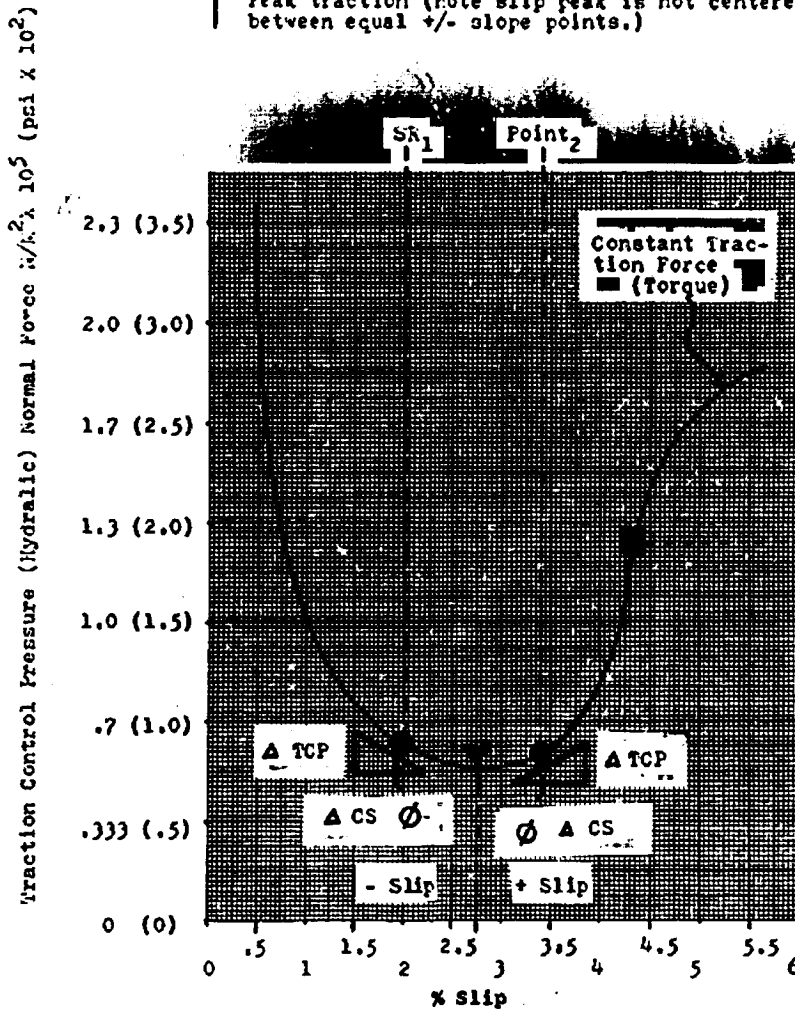
Unlike the basic slip system this system would prefer $\Delta TCP / \Delta CS$ instead of $\Delta CS / \Delta TCP$ because as shown a slope calculation of 0/X results in "0". If $\Delta CS / \Delta TCP$ were used then the peak is X/0 = - and saturation of computer circuits would result in data loss near the peak.

The operating slope (OS) calculation and the desired slope reference (selected operating point at or near the peak) are applied to a DF. The DF output is +/- slope error (SE). SE is applied to the - terminal of an integrator such that - SE produces a + voltage rise out of the integrator. Referring to Figure 38, page 98, it may be seen that - SE means a slope value less than the reference (SR), hence closer to the peak than desirable. The + integrator response will produce a demand for increased pressure which will reduce slip, bringing the operating point back toward SR_1 .

Just as a typical traction curve reflects two equal torque (Traction Force) points for given values of slip and normal load, see Figure 34, page 93, equal slope values also exist (See SR_1 and point 2 of Figure 35, page 95). A shock load could transient the operating condition into the + slip regime. The problem is that reverse logic is produced by control systems for that slip condition. Such that at point 3, for example,

● Equal +/- Slope Points (Note slight offset in pressure values due to asymmetrical curvature.)

∩ Peak traction (note slip peak is not centered between equal +/- slope points.)



Typical Traction Curve Pressure VS % Slip

Figure 35,

(Invert for $\Delta TCP / \Delta CS, \omega = 0$)

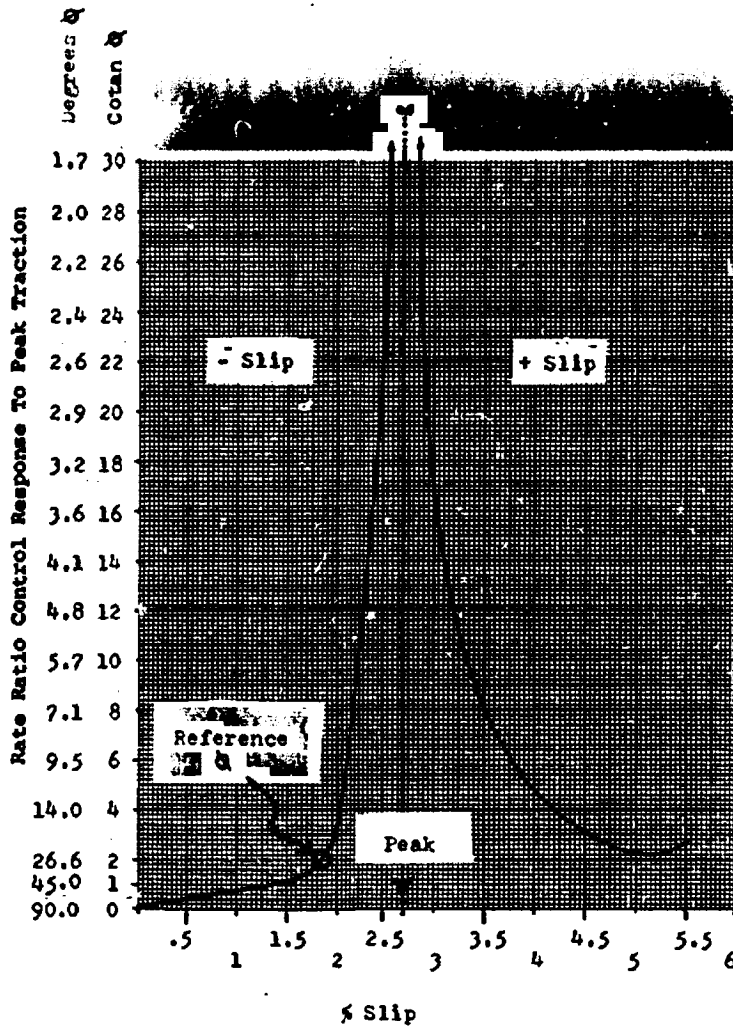


Figure 36 :

Typical Rate Control Curve
($\Delta CS / \Delta TCP$)

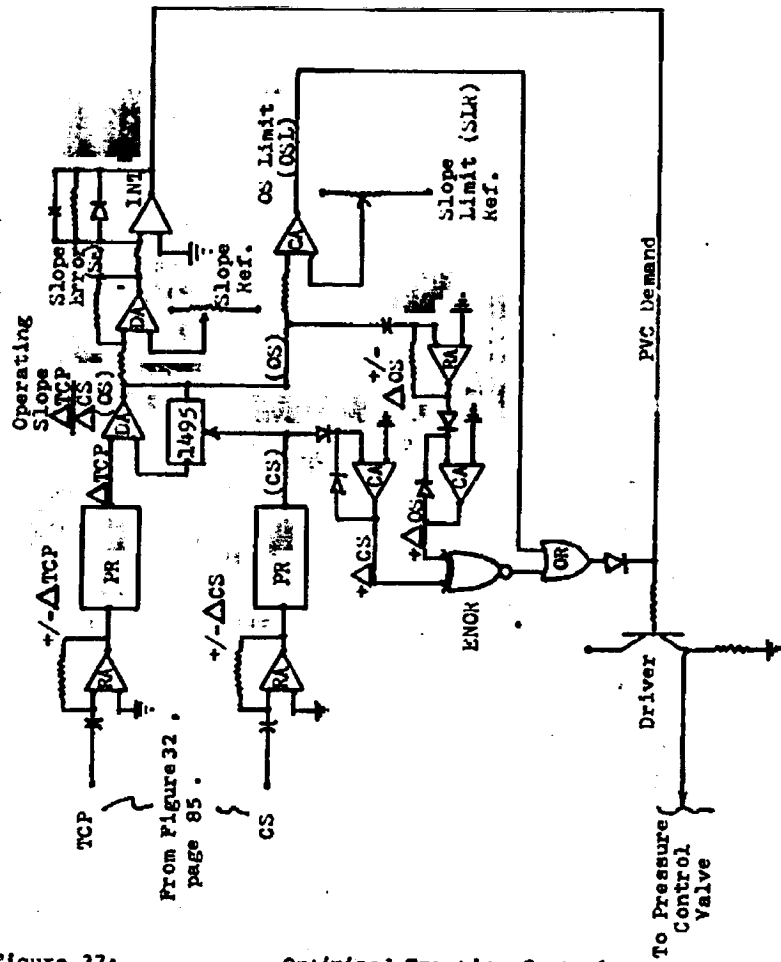
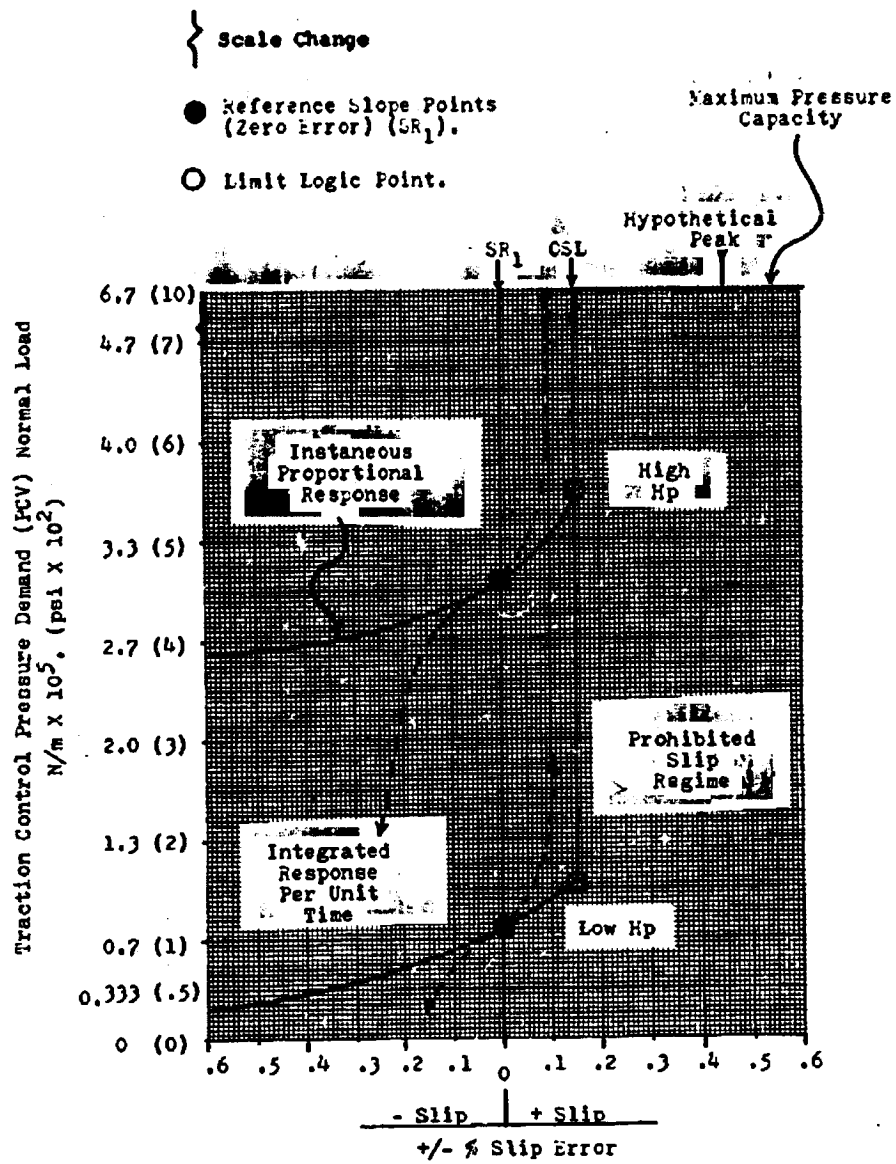


Figure 37:

Optimized Traction Control (OTC) Diagram



Computer Response To Error

Figure 38 :

the slope is too large and the normal response for correction in the - slip regime is to decrease pressure but in the + slip regime must increase pressure. That condition is disallowed by the system rather than developing reverse logic control.

This is accomplished first by driving a comparator with the OS signal. The Slope Limit Reference (SLR) will demand maximum correction anytime OS falls below the preset SLR. It will continue to demand maximum pressure for as long as OS calculations fall below the SLR settings.

With adequate hydromechanical response designed into the system initially the OS Limit (OSL) should preclude a + slip condition from occurring.

However, the closer to the peak we can operate the more dramatic the benefits of OTC. But consequently a greater hydromechanical response must be available to maintain control and the easier it becomes for shock loads to cause an uncontrollable transient into the + slip regime.

Therefore CS and OS signals are analyzed for their trends. It may be seen in Figure 35, page 95, that as the traction peak is approached in the - slip regime the slope values decrease with increased slip and slope values increase as slip decreases. But in the + slip regime slope values increase as slip increases and vice-versa. In the + slip regime "parity" occurs in the slope and slip trends.

This fact is used to identify and prohibit continued operation in the regime by constant demand for increased pressure.

This is accomplished by isolating +/-ACS from a comparator using a diode. Only +CS becomes applied to the CA input. The other input is grounded such that any +ACS caused maximum output. The feedback diode precludes spurious - saturation.

OS is applied to an RA to provide +/- Δ OS and an identical structure reduces the signal to an "0" or "1" (+ Δ OS) output.

OS and CS logic signals are applied to an "Exclusive NOR" (ENOR) Gate. The ENOR output is "0" for any conditions except two "0" inputs or two "1" inputs. Anytime CS and Δ OS are the same, both "0" or both "1", we are operating in the + slip regime and ENOR response is a "1" output.

The ENOR output is applied to an OR Gate in conjunction with the OSL logic output. Anytime a "1" appears out the OR Gate, maximum pressure is demanded by the PCV Driver.

The result is a control system that controls pressure to maintain the traction junction operating at slope calculations

around a reference value near peak traction. Once error in control exists beyond a preset CSL amount, full pressure is demanded until the return to the normal control range -- even if the peak is transient in the interim. This may be insured by using a "sample and hold" of the slip value at the time OSL indicates the transient may be imminent (not shown), as a reference.

Just as in the basic slip controller other modifier signals are readily available for OTC.

Since basic slip control can only do what we tell it to do, and cannot tell if that is right or wrong, we must test empirically the effects of temperature, speed, etc., and modify the control response to maintain maximum benefit. The OTC system just described will control the pressure to maintain optimum conditions even if regular oil is substituted for traction fluid. And automatically compensates for all variable effects without the necessity of measuring those factors or without knowing what effect such variables have, because OTC analysis is of the traction slope produced, after the influence of such variables.

Figure 38, page 98, is a typical control response to conditions in the junction. The area between the solid line and dashed line represents the effect of the integrator with time. The solid line therefore is an instantaneous response and if the error continues the demand for correction will correspondingly drive the PCV to full pressure or no pressure in an attempt to bring conditions exactly to the SR point.

The problem with the OTC system just described is that it only works with a fixed load condition where ΔCS is only in response to ΔTCP .

The automotive application presents varying external load conditions and slip would vary with that load, without a change in TCP. This would produce false $\Delta TCP / \Delta CS$ slope calculations and the system becomes lost.

Also the system would become lost under quiescent conditions of constant load where ΔTCP and ΔCS both equal zero. However, in this case the system produces its own change and will oscillate thereby producing its own ΔTCP which would cause a ΔCS response.

Many options exist to overcome these problems.

First, a torque sensing device could be installed to permit computation of the % of ACS due to load change and thereby leave the appropriate ACS for the $\Delta TCP / \Delta CS$ slope calculation. This adds cost and complexity.

A hybrid control philosophy can replace the need for torque sensing in light of the improved cone mounting using the spiral bevel to assist loading as a function of traction torque.

It can be seen that low slope values will result from operating too near the peak or from external load influences. But the correct response is increased pressure in both cases.

It can be seen that an external load increase causing slip to increase actually moves the operating point toward the peak and also produces the correct slope calculation change to produce a corrective response.

But a load decrease (which is in the safe direction) could falsely indicate near peak conditions and improper response (but safe) of increased pressure would result.

If a basic slip controller therefore were used as the primary control and slope calculations as a modifier are introduced, a system of pressure response to slip (load influence) around a selected slope point evolves.

In this technique slope error values would be averaged and applied to the slip circuit reference via a summing amplifier. An oscillator could be used to insure continuous Δ TCP by providing a fixed dither signal to the demand; although the use of the integrator in the system as well as dynamic loads may prove adequate on their own. See Figure 39, page 102.

In this manner a reasonable (safe) starting slip value may be established and the average slope error used to bring the reference into line with environmental conditions but under short term transient conditions, respond to Δ CS as load signals.

The net effect is a traction drive under torque feedback response with slip calculations used to fine tune control responses to operate at or near peak traction conditions. And slope logic as well as Δ CS and CS modifiers to preclude operation in + slip regime.

Unenhanced OTC control would necessitate a high degree of compliance to the dither signal as the slope values would need to be predominately based on controlled Δ TCP effects on Δ CS in time frames much faster than Δ CS produced by normal vehicle load changes.

This all becomes possible because for a given set of conditions there is a particular Δ CS in response to Δ TCP at specific operating slopes and lower frequency dither may now be applied and the baseline Δ TCP/ Δ CS filtered out. The remaining Δ TCP and Δ CS are vehicle load effects and slip

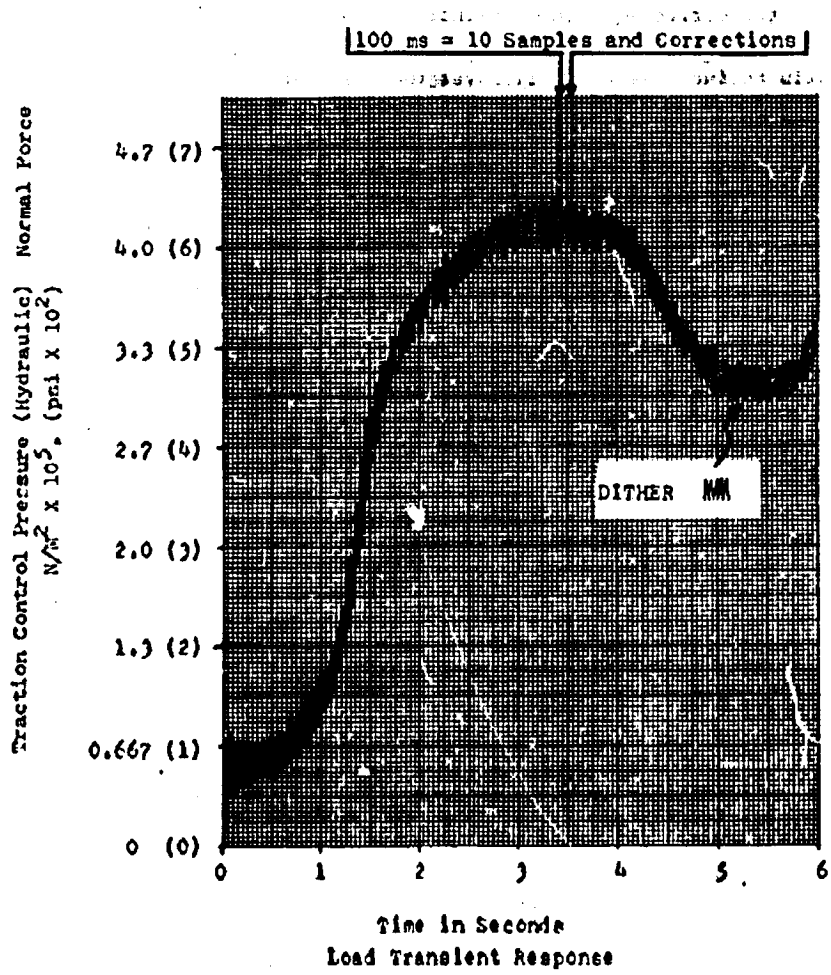


Figure 39:

control response induced. The specific relationship of a TCP to ACS need not be known as it will change as a function of environmental variables. But on the average that information filters into the basic slip control and updates the slip reference.

In terms of time, the system hydromechanical response from no pressure to maximum pressure is 50-100 milli-seconds.

The pressure available is calculated at twice that required to handle peak design horsepower. So from zero to full load control capability in 25-50 milli-seconds; usual vehicle load changes are much slower than that and even shock loads (transients) would range from 100-500 milli-seconds. Rubber tires, axles, drive shafts and the like, absorb most load spikes but if necessary a torsional coupling may be added to smooth out road shock permitting the computer adequate time to respond.

Optimum operating slip will only change over a period of 1-5 seconds with temperature, speeds or ratio setting and slope averaging would allow 0.5-1 second to make corrections to the slip reference.

These basic concepts were provided in analog form to better facilitate comprehension. Obviously such a system may be converted to digital and placed under the control of a microprocessor.

The analog system would suffer from calibration requirements, temperature drift, non-linearities and physical size. Its advantage is constant monitoring and a dedicated system performing control.

The microprocessor (MPU) (programmable) provides greater flexibility during development; smaller packaging and higher speed as well as is available to perform other tasks on a time sharing basis. It suffers from sensitivity to environmental electrical noise such as fans, turnlight flashers and spark plug firings. It can soon lose in terms of speed because of the program required to fulfill complex computations.

The best all around system would appear to be a hybrid between an MPU and analog conversions. By converting monitored data into analog form, then multiplex that data either directly or through a logarithmic converter, to an "analog to digital" converter, allows us to supply a high speed MPU with digital numbers that need only to be added or subtracted (4 computer cycles) to achieve addition, subtraction, multiplication, or division.

Without logarithmic data, multiplication and division time by the normal multiple precision addition or subtraction method will vary with the value of the number being processed and usually requires a few hundred cycles if numbers large enough to provide 0.1% accuracy or resolution are used, (i.e., 1,000 or greater is 10 bits minimum in binary).

An alternative is to supply a ROM (Read Only Memory) for logarithmic values over operating-ranges and let input data address its logarithmic equivalent for use by the MPU. This would basically double MPU cycles to 8 but eliminates multiplier and analog-logarithmic and analog ant' log conversions. This would be an overall preferred technique. It allows minimizing processing time without the bulk and complications of added external analog processing.

For example if the TSO and TSI disc has 60 aperatures and TSO is spinning at 10,000 Rpm, each aperature would occupy 0.0001 of a second or 100 μ seconds (100 millionths at a second). Using an internal clock frequency of 10 MHz (10 million cycles per second) 1,000 clock pulses would be counted per aperature. TSI at 5,000 Rpm means 2,000 counts would accumulate. If speed were important for display, the MPU would divide 10,000,000 by the counts accumulated.

$$10,000,000/1,000 = 10,000 \text{ Rpm}$$

$$10,000,000/2,000 = 5,000 \text{ Rpm}$$

However, that step is not necessary to control, as previously shown, since the system is looking at ratios. Therefore the counts would address a log equivalent memory and the respective logs would be subtracted. The \log_{10} of 1,000 = 3.000 the \log_{10} of 2,000 = 3.3010.

3.3010 - 3.000 = 0.3010. The antilog of 0.3010 = 2.000 or is equivalent to 10,000/5,000 = 2.000. If the clock frequency is not exact such that 10,000 = 8,260 for example.

8,260 Rpm = 1,210.65 counts (1,210) and the \log_{10} 1,210 = 3.0828. 16,520 Rpm = 605. \log_{10} 605 = 2.7818.

3.0828 - 2.7818 = 0.3010 the antilog of which = 2.000. Drift becomes relatively unimportant.

TSR (as well as TCP) would provide a variable voltage to a voltage controlled oscillator (VCO). The VCO would be calibrated to produce a frequency of 2,000 Hz at the 2/1 roller-cone position. One VCO cycle would be timed. At 2,000 Hz the pulse width would cause 5,000 counts to accumulate. This would be

converted to \log_{10} of 5,000 = 3.6990 and would be subtracted from a memory fixed of 4,000. (\log_{10} of 10,000 counts)
 $4,000 - 3.6990 = 0.3010$.

The 2/1 roller-cone ratio computed above in \log_{10} form of 0.3010 is subtracted from TSR = 0.3010 and the results = 0.0000. The antilog of 0.000 = 1.000 or 1/1 = no slip!

Under the above assumptions it may be seen that if the roller speed was 5,000 Rpm but the cone speed of 10,000 Rpm was not present because of 5% slip + (a cone speed of 10,500 would exist) the cone count would equal 952.38 (952). The \log_{10} 952 = 2.9786.

$3.3010 - 2.9786 = 0.3224$ as the \log_{10} of roller-cone ratio. This ratio minus the predicted ratio by TSR of 0.3010 equals $0.3224 - 0.3010 = 0.0214$. The antilog of 0.0214 = 1.05 or 5% more speed than there should be.

This philosophy can be extended throughout the system and need not be duplicated in this presentation. Due to the control complexity and the amount of multiplication and division data, \log_{10} conversion before MPU processing is dictated. The appropriate Bytes of log ROM is preferred but may be achieved by other means.

A logarithmic amplified could convert analog inputs before the analog to digital conversion. In which case the frequency conversion would need to be made or preferably use small voltage generators. But since $\log_{10} 1.111 = 0.0457$, $\log_{10} 11.11 = 1.0457$, \log_{10} of 111.1 = 2.0457 and \log_{10} of 1,111 = 3.0457, a ranging unit can be used to assign the characteristic while digit decoding may be used to address the \log_{10} of four (1's). This cuts memory capacity requirements to 4.

To minimize mechanical fabrication requirements for extreme tolerance between open and closed duty cycle (See Figure 40, page 106, the MPU is edge triggered and begins counting the clock with positive or negative transition of the incoming signal. It continues to count until the next "like", rising or falling signal is received. It counts from leading edge to leading edge or trailing edge to trailing edge. This eliminates cutter size to disc circumference relationship problems otherwise required to keep the duty cycle balanced. In the preceding example only the aperatura was considered and that also eliminates duty cycle balance but if the MPU is to wait for an

Cutter diameter matched to disc diameter - symmetrical ON/OFF duty cycle.

time $A + B = C$

ON OFF ON

time $D + E = F$

ON OFF ON

$C = F$, Duty cycle error eliminated.

Standard cutter to desired disc diameter (duty cycle error exaggerated).

ON/OFF

time $D + E = F$

ON OFF ON

$C \neq F$, Duty cycle error exaggerated.

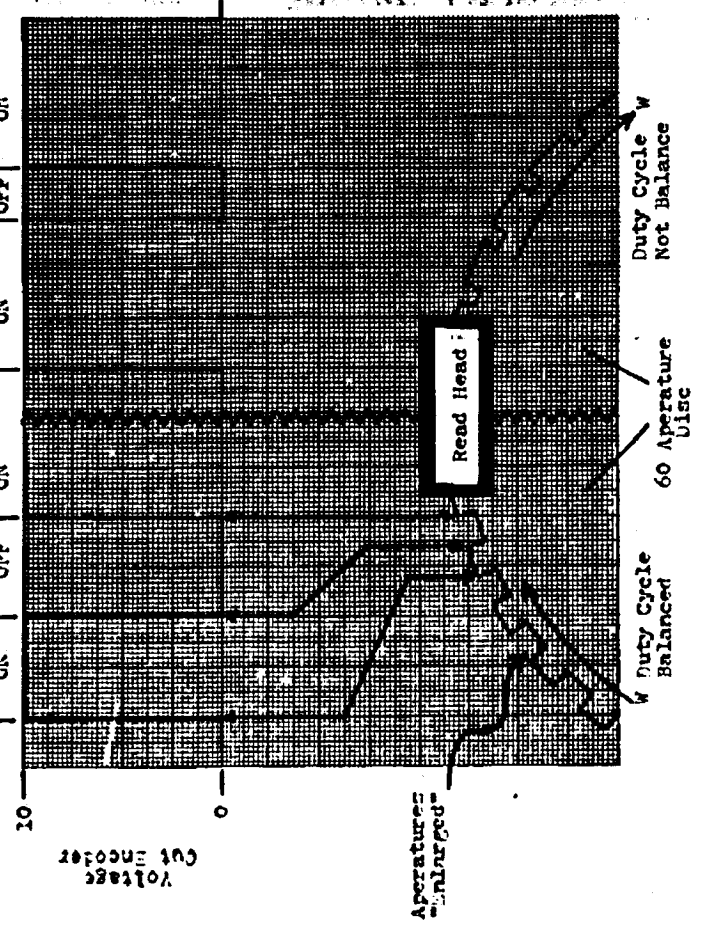


Figure 40: Duty Cycle Error and Correction

perature, it is preferable for it to count during that time since more counts improve resolution. Comparable counts are accomplished by going to 120 apertures providing twice the sampling rate.

The final output integration will be accomplished by repeated addition of error value into an output accumulator. This accumulation is continuously applied to a digital to analog converter to drive the PCV amplifier.

Rates are developed by operating sampling on fixed cycles so that time need not be computed but is inherent to the data collection $(\text{Cycle}_1 - \text{Cycle}_2) / \text{fixed sample time interval} =$

Δ counts.

With a fixed sample time Δ may be used as rate, disregarding the sampling time used.

Keeping computer time to a minimum permits time for more computations. Some useful computations as far as traction goes would be $\Delta \text{TCP} / \Delta \text{PCV}$. This is a measure of hydromechanical response not only inherent in any given design but is also sensitive to temperature and fluid used. Such that the computed pressure lag could be used in the program to vary the frequency of adding error into the output accumulator.

This causes the integrator to respond faster in cold weather (assuming oil viscosity change has caused an increase in hydromechanical response time).

Adding the slope over 10 cycles can reflect a change in terrain by successive excursions toward the peak. - Unlike slip error \pm which would average zero for any given amount of error ($\pm 1\%$ or $\pm 5\%$ around a set point), slope is $\tan \theta$ and the trigometric function means the average will shift dramatically as the oscillations vary from $\pm 1\%$ or $\pm 5\%$ around the set point. Such that transient conditions and responses become easily detected. That information can be used to either offset the slip reference downward or preferably to increase PCV (integrator) response. This increases the tautband of the control by changing the error addition frequency into the integrator.

It is recommended therefore that a small programmable MPU be used, with a 10 MHz internal clock. And a minimum of 4 edge triggered I/O ports for TCP, TSR, TSI and ISO signals. A 10 Bit wide O port to provide better than 0.1% pressure control resolution, and at least 1,000 memories for \log_{10} value storage; plus appropriate processing space.

Having developed the described control response in actual hardware a custom system can be developed on a single chip for mass production which uses ROM for the fixed program.

VCS (Vehicle Control System):

VCS units are already available commercially in terms of optimizing the performance of an electric motor or proper throttle setting for best BSFC of an IC engine. So only those aspects of VCS as applies in a unique way to the traction CVT and/or flywheel are discussed.

In the prior discussion it was noted that (computed slip) CS was made available to the VCS unit.

The purpose is several-fold.

1. Slip may be used to offset Transmission Speed Control (TSC), thereby reducing the rate of shift to preclude driver demand from placing uncontrollable slip conditions on the unit. This would not normally be a problem but it is possible that the driver could attach a trailer to the vehicle or in some other fashion induce abnormal vehicle loads into the system (such as attempting to push a second vehicle or operate with the brakes locked up). By interlocking the MPU demand for shift of the transmission, to slip in the traction junction, hundreds of potentially destructive possibilities are precluded. The transmission would only shift to the point that slip limits would allow. There it would stop trying and when maximum control pressure is reached an overload warning light would tell the driver his problem.

2. Also should any condition such as plugged filter or pump failure preclude continued control of pressure, the basic slip/OTC system would set the safety shutdown. The set signal would then instruct the MPU to operate TSC to maintain zero slip, or track output speed with no clamping pressure being applied.

Obviously ΔP monitoring should warn the driver well in advance that a filter problem is imminent but if that minor problem is not fixed we should still preclude the destruction of the transmission. Indeed if the problem is a slowly growing one, warnings and automatic steps could be taken to preclude the undesirable total shutdown on the open road. Such a possibility would be TSC feedback from filter ΔP . The vehicles performance would diminish demanding attention as well as providing a warning indication to the driver.

The TSC normally functions by the difference between vehicle speed out (VSO) and Vehicle Speed Demand (VSD). VSD is derived from the floor pedal and brake pedal pressure (BPD).

VSO may be developed by normal speed-o-meter means at the output shaft or it may be derived by the MPU.

The output speed of the planetary is a fixed relationship to the sun gear speed (TSI) and ring gear speed (TSO): Where:

WS = Sun Rpm = TSI
WR = Ring Rpm = TSO
WC = Carrier Rpm = Output = VSO
Sr = Sun radius
Rr = Ring radius
Cr = Carrier radius = center of planet gears to sun gear center.
K = Constant taking tire size, rear axle ratio, etc. into account for conversion into Mph

$$W_C = \frac{W_{SSr} - W_{RRr}}{2Cr}$$

Cone gear coupling ratio = (Cgr)

$$VSO = K \left(\frac{TSI(Sr) - TSO(Cgr)(Rr)}{2Cr} \right)$$

Since these signals are available the additional conventional speed-o-meter can be eliminated.

TSC is further modified to take into account the current operating conditions of the motor. In other words, a large differential between VSD and VSO would generally mean rapid shift of TSC to increase VSO, such that vehicle acceleration corresponds to driver demand. But TSC is offset if the engine is being overloaded (Rpm below optimum for demand) and a decision to downshift TSC and increase throttle could result. But the final vehicle response is still heavy acceleration for large demand differential to current speed.

If VSD-VSO is negative the results may be ignored and a coast down would occur. To best simulate today's driver feel the - result can cause a slow downshift of TSC or CREEP signal, duplicating normal vehicle coast down with the driver's foot removed from the pedal.

BPD becomes a modifier for Creep. As a larger BPD is detected creep is increased causing a more rapid downshift of TSC resulting in regenerative braking. BPD is set as "master" so that pressing both pedals produces braking.

The combination of regenerative braking with normal brakes provides a most suitable arrangement in that under gentle braking TSC is causing recovery of energy. But should more rapid braking be dictated and slip starts to override TSC then the increased pedal pressure (which is normal driver response even with power brakes) causes normal braking to become

predominate. This is less efficient because regenerative energy is being lost but getting stopped safely is more important than capturing energy at this point. This system not only provides smooth transition from TSC regenerative braking to normal braking but insures maximum regeneration will be utilized and even with transmission failure leaves the driver with ample normal brakes as a safety backup.

Having TSC shift speed tied to the magnitude of VSD-VSO makes the response duplicate conventional driving of torque demand with an accelerator pedal.

Cruise may be accomplished in a conventional manner by storing VSO, at the moment cruise is set, into the memory for reference in lieu of VSD. VSD can override VSO memory for temporary increases in speed, larger value as demand result, by OR logic.

TSC - (VSO Memory or VSD) - VSO.

Notice that a - TSC means road speed greater than desired. In the cruise mode TSC may respond to maintain constant road speed resulting in slight regenerative braking in hilly country, to be used to climb the next hill.

BPD will clear cruise as normal. I would add to the usual array of buttons an Increment (increase) and Decrement (decrease) memory button. This would provide finite trimming of cruise speed to suit speed limits, traffic or weather conditions.

Logic may be provided to preclude going into reverse with + VSO computed and vice-versa. A bottom limit to this interlock should be provided to permit rocking the vehicle as a means of removal from mud or snow, i.e., below 2-3 mph.

With the computer on board one added safety feature can be easily accomplished.

By monitoring VSO, and comparing it with a frame accelerometer, skidding may be precluded. The computer would know when tire traction was being lost and could override normal TSC or BPD signals. To take advantage of the possibility for antiskid circuitry the direct pressure link between the pedal (BPD) and the wheels would need to be broken so that a composite pressure signal from the pedal and the computer activates cylinder pressure.

This excluding any desired startup or shutdown sequences, added safety, or auxiliary indicator functions and flywheel monitoring and clutch control, would conclude a controls package for the CVT presented.

The flywheel may engage only during braking until an operating speed range is achieved, at which time it remains engaged. The motor controls in conjunction with TSC will maintain operating speed on the flywheel as well as control vehicle speed. A shutdown sequence by removing the key could cause an output clutch to disengage and engage the motor, causing it to brake the flywheel by generating into the batteries. (If the motor is designed to produce counter emf).

In the final analysis the control technology exists. The final design to be predicated by details of the application and desired features in performance, which must be weighed against size and cost of an MPU to achieve all the functions reliably in acceptable time frames.

APPENDIX D

GEAR WINDAGE POWER LOSS

$$P.L. = \left[\frac{L}{r} \right] (N^3) (r^5) (L^7) / 10^{17}$$

$\left[\frac{L}{r} \right] = 1.5$ FOR JET LUBRICATION NO ROTATING PARTS SUBMERGED.

BEVEL PINION:

$$P.L. = (1.5) (23479)^3 (1.54)^5 (.5)^7 / 10^{17}$$

$$P.L. = .0001 \text{ HP}$$

BEVEL GEAR:

$$P.L. = (1.5) (16552)^3 (2.1)^5 (.5)^7 / 10^{17}$$

$$P.L. = .00017 \text{ HP}$$

IDLER HELICAL:

$$P.L. = (1.5) (16552)^3 (1.54)^5 (.5)^7 / 10^{17}$$

$$P.L. = .00004 \text{ HP}$$

APPENDIX E

BEARING LUBRICATION FACTOR(REF. 5)

BEARING	$m(\mu \alpha)^{.7} (N)^{.7} (Po)^{-.09} \sqrt{F}$
ROLLER CONE SUPPORT	$(6.5)(10^4) (5.5)(10^{-8}) (1146)(.59)(2.14) > 3.0$
BALL, DUPLEX CONE SUPPORT	$(8)(10^4) (55)(10^{-8}) (1080)(.65)(30.9) > 3.0$

APPENDIX F

TRANSMISSION RATIO ANALYSIS

N_{Os} = OUTPUT SHAFT SPEED, SUN DRIVING = (RPM_s) (R_p)

$$R_p = \frac{N_s}{N_s + N_r} = \frac{40}{40 + 100} = .2857$$

RPM_s = SUN SPEED = Flywheel RPM_n/2.9166

$N_{Os} = .2857 \text{ RPM}_s$

N_{Or} = OUTPUT SHAFT SPEED, RING DRIVING = (RPM_r) (R_r)

$$R_r = \frac{N_r}{N_s + N_r} = \frac{100}{40 + 100} = .7143$$

$N_{Or} = .7143 \text{ RPM}_r$

$\text{RPM}_r = (\text{RPM}_s) \frac{\text{ROLLER DIA}}{\text{CONE DIA}}$ (BEVEL IDLER RATIO)
= (RPM_s) (R_c) (R_B)

N_o = OUTPUT SHAFT SPEED
 $= N_{Or} - N_{Os}$

$N_o = (.7143 R_c R_B - .2857) \text{ RPM}_s$

$$R_B = \frac{19}{27} \cdot \frac{21}{49} = .3016$$

$$N_o = (.2154 R_c - .2857) \text{ RPM}_s$$

<u>Flywheel RPM</u>	<u>RPM_s</u>	<u>R_c</u>	<u>RPM_{out}</u>
14,000	4800	4.65/.75	5038
21,000	7200	4.65/1.426	3000
28,000	9600	4.65/2.68	845

Table 10:

APPENDIX G

INPUT PLANETARY GEAR DATA

	<u>SUN</u>	<u>PLANET</u>	<u>RING</u>
N	48	22	92
P _T	20.0		
θ _T	22.5°		
ψ	30°		
P _N	23.09		
θ _N	19.73°		
C.D.	1.75		
D	2.40	1.10	4.60
D _o	2.50	1.20	4.70
D _R	2.28	.98	4.48
r _f	.02	.02	.02
t	.077	.077	.079
F	.50	.50	.50

Table 11:

APPENDIX H

INPUT PLANETARY SUN LOSS FACTOR

$$P_L = \frac{50 f \cos^2 \gamma}{\cos \theta_N} \left[\frac{H_T^2 + H_S^2}{H_T + H_S} \right]$$

$$H_S = \left(\frac{M_E + 1}{M_E} \right) \left[\sqrt{\left(\frac{r_o}{r} \right)^2 - \cos^2 \theta_N} - \sin \theta_N \right]$$

$$= \left(\frac{41/19 + 1}{41/19} \right) \left[\sqrt{\left(\frac{1.05}{.95} \right)^2 - \cos^2 19.7339} - \sin 19.7339 \right]$$

$$H_S = .353$$

$$H_T = (M_E + 1) \left[\sqrt{\left(\frac{R_o}{R} \right)^2 - \cos^2 \theta_N} - \sin \theta_N \right]$$

$$= (41/19 + 1) \left[\sqrt{\left(\frac{2.15}{2.05} \right)^2 - \cos^2 19.7339} - \sin 19.7339 \right]$$

$$H_T = .394$$

$$P_L = \frac{(50) (.03) (\cos^2 30^\circ)}{\cos 19.7339} \left[\frac{.353^2 + .394^2}{.353 + .394} \right]$$

$$P_L = .448\%$$

APPENDIX I

INPUT PLANETARY RING GEAR LOSS FACTOR

$$P_L = \frac{50 f \cos^2 \psi}{\cos \phi_N} \left[\frac{H_T^2 + H_S^2}{H_T + H_S} \right]$$

$$H_S = \frac{M_g - 1}{M_g} \left[\sqrt{\left(\frac{r_o}{r}\right)^2 - \cos^2 \phi_N} - \sin \phi_N \right]$$

$$= \frac{79/19 - 1}{79/19} \left[\sqrt{\left(\frac{1.05}{.95}\right)^2 - \cos^2 19.7339} - \sin 19.7339 \right]$$

$$H_S = .1835$$

$$H_T = (M_g - 1) \left[\sqrt{\left(\frac{R_o}{R}\right)^2 - \cos^2 \phi_N} - \sin \phi_N \right]$$

$$= (79/19 - 1) \left[\sqrt{\left(\frac{3.95}{3.85}\right)^2 - \cos^2 19.7339} - \sin 19.7339 \right]$$

$$H_T = .2228$$

$$P_L = \frac{(50)(.03)(\cos^2 30)}{\cos 19.7339} \left[\frac{.1835^2 + .2228^2}{.1835 + .2228} \right]$$

$$P_L = .245\% \text{ (PER MESH)}$$

APPENDIX J

INPUT PLANETARY ASSY POWER DERIVATION

$$T_{in} = \frac{6300 \text{ HP}_{in}}{\text{RPM}_{in}}$$

AT MEAN CONDITION:

$$T_{in} = \frac{(6300)(22)}{21000}$$

$$= 66 \text{ IN.LB.}$$

$$W_{TS} = \frac{2 T_{in}}{(D_p) (\text{No. PLANETS})}$$

$$= \frac{2 T_{in}}{(2.05)(3)}$$

$$= .325 T_{in}$$

$$T_{pc} = (W_{TS}) R_{pL}$$

$$= (W_{TS}) \frac{.95}{2}$$

$$= .154 T_{in}$$

Table 12:

<u>FLYWHEEL RPM</u>	<u>PLANET</u>
28000	39780
21000	29830
14000	19890

APPENDIX K

OUTPUT PLANETARY GEAR DATA

	<u>SUN</u>	<u>PLANET</u>	<u>RING</u>
N	40	30	100
P_T	20		
θ_T	22.796°		
ψ	30°		
D_P	2.00	1.500	5.00
D_O	2.10	1.60	4.90
D_R	1.86	1.36	5.14
R_F	.03	.03	.03
F	.50	.75	.50
t	.077	.077	.081
P_N	23.094		
θ_N	20°		

Table 13:

APPENDIX L

OUTPUT PLANET SPEED DERIVATION

$$\begin{aligned}
 \text{RPM}_{\text{PL}} &= \left(\frac{N_I}{N_P}\right) \text{RPM}_I \left(\frac{N_S}{N_P}\right) \text{RPM}_S \\
 \text{RPM}_I &= (\text{RPM}_S) (R_C) (R_B) \\
 &= (\text{RPM}_S) (R_C) (.3016) \\
 \text{RPM}_{\text{PL}} &= \left[(.3016) \left(\frac{100}{40}\right) R_C + 1 \right] \text{RPM}_S \\
 &= (.754 R_C + 1) \text{RPM}_S
 \end{aligned}$$

	<u>RPM_{PL}</u>		
*RPM_S →	9600	7200	4800
RPM _O ↓			
5000	36700	31901	27102
4000	33204	28405	23602
3000	29701	24903	20102
1500	24453	19654	14851
850	22173	17374	12578

*RPM_S = Flywheel RPM_n / 2.9166

Table 14 :

APPENDIX M

OUTPUT PLANETARY SUN-PLANET POWER LOSS FACTOR

$$P_L = \frac{50 f \cos^2 \Psi}{\cos \beta_N} \left[\frac{H_S^2 + H_T^2}{H_S + H_T} \right]$$

$$H_T = \frac{M_E + 1}{M_E} \left[\sqrt{\left(\frac{r_o}{r}\right)^2 - \cos^2 \theta} - \sin \theta \right]$$

$$= \frac{40/30 + 1}{40/30} \left[\sqrt{\left(\frac{1.6}{1.5}\right)^2 - \cos^2 20} - \sin 20 \right]$$

$$H_T = .2847$$

$$H_S = (40/30 + 1) \left[\sqrt{\left(\frac{2.1}{270}\right)^2 - \cos^2 20} - \sin 20 \right]$$

$$H_S = .2951$$

$$P_L = \frac{(50)(.03)(\cos^2 30)}{\cos 20} \left[\frac{(.2847)^2 + (.2951)^2}{.2847 + .2951} \right]$$

$$P_L = .347\%$$

APPENDIX N

OUTPUT PLANETARY PLANET-RING POWER LOSS FACTOR

$$P_L = \frac{(50)(.03)(\cos^2 \psi)}{\cos 20} \frac{H_S^2 + H_T^2}{H_S + H_T}$$

$$H_T = \frac{M_E - 1}{M_E} \left[\sqrt{\left(\frac{r_o}{r_i}\right)^2 - \cos^2 \theta} - \sin \theta \right]$$

$$= \frac{100/30 - 1}{100/30} \left[\sqrt{\left(\frac{1.6}{1.5}\right)^2 - \cos^2 20} - \sin 20 \right]$$

$$H_T = .1139$$

$$H_S = (100/30 - 1) \left[\sqrt{\left(\frac{5.1}{5.0}\right)^2 - \cos^2 20} - \sin 20 \right]$$

$$H_S = .1276$$

$$P_L = \frac{(50)(.03)(\cos^2 30)}{\cos 20} \left[\frac{(.1139)^2 + (.1276)^2}{.1139 + .1276} \right]$$

$$P_L = .145\%$$

APPENDIX O

OUTPUT PLANETARY ASSY POWER DERIVATION

$$T_o = \frac{63000 \text{ HP}_o}{\text{RPM}_o}$$

$$T_s = \frac{T_o}{3.50} = .2857 T_o$$

$$W_T = \frac{2 T_s}{D_s}$$

$$\begin{aligned} T_{PL} &= (W_{Ts}) (R_{PL}) \\ &= \frac{2 T_s}{D_s} (R_{PL}) \\ &= \frac{2 T_o}{(3.5) D_s} (R_{PL}) \\ &= \frac{63000 \text{ HP}_o}{(3.5)(\text{RPM}_o)} \left(\frac{D_p}{D_s} \right) \\ &= \frac{13500 \text{ HP}_o}{\text{RPM}_o} \end{aligned}$$

$$\text{HP}_{PL} = \frac{T_{PL} \text{ RPM}_{PL}}{(63000)(4)} \quad (\text{FOR 4 PLANETS})$$

$$= \frac{13500 \text{ HP}_o}{\text{RPM}_o} \frac{\text{RPM}_{PL}}{(63000)(4)}$$

$$\text{HP}_{PL} = .0536 (\text{HP}_o) \left(\frac{\text{RPM}_{PL}}{\text{RPM}_o} \right)$$

APPENDIX P

OUTPUT PLANET POWER

$$HP_{PL} = .0536 HP_o \left(\frac{RPM_{PL}}{RPM_o} \right)$$

7.5KW (10 HP)

	$RPM_n \rightarrow$	28,000	21,000	14,000
$RPM_o \downarrow$				
5000		3.93	3.42	2.91
4000		4.45	3.81	3.16
3000		5.31	4.45	3.59
1500		8.74	7.02	5.31
850		13.98	10.96	7.93

15KW (20 HP)

5000	7.87	6.84	5.81
4000	8.89	7.61	6.33
3000	10.61	8.90	7.18
1500	17.48	14.05	10.61
850	27.96	21.91	15.86

30KW (40 HP)

5000	15.74	13.68	11.62
4000	17.78	15.23	12.65
3000	21.23	17.80	14.37
1500	34.95	28.09	21.23
850	55.93	43.82	31.73

APPENDIX P (continued)

52KW (70 HP)

5000	27.54	23.94	20.34
4000	31.12	26.64	22.14
3000	37.15	31.15	25.14
1500	61.16	49.16	37.15
850	*97.87	*76.69	*55.52

75KW (100 HP)

5000	39.34	34.20	29.05
4000	44.45	38.06	31.63
3000	53.07	44.49	35.92
1500	*87.38	*70.23	*53.07
850	*139.82	*109.56	*79.32

*NOTE: The values shown do not reflect the limiting wheelslip torque of 330 FT. LBS.

APPENDIX Q

SPIRAL BEVEL GEAR DATA

	<u>PINION</u>	<u>GEAR</u>
N	19	27
P	13.570	
ϕ	22° 30'	
ψ	30°	
D_p	1.400	1.990
F	.600	.600
SHAFT ANGLE	9° 41'	
OUTER CONE DISF.	10.522	
WHOLE DEPTH	.136	.136
HAND OF SPIRAL	RH	LH
OUTSIDE DIA.	1.539	2.095

Table 16:

APPENDIX R

SPIRAL BEVEL GEAR POWER LOSS FACTOR

$$P_L = 50 f (\cos \Gamma + \cos \gamma) \frac{\cos \Psi^2}{\cos \phi} \left[\frac{H_S^2 + H_T^2}{H_S + H_T} \right]$$

$$\begin{aligned} \Gamma &= 5.433^\circ \\ \gamma &= 3.817^\circ \\ \Psi &= 30^\circ \\ \phi &= 22.5^\circ \\ f &= .03 \end{aligned}$$

$$\begin{aligned} H_T &= \frac{M_g + 1}{M_g} \left[\sqrt{\left(\frac{r_o}{r}\right)^2 - \cos^2 \theta_N} - \sin \theta \right] \\ &= \frac{27/19 + 1}{27/19} \left[\sqrt{\left(\frac{1.539}{1.400}\right)^2 - \cos^2 22.5} - \sin 22.5 \right] \end{aligned}$$

$$H_T = .3629$$

$$H_S = (M_g + 1) \left[\sqrt{\left(\frac{R_o}{R}\right)^2 - \cos^2 \theta} - \sin \theta \right]$$

$$H_S = (27/19 + 1) \left[\sqrt{\left(\frac{2.095}{1.99}\right)^2 - \cos^2 22.5} - \sin 22.5 \right]$$

$$H_S = .2955$$

$$P_L = (50)(.03)(\cos 5.433 + \cos 3.817) \left[\frac{.3629^2 + .2955}{.3629 + .2955} \right]$$

$$P_L = .807\%$$

APPENDIX S

HELICAL IDLER GEAR DATA

	<u>PINION</u>	<u>GEAR</u>
N	21	49
P_T	14.894	
θ_T	21.789°	
ψ	24.427°	
D_P	1.41	3.2899
D_O	1.544	3.4242
D_R	1.222	3.1019
R_F	.035	.035
F	.50	.50
t	.104	.103
P_N	16.358	
θ_N	20°	
C	2.350	

Table 17:

APPENDIX T

HELICAL IDLER POWER LOSS FACTOR

$$P_c = \frac{50 f \cos^2 \psi}{\cos N} \left[\frac{H_S^2 + H_T^2}{H_S + H_T} \right]$$

$$H_S = \frac{M_g + 1}{M_g} \left[\left(\frac{r_o}{r} \right)^2 - \cos^2 \theta - \sin \theta \right]$$

$$= \frac{49/21 + 1}{49/21} \left[\left(\frac{1.544}{1.41} \right)^2 - \cos^2 20^\circ - \sin 20^\circ \right]$$

$$H_S = .3146$$

$$H_T = (M_g + 1) \left[\left(\frac{R_o}{R} \right)^2 - \cos^2 \theta_N - \sin \theta \right]$$

$$= (49/21 H) \left[\left(\frac{3.4242}{3.2899} \right)^2 - \cos^2 20 - \sin 20 \right]$$

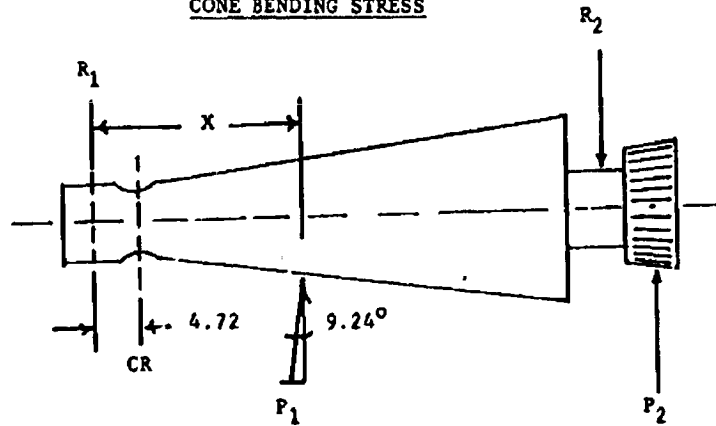
$$H_T = .3517$$

$$P_L = \frac{(50)(.03)(\cos^2 24.427)}{\cos 20} \left[\frac{(.3146)^2 + (.3517)^2}{.3146 + .3517} \right]$$

$$P_L = .4447$$

APPENDIX U

CONE BENDING STRESS



MEAN CONDION:

$$R_1 = \text{RESULTANT LOAD} = \frac{a}{\sqrt{a^2 + b^2}} \rightarrow 345.6 = 345.8 \text{ LB.}$$

$$M_{CR} = (R_1) (l) = (346.8)(.472) = 163.8 \text{ IN. LB.}$$

$$I = .049 D^4 = (.049)(.67)^4 = .0099 \text{ IN.}^4$$

$$S_B = \frac{Mc}{I} = \frac{(163.8)(.333)}{.0099} = \underline{5360 \text{ PSI}}$$

MAXIMUM CONDION:

$$S_B = M' \frac{c}{I} = R_1' \frac{l c}{I} = \frac{(2330)(.472)(.333)}{.0099}$$

$$S_B = 37,530 \text{ PSI}$$

$$* \rightarrow = \sqrt{a^2 + b^2}$$

APPENDIX V

CONE HORSEPOWER DERIVATION

HP_c FORMULA:

$$T_o = \frac{(HP_o)(6300)}{RPM_o}$$

$$T_r = (T_o)(1 - R_p)$$

$$HP_c = \frac{(T_c)(RPM_c)}{(63000)(4)}$$

$$= \frac{(T_r)(R_p)(RPM_c)}{(63000)(4)}$$

$$= \frac{(HP_o)(63000)(RPM_c)(1 - R_p)}{(RPM_o)(63000)(4)}$$

$$HP_c = \frac{(HP_o)(R_p)(RPM_c)(1 - R_p)}{(4)(.2154 R_c - .2857)(RPM_g)}$$

$$HP_c = \frac{(HP)(.3016)(R_c)(.7143)}{(4)(.2154 R_c - .2857)}$$

$$HP_c = \frac{(.0539)(HP_o)(R_c)}{(.2154 R_c - .2857)}$$

APPENDIX W

TRACTION CONE LIFE AT
MEAN CONDITION (REF. 3)

$$L = K_4 (K_2)^{-9} (Q)^{-3} (E)^{-6.3} (R)^{-9}$$

$$K_4 = 6.43 \times 10^8$$

$$K_2 = 1.3 \times 10^6$$

$$Q = 498.5 \text{ LB.}$$

$$E = \frac{1}{2.325} + \frac{1}{5} + \frac{1}{.722} = 2.015$$

$$\begin{aligned} L &= (6.43 \times 10^8) (1.3 \times 10^6)^{-9} (498.5)^{-3} (2.015)^{-6.3} (.722)^{-9} \\ &= 2.68 \times 10^4 \text{ (MR)} \end{aligned}$$

$$L_{10} = \frac{2.68 \times 10^4 \text{ MR}}{(60) (23479)} = 19,020 \text{ HOURS (Single cone life)}$$

APPENDIX X

TRACTION ROLLER LIFE AT
MEAN CONDITION (REF. 3)

$$L = K_4 (K_2)^{.9} (Q)^{-3} (E)^{-6.3} (R)^{-.9}$$

$$K_4 = 6.43 \times 10^8$$

$$K_2 = 1.3 \times 10^6$$

$$Q = 498.5 \text{ LB.}$$

$$E = \frac{1}{2.325} + \frac{1}{5} + \frac{1}{.722} = 2.015$$

$$L = (6.43 \times 10^8)(1.3 \times 10^6)^{.9} (498.5)^{-3} (2.015)^{-6.3} (2.325)^{-.9}$$

$$L = 9.36 \times 10^3 \text{ HR}$$

$$L_{10} = \frac{(9.36 \times 10^3)(10^6)}{(7200)(60)(4)} = 5420 \text{ HOURS}$$

APPENDIX Y

TRACTION CONTACT COMPOSITE LIFE
AT MEAN CONDITION

$$L_c = \left[\frac{N_c}{(H_1)^{10/9}} + \frac{N_r}{(H_2)^{10/9}} \right]^{-9/10}$$

N_c = NUMBER OF CONES = 4

N_r = NUMBER OF ROLLERS = 1

H_1 = INDIVIDUAL CONE LIFE, HRS. 19020

H_2 = ROLLER LIFE, HRS. = 5420

$$L_c = \left[\frac{4}{(19020)^{10/9}} + \frac{1}{(5420)^{10/9}} \right]^{-9/10}$$

L_c = 2920 HOURS

APPENDIX 2

CONE TORQUE (IN. LB.)

$$T_c = HP_c \times \frac{63025}{RPM_c}$$

<u>7.5KW (10 HP)</u>				
RPM _c	RPM _n →	28,000	21,000	14,000
5000		6.79	6.79	6.79
4000		8.49	8.49	8.49
3000		11.32	11.32	11.32
1500		22.63	22.63	22.63
850		39.99	39.99	39.99
<u>15KW (20 HP)</u>				
5000		13.58	13.58	13.58
4000		16.98	16.98	16.98
3000		22.64	22.64	22.64
1500		45.26	45.26	45.26
850		79.98	79.98	79.98
<u>30KW (40 HP)</u>				
5000		27.16	27.16	27.16
4000		33.96	33.96	33.96
3000		45.28	45.28	45.28
1500		90.52	90.52	90.52
850		159.96	159.96	159.96

Table 121

APPENDIX Z (continued)

<u>52KW (70 HP)</u>				
	5000	47.53	47.53	47.53
	4000	59.43	59.43	59.43
	3000	79.24	79.24	79.24
	1500	158.41	158.41	158.41
39.8KW(53.4 Hp)	850	279.93*	279.93*	279.93*
<u>75KW (100 HP)</u>				
	5000	67.90	67.90	67.90
	4000	84.90	84.90	84.90
	3000	113.20	113.20	113.20
70.4KW(94.3 Hp)	1500	226.30*	226.30*	226.30*
39.8KW(53.4 Hp)	850	399.90*	399.90*	399.90*

* THE NUMBERS SHOWN ARE THEORETICAL ONLY. THE MAXIMUM WHEEL SLIP TORQUE OF 310 FT. LBS. LIMITS THE CONE TORQUE.

Table 13: Continued

APPENDIX AA

SINGLE CONE HORSEPOWER (HP)

$$HP = \frac{(.0539)(HP_o)(Rc)}{(.2154)(Rc) - .2857}$$

<u>7.5KW (10 HP)</u>				
	RPM _n →	28,000	21,000	14,000
RPM _o ↓				
5000		3.88	3.53	3.19
4000		4.22	3.79	3.36
3000		4.79	4.22	3.65
1500		7.08	5.93	4.79
850		10.59	8.56	6.54
<u>15KW (20 HP)</u>				
5000		7.75	7.06	6.38
4000		8.43	7.58	6.72
3000		9.58	8.44	7.29
1500		14.15	11.86	9.58
850		21.17	17.13	13.07
<u>30KW (40 HP)</u>				
5000		15.50	14.13	12.75
4000		16.87	15.16	13.44
3000		19.16	16.87	14.58
1500		28.30	23.73	19.16
850		42.34	34.25	26.15

Table 19i

ORIGINAL PAGE IS
OF POOR QUALITY

APPENDIX AA (continued)

52KW (70 HP)

5000	27.13	24.72	22.32
4000	29.53	26.52	23.52
3000	33.53	29.53	25.52
1500	49.53	41.53	33.53
850	74.10 (56.53)	59.94 (45.73)	45.76 (34.91)

75KW (100 HP)

5000	38.75	35.39	31.89
4000	42.18	37.89	33.60
3000	47.90	42.18	36.46
1500	70.63(66.69)	59.32(55.91)	47.90 (45.15)
850	105.85(56.53)	85.63(45.73)	65.37 (34.91)

NOTE: THE MAXIMUM WHEEL SLIP TORQUE OF 330 FT. LBS. LIMITS
THE CONE HORSEPOWER TO THE VALUES IN PARENTHESIS.

Table 19: Continued

APPENDIX BB

TOTAL CONE HORSEPOWER (HP): FOUR (4) CONES

$$HP = \frac{(.539)(HP_o)(R_c)}{(.2154)(R_c) - .2857} \times 4 \quad "n" = \frac{\text{Total cone power}}{\text{Power out}}$$

7.5KW (10 HP)

RPM _o	RPM _n →	28,000	21,000	14,000
5000		15.52	14.12	12.76
4000		16.88	15.16	13.44
3000		19.16	16.88	14.60
1500		28.32	23.72	19.16
850		42.36	34.24	26.16

15KW (20 HP)

5000	31.00	28.24	25.52
4000	33.72	30.32	26.88
3000	38.32	33.76	29.16
1500	56.60	47.44	38.32
850	84.68	68.52	52.28

30KW (40 HP)

5000	62.00	56.56	51.00
4000	67.48	60.64	53.76
3000	76.64	67.48	58.32
1500	113.20	94.92	76.64
850	169.36	137.0	104.6

Table 201

APPENDIX BB (continued)

52KW (70 HP)

5000	108.5	98.88	89.28
4000	118.1	106.1	94.08
3000	134.1	118.1	102.1
1500	198.1	166.1	134.1
850	296.4(226.1)	239.8(182.9)	183(139.6)

75KW (100 HP)

5000	155.0	141.6	127.6
4000	168.7	151.6	134.4
3000	191.6	168.7	145.8
1500	282.5(266.8)	237.3(223.6)	191.6(180.6)
850	423.4(226.1)	342.5(182.9)	261.5(139.6)

NOTE: THE MAXIMUM WHEEL SLIP TORQUE OF 330 FT. LBS. LIMITS
THE CONE HORSEPOWER TO THE VALUES IN PARENTHESES ().

Table 20: Continued

APPENDIX CC

CONE NORMAL LOAD (LB.)

$$W_N = \frac{2 T_c}{.07 D_{\text{cone}}}$$

7.5KW (10 HP)

	RPM _n →	28,000	21,000	14,000
RPM _o				
5000		155.20	189.82	256.95
4000		170.11	203.67	271.03
3000		193.09	226.81	294.03
1500		285.34	318.98	386.01
850		426.81	460.53	527.99

15KW (20 HP)

5000	312.40	379.65	513.91
4000	340.21	407.34	542.06
3000	386.18	436.62	588.05
1500	570.67	637.96	772.02
850	853.62	921.06	1055.98

30KW (40 HP)

5000	624.80	759.30	1027.81
4000	680.42	814.68	1084.12
3000	772.37	907.23	1176.10
1500	1141.34	1275.92	1544.05
850	1707.24	1842.11	2111.96

52KW (70 HP)

5000	1093.40	1328.77	1798.68
4000	1190.74	1425.69	1897.21
3000	1351.64	1587.66	2058.18
1500	1997.35	2234.86	2702.09
850	2987.99 (2273.33)	3224.06 (2452.93)	3696.33 (2812.25)

Table 210

APPENDIX CC (continued)

<u>75KW (100 HP)</u>			
5000	1562.00	1898.24	2569.54
4000	1701.06	2036.70	2710.30
3000	1930.92	2268.08	2940.26
1500	2853.36 (2685.66)	3189.79 (3002.32)	3860.13 (3633.26)
850	4268.10 (2273.33)	4605.28 (2452.93)	5279.90 (2812.25)

NOTE: THE MAXIMUM WHEEL SLIP TORQUE OF 330 FT. LB.
LIMITS THE CONE NORMAL LOAD TO THE VALUES
SHOWN IN PARENTHESES.

Table 21: Continued

APPENDIX DD

CONE BEARING LOSS

(4 cones)

<u>7.5 KW (10 HP)</u>				
RPM _o	RPM _n	28,000	21,000	14,000
5000		.394	.383	.420
4000		.260	.360	.310
3000		.266	.342	.250
1500		.320	.340	.230
850		.390	.311	.242
<u>15 KW (20 HP)</u>				
5000		.720	.700	.680
4000		.460	.510	.600
3000		.480	.500	.560
1500		.760	.700	.540
850		.950	.800	.580
<u>30 KW (40 HP)</u>				
5000		1.240	1.368	1.840
4000		.960	1.180	1.640
3000		1.158	1.206	1.510
1500		2.140	1.870	1.550
850		2.737	2.295	1.573
<u>52 KW (70 HP)</u>				
5000		2.66	3.32	4.60
4000		2.20	2.60	3.92
3000		2.54	2.75	3.70
1500		4.44	4.15	3.71
(39.8 KW)	850 (53.4 HP)	6.50 (4.3)	5.55 (3)	3.82 (1.9)
<u>75 KW (100 HP)</u>				
5000		4.31	5.46	8.10
4000		3.83	4.54	6.37

Table 22:

APPENDIX DD

CONE BEARING LOSS (CONTINUED)

(4 CONES)

3000	4.13	4.47	6.22
(90KW) 1500 (94.3 HP)	6.45 (6.4)	6.20 (4.8)	6.95 (3.4)
(39.8KW) 850 (53.4 HP)	11.11 (4.3)	9.29 (3)	7.65 (1.9)

() WHEEL SLIP TORQUE LIMITED VALUES.

Table 22: Continued

APPENDIX EE

SPIN VELOCITY DERIVATION

TANGENTIAL VELOCITY = $\frac{D_{roll}}{2} \cdot (RPM_s)$

$RPM_s = \text{Flywheel } RPM_n / 2.9166$

$\gamma = \left(\frac{27}{60}\right) \left(\frac{1}{2}\right) \left(\frac{4.65}{39.37}\right) (RPM_s)$

$\gamma = .00618 (RPM_s) \text{ M/SEC}$

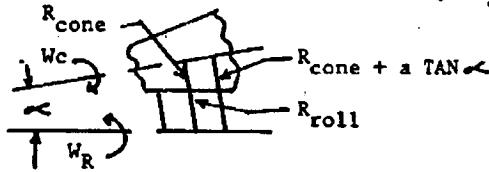
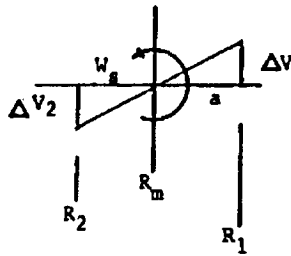
$W_s = \frac{\Delta V_1}{a}$

$\Delta V_1 = W_c (R_1) - (W_R) R_{Roll}$

$\Delta V_1 = W_c (R_{cone} + a \text{ TAN } \alpha) - (W_R) R_{Roll}$

$\alpha = (\text{CONE ANGLE}) / 2$

$W_s = \frac{W_c (R_{cone} + a \text{ TAN } \alpha) - (W_R) R_{Roll}}{a}$



$W_c = R_c (W_R)$

$R_{cone} = R_{roll} / R_c$

$W_s = R_c (W_R) \text{ TAN } \alpha$

*RPM _n	→ 28000	21000	14000
*RPM _s	→ 9600	7200	4800
W _{Roll} RAD/SEC	1005	754	503
V (M/SEC)	59.37	44.53	29.69

$W_s = (\text{RAD/SEC}) = (R_c) (W_{roll}) \text{ TAN } \alpha$

RPM _o	RPM _s	9600	7200	4800
5000		612	558	504
4000		533	479	425
3000		454	400	346
1500		335	281	227
850		284	230	176

Table 23:

APPENDIX FF

J₆, DIMENSIONLESS SPIN TORQUE FACTOR (REF. 1)

7.5 KW (10 HP)

RPM _o \ RPM _n →	28,000	21,000	14,000
5000	.009	.007	.004
4000	.008	.0065	.0035
3000	.007	.006	.0028
1500	.0065	.005	.0022
850	.006	.004	.002

15 KW (20 HP)

5000	.012	.009	.006
4000	.010	.008	.0045
3000	.009	.007	.0038
1500	.008	.006	.0032
850	.0075	.005	.0027

30 KW (40 HP)

5000	.014	.010	.007
4000	.013	.009	.006
3000	.012	.008	.005
1500	.011	.007	.004
850	.010	.006	.0035

52 KW (70 HP)

5000	.016	.012	.008
4000	.015	.011	.007
3000	.014	.009	.006
1500	.013	.008	.005
850	.012	.007	.004

75 KW (100 HP)

5000	.019	.015	.0085
4000	.018	.012	.0075
3000	.017	.010	.0065
1500	.016	.009	.0055
850	.015	.008	.0045

Table 24:

APPENDIX GG

TRACTION LOAD DETERMINATION

MEAN CONDITION:

$$HP_{out} = 22 \text{ HORSEPOWER}$$

$$RPM_{out} = 3000 \text{ RPM}$$

$$T_o = \frac{(HP_{out})(63000)}{RPM_{out}} = 462 \text{ in. lb.}$$

$$T_{sum} = (T_o)(R_p) = (462)(.2857) = 132 \text{ in. lb.}$$

$$T_{ring} = (T_o)(1-R_p) = (462)(1-.2857) = 330 \text{ in lb.}$$

$$T_{cone} = (T_{ring})(R_B) = (330)(.3016) = 99.5 \text{ in. lb.}$$

FOR 4 CONES:

$$T_{cone} = \frac{99.5}{4} = 24.88 \text{ in. lb./cone}$$

$$W_{T_{cone}} = \frac{T}{R_{cone}} = \frac{24.88}{(1.426)} = 34.9 \text{ lbs.}$$

$$W_{N_{cone}} = \frac{W_T}{.07} = \frac{34.9}{.07} = 498.5 \text{ lbs.}$$

MAXIMUM CONDITION:

$$HP_{out} = 100 \text{ HP}$$

$$T_o = 330 \text{ FT. LB.} = 3960 \text{ IN. LB.}$$

$$RPM_o = 100 \times 63025/3960 = 1592 \text{ RPM}$$

$$RPM_{in} = 14,000 \text{ RPM}$$

$$R_c = \frac{n_o}{RPM_s} + .2857 = \frac{1592}{4800} + .2857 = 2.866$$
$$\frac{.2154}{.2154}$$

APPENDIX GG

TRACTION LOAD DETERMINATION (CONTINUED)

$$D_c = 4.65/R_c = 4.65/2.866 = 1.622 \text{ in.}$$

$$\text{RPM}_c = R_c \text{ RPM}_x = 2.866 (4800) = 13757 \text{ RPM}$$

$$T_{\text{ring}} = T_o (1 - R_p) = 3960 (1 - .2857) = 2829 \text{ IN. LB.}$$

$$T_{\text{cone}} = T_{\text{ring}} R_B = 2829 (.3016) = 853 \text{ IN. LB. (4 cones)}$$

PER CONE:

$$T_{\text{cone}} = 853/4 = 213 \text{ IN. LB.}$$

$$W_{N\text{cone}} = \frac{W_T}{\mu} = \frac{T_{\text{cone}}}{\frac{D_c \mu}{2}} = \frac{213}{1.622 \frac{(2)}{(.07)}} = 3750 \text{ LB.}$$

APPENDIX HH

TRACTION POWER LOSS (HP, FOR 4 CONTACTS) (REFERENCE 2)

$$\text{POWER LOSS} = \frac{(.015)^{J_7/J_4} (\text{HP}_c)}{\sqrt{K}}$$

<u>7.5 KW (10 HP)</u>			
RPM _o \ RPM _n →	28,000	21,000	14,000
5000	.25	.23	.21
4000	.27	.25	.22
3000	.31	.27	.24
1500	.46	.38	.31
850	.69	.56	.42
<u>15 KW (20 HP)</u>			
5000	.50	.46	.41
4000	.55	.49	.44
3000	.62	.55	.47
1500	.92	.77	.62
850	1.37	1.11	.85
<u>30 KW (40 HP)</u>			
5000	1.00	.91	.83
4000	1.09	.98	.89
3000	1.24	1.10	.94
1500	1.83	1.54	1.24
850	2.74	2.22	1.70
<u>52 KW (70 HP)</u>			
5000	1.75	1.60	1.45
4000	1.91	1.72	1.55
3000	2.17	1.92	1.65
1500	3.21	2.69	2.17
850	4.80 (3.69)	3.89 (2.99)	2.97 (2.24)
<u>75 KW (100 HP)</u>			
5000	2.50	2.80	2.07
4000	2.73	2.45	2.22

Table 25:

APPENDIX HH

TRACTION POWER LOSS (HP, FOR 4 CONTACTS) (REFERENCE) (CONTINUED)

$$\text{POWER LOSS} = \frac{(.015) J_7/J_4 (\text{HP}_c)}{\sqrt{k}}$$

3000	3.10	2.74	2.36
1500	4.58 (4.33)	3.84 (3.58)	3.10 (2.92)
850	6.86 (3.69)	5.55 (2.99)	4.24 (2.24)

NOTE: THE MAXIMUM WHEEL SLIP TORQUE OF 330 FT. LBS LIMITS THE POWER LOSS TO THE VALUES SHOWN IN PARENTHESES.

Table 25: Continued

APPENDIX II

CONTACT ELLIPSE DIMENSIONS, a/b (IN.) (REF. 6)

RPM _o ↓ 7.5 KW (10 HP)	b = μ g		a = ν g	
	28,000	21,000	14,000	
	a/b in.			
5000	.0456/.0101	.0492/.0098	.0507/.0086	
4000	.0462/.0109	.0499/.0108	.0561/.0105	
3000	.0478/.0122	.0508/.0120	.0566/.0118	
1500	.0531/.0155	.0556/.0155	.0600/.0153	
850	.0601/.0188	.0618/.0188	.0656/.0188	
<u>15 KW (20 HP)</u>				
5000	.0574/.0127	.0619/.0124	.0702/.0120	
4000	.0581/.0138	.0630/.0136	.0708/.0132	
3000	.0600/.0153	.0645/.0153	.0713/.0148	
1500	.0670/.0195	.0702/.0192	.0758/.0193	
850	.0757/.0237	.0779/.0237	.0825/.0236	
<u>30 KW (40 HP)</u>				
5000	.0723/.0160	.0780/.0157	.0886/.0151	
4000	.0733/.0174	.0793/.0171	.0892/.0167	
3000	.0758/.0193	.0806/.0191	.0900/.0187	
1500	.0843/.0246	.0884/.0246	.0955/.0244	
850	.0953/.0299	.0981/.0299	.1041/.0298	
<u>52 KW (70 HP)</u>				
5000	.0872/.0192	.0941/.0189	.1068/.0182	
4000	.0884/.0209	.0956/.0207	.1073/.0201	
3000	.0914/.0233	.0972/.0230	.1085/.0226	
1500	.1017/.0296	.1067/.0297	.1150/.0293	
850	.1147/.0360 (.1047/.0329)	.1183/.0360 (.1079/.0328)	.1253/.0359 (.1145/.0328)	

Table 26:

APPENDIX II

CONTACT ELLIPSE DIMENSIONS, a/b (IN.) (REF. 6) (CONTINUED)

<u>75 KW (100 HP)</u>			
5000	.0980/.0216	.1060/.0213	.1201/.0205
4000	.0995/.0236	.1075/.0232	.1210/.0226
3000	.1028/.0262	.1096/.0259	.1222/.0254
1500	.1145/.0334 (.1121/.0327)	.1200/.0334 (.1177/.0327)	.1295/.0330 (.1269/.0324)
850	.1292/.0405 (.1047/.0329)	.1332/.0405 (.1079/.0328)	.1412/.0404 (.1145/.0328)

NOTE: THE MAXIMUM WHEEL SLIP TORQUE OF 330 FT. LB LIMITS
"b/a" TO THE VALUES SHOWN IN PARENTHESES.

Table 26; Continued

APPENDIX JJ

g (REF. 6)

	RPM _n → 28,000	21,000	14,000
RPM _o ↓			
<u>7.5 KW (10 HP)</u>			
5000	.0190	.0193	.0197
4000	.0201	.0205	.0201
3000	.0218	.0221	.0227
1500	.0264	.0268	.0274
850	.0312	.0315	.0322
<u>15 KW (20 HP)</u>			
5000	.0239	.0243	.0248
4000	.0253	.0259	.0265
3000	.0274	.0281	.0286
1500	.0333	.0338	.0346
850	.0393	.0397	.0405
<u>30 KW (40 HP)</u>			
5000	.0301	.0306	.0313
4000	.0319	.0326	.0334
3000	.0346	.0351	.0361
1500	.0419	.0426	.0436
850	.0495	.0500	.0511
<u>52 KW (70 HP)</u>			
5000	.0363	.0369	.0377
4000	.0385	.0393	.0402
3000	.0417	.0423	.0435
1500	.0505	.0514	.0525
850	.0596 (.0544)	.0603 (.0550)	.0615 (.0562)
<u>75 KW (100 HP)</u>			
5000	.0408	.0416	.0424
4000	.0433	.0442	.0453

Table 27:

APPENDIX JJ

g (REF. 6) (CONTINUED)

3000	.469	.0477	.0490
1500	.0569 (.0557)	.0578 (.0567)	.0591 (.0579)
850	.0671 (.0544)	.0679 (.0550)	.0693 (.0562)

NOTE: THE MAXIMUM WHEEL SLIP TORQUE OF 330 FT. LB. LIMITS
"g" TO THE VALUES SHOWN IN PARENTHESES.

Table 27:

APPENDIX KK

ELASTOHYDRODYNAMIC
(EHD) FILM THICKNESS AT
TRACTION CONTACT (REF. 7)

$$h = 2.04 \left(1 + \frac{2R_1}{3R_2} \right) \left(\mu_0 \frac{u_1 + u_2}{2} \right)^{.74} (R_1)^{.407} \left(\frac{F}{(1 - \rho^2)Q} \right)^{.074}$$

AT MEAN CONDITION:

$$R_1 = \frac{1}{\frac{1}{2.325} + \frac{1}{.722}} = .551$$

$$R_2 = \frac{1}{\frac{1}{5.0} + \frac{1}{\infty}} = 5.0$$

$$\mu_0 = .87 \times 10^{-6} \text{ AT } 176^\circ\text{F}$$

$$\rho = 1.5 \times 10^{-4}$$

$$\frac{u_1 + u_2}{2} = \pi(4.65) \left(\frac{7200}{60} \right) = 1753 \text{ IN./SEC.}$$

$$Q = 498.5 \text{ LB.}$$

$$h = 2.04 \left(1 + \frac{3(.551)}{2(5.0)} \right)^{.74} \left(.87 \times 10^{-6} \times 1.5 \times 10^{-4} \times 1753 \right)^{.74} \\ (.551)^{.407} \left(\frac{30 \times 10^6}{(1 - .32^2)(498.5)} \right)^{.074} = 39.6 \mu \text{ in.}$$

$$h = 39.6 \mu \text{ in.}$$

$$\sigma = (\sigma_1^2 + \sigma_2^2)^{.5} = (6^2 + 6^2)^{.5} = 8.49$$

$$h/\sigma = 39.6/8.49 = 4.66$$

APPENDIX KK

EHD FILM THICKNESS AT
TRACTION CONTACT (REF. 7)
 (CONTINUED)

AT MAXIMUM CONDITION:

$$R_1 = \frac{1}{\frac{1}{2.325} + \frac{1}{.822}} = .607 \text{ IN.}$$

$$R_2 = 5.0 \text{ IN.}$$

$$Q = 3750 \text{ LB.}$$

$$\frac{u_1 + u_2}{2} = \frac{7(4.65)(4800)}{60} = 1169 \text{ IN./SEC.}$$

$$h = 2.04 \left(1 + \frac{2(.607)}{3(5.0)} \right)^{-.74} \left(.87 \times 10^{-6} \times 1.5 \times 10^{-4} \times 1169 \right)^{.74}$$

$$\left(.607 \right)^{.407} \left(\frac{30 \times 10^6}{(1 - .32)(3750)} \right)^{.074} = 27.8 \mu \text{ in.}$$

$$h = 27.8 \mu \text{ IN.}$$

$$h/\sigma = 27.8/8.49 = 3.27$$

APPENDIX LL

HERTZIAN
TRACTION CONTACT STRESS
(REF. 6)

MEAN CONDITION:

$$P = 498.5 \text{ LB.}$$

$$R_{A1} = 2.235 \text{ IN.}$$

$$R_{A2} = 5.0 \text{ IN.}$$

$$R_{B1} = \frac{1.426}{2 \cos 9.24^\circ} = .722 \text{ IN.}$$

$$R_{B2} = \infty$$

$$\epsilon = .00459 \left(\frac{498.5}{\frac{1}{2.325} + \frac{1}{5} + \frac{1}{.722}} \right)^{1/3} = .0288$$

$$\cos \gamma = \frac{\frac{1}{2.325} - \frac{1}{5.0} + \frac{1}{.722}}{\frac{1}{2.35} + \frac{1}{5.0} + \frac{1}{.722}} = .8015$$

$$\mu = 2.300$$

$$\gamma = .543$$

$$b = \mu g = (2.300)(.0287) = .0662$$

$$a = \gamma g = (.543)(.0287) = .0156$$

$$\text{ASPECT RATIO} = .0662 / .0156 = 4.24$$

$$S_{\max} = \left(\frac{3}{2\pi} \right) \left(\frac{498.5}{(.0662)(.0156)} \right) = 230,480 \text{ PSI (MEAN)}$$

MAXIMUM CONDITION:

$$P = W_N = 3750 \text{ LB.}$$

APPENDIX LL

TRACTION CONTACT STRESS (CONTINUED)
(REF. 6)

$$R_{B-1} = 1.622 / (2 \cos 9.24^\circ) = .822 \text{ IN.}$$

$$g = (.00459) \left(\frac{3750}{\frac{1}{2.325} + \frac{1}{5} + \frac{1}{.822}} \right)^{1/3} = .0581$$

$$\cos \tau = \frac{\frac{1}{2.325} - \frac{1}{5} + \frac{1}{.822}}{\frac{1}{2.325} + \frac{1}{5} + \frac{1}{.822}} = .783$$

$$\mu = 2.208$$

$$\nu = .566$$

$$b = \mu g = 2.208 (.0581) = .1283$$

$$a = \nu g = 0.556 (.0581) = .0323$$

$$\text{ASPECT RATIO} = .1283 / .0323 = 3.972$$

$$S_{\max} = \frac{3}{2\pi} \frac{3750}{(.1283)(.0323)} = 432,060 \text{ PSI (MAX)}$$

APPENDIX MM

EXAMPLE: TRACTION LOSS CALCULATION

From Reference 1, page 15.

$$\text{Loss factor} = \frac{3\pi}{8} \cdot \sqrt{k} \cdot \frac{m}{\mu} \cdot \left(\frac{\text{power loss}}{\text{power input}} \right)$$

$$\text{Power Loss} = \text{Loss factor (8)} (\text{power input}) / 3\pi \cdot \sqrt{k} \cdot \left(\frac{m}{\mu} \right)$$

$$\text{Loss factor} = J_7/J_4$$

$$\text{Power Loss} = \frac{.849 (J_7/J_4) (\text{power input})}{\sqrt{k} \cdot \left(\frac{m}{\mu} \right)}$$

For four contacts, and assuming $m/\mu = 220$

$$\text{Power loss} = \frac{.015 (J_7/J_4) (\text{power input})}{\sqrt{k}}$$

$$J_7/J_4 = (J_6 \times J_3) + (J_4 \times J_1) \quad (\text{Ref. 1, page 15})$$

$$J_1 = \frac{3\pi}{8} \cdot \frac{m}{\mu} \cdot \frac{\Delta u}{u} \cdot \sqrt{k} \quad (\text{Slip Factor, Ref. 1, page 9})$$

$$\text{Assuming } \frac{\Delta u}{u} = .016$$

$$J_1 = 4.15 \sqrt{k} = 8.30$$

$k = \text{aspect ratio of Hertzian contact} = 4.0$

$$J_3 = \frac{3\pi}{8} \cdot \frac{m}{\mu} \cdot \frac{W_s}{u} \cdot \sqrt{a \cdot b} \cdot \sqrt{k} \quad (\text{Spin Factor, Ref. 1, page 9})$$

For $W_s = 600 \text{ rad/sec.}$ (Spin Velocity)

APPENDIX MM

EXAMPLE: TRACTION LOSS CALCULATION (CONTINUED)

and $u = 60$ m/sec (Velocity)

and since $k = a/b$

$$J_3 = 2592 b$$

For $b = .0013$ m

$$J_3 = 3.37$$

$$J_1/J_3 = 8.30/3.37 = 2.46$$

From Reference 1, page 30:

$$J_4 = 1.0$$

From Reference 1, page 33:

$$J_6 = .06$$

$$\begin{aligned} J_7/J_4 &= \frac{J_6 \times J_3 + J_4 \times J_1}{J_4} \\ &= \frac{.06 \times 3.37 + 1.0 \times 8.30}{1.0} \end{aligned}$$

$$J_7/J_4 = 8.50$$

Therefore,

$$\text{Power Loss} = \frac{.015 (8.50) (\text{power input})}{\sqrt{4}}$$

$$\text{Power loss} = .064 (\text{power input})$$

APPENDIX MM

EXAMPLE: TRACTION LOSS CALCULATION (CONTINUED)

Where power loss is per four contacts and
power input is horsepower per contact.

APPENDIX NN

J_7 / J_4
LOSS FACTOR (REF. 1)

$$J_7/J_4 = \frac{J_6 \cdot J_3 + J_4 \cdot J_1}{J_4}$$

$RPM_n \rightarrow$	28,000	21,000	14,000
$RPM_o \downarrow$			
5000	8.78	9.32	10.22
4000	8.44	9.09	9.70
3000	8.21	8.44	9.23
1500	7.71	7.78	8.21
850	7.47	7.60	7.69

Table 28:

APPENDIX OO

J_1 , DIMENSIONLESS SLIP FACTOR (Ref.1)

$$J_1 = \left(\frac{3\pi}{8}\right) \left(\frac{H}{\mu}\right) \left(\frac{\Delta u}{u}\right) \sqrt{K}$$

$$J_1 = \left(\frac{3\pi}{8}\right) (220) (.016) \sqrt{K} = 4.15 \sqrt{K}$$

	RPM _s →	9600	7200	4800
RPM _o ↓				
5000		8.82	9.26	10.05
4000		8.54	8.92	9.59
3000		8.21	8.54	9.09
1500		7.68	7.86	8.22
850		7.42	7.52	7.75

Table 29:

APPENDIX PP

J_3

DIMENSIONLESS SPIN FACTOR (REF. 1)

$$J_3 = \left(\frac{3\pi}{8}\right) \left(\frac{M}{\mu}\right) \left(\frac{W_s}{U}\right) (a \cdot b) \sqrt{K}$$

$$\left(\frac{3\pi}{8}\right) (220) \left(\frac{W_s}{U}\right) (a \cdot b) \sqrt{K}$$

$$J_3 = 4.366 W_s \cdot b \quad (\text{AT } 28,000 \text{ RPM}_n)$$

$$J_3 = 3.275 W_s \cdot b \quad (\text{AT } 21,000 \text{ RPM}_n)$$

$$J_3 = 2.183 W_s \cdot b \quad (\text{AT } 14,000 \text{ RPM}_n)$$

(b is in meters)

7.5 KW (10 HP)

RPM _o \ RPM _n →	28,000	21,000	14,000
5000	3.09	2.24	1.42
4000	2.73	1.99	1.32
3000	2.41	1.69	1.09
1500	1.97	1.30	.76
850	1.89	1.18	.64

15 KW (20 HP)

5000	3.90	2.87	1.96
4000	3.43	2.51	1.67
3000	3.02	2.15	1.37
1500	2.49	1.64	.93
850	2.38	1.49	.81

30 KW (40 HP)

5000	4.91	3.62	2.48
4000	4.33	3.16	2.10
3000	3.82	2.68	1.73

Table 30:

APPENDIX PP

J_3

DIMENSIONLESS SPIN FACTOR (REF. 1) (CONTINUED)

1500	3.13	2.07	1.20
850	3.00	1.88	1.02
<u>52 KW (70 HP)</u>			
5000	5.92	4.37	2.98
4000	5.23	3.81	2.53
3000	4.60	3.23	2.08
1500	3.78	2.49	1.45
850	3.61 (3.30)	2.26 (2.06)	1.22 (1.12)
<u>75 KW (100 HP)</u>			
5000	6.65	4.92	3.36
4000	5.88	4.28	2.85
3000	5.18	3.65	2.34
1500	4.25 (4.16)	2.80 (2.75)	1.63 (1.60)
850	4.07 (3.30)	2.55 (2.06)	1.38 (1.12)

() NOTE: Values at wheelslip torque limit values.

Table 30: (Continued)

APPENDIX QQ

RPM _o \ RPM _n →	$\frac{g/(W_H)^{1/3}}{\text{(REF. 6)*}}$		
	28,000	21,000	14,000
5000	.00352	.00336	.00310
4000	.00363	.00349	.00325
3000	.00377	.00363	.00342
1500	.00401	.00393	.00377
850	.00414	.00408	.00398

	$R_B - 1 = D_c / (2 \cos 9.24^\circ) \text{ in.}^*$		
5000	.629	.518	.382
4000	.722	.603	.453
3000	.849	.722	.557
1500	1.148	1.027	.849
850	1.356	1.257	1.096

	$\cos \tau^*$		
5000	.820	.843	.877
4000	.801	.825	.859
3000	.779	.801	.835
1500	.734	.751	.779
850	.707	.719	.741

	μ^*		
5000	2.402	2.549	2.832
4000	2.297	2.432	2.670
3000	2.191	2.297	2.494
1500	2.013	2.076	2.191
850	1.925	1.962	2.038

Table 31:

APPENDIX QQ

$\frac{g}{(W_H)^{1/3}}$ (REF. 6)* (CONTINUED)

RPM _o ↓	RPM _n →	γ^*		
		28,000	21,000	14,000
5000		.530	.512	.483
4000		.544	.526	.499
3000		.559	.544	.519
1500		.587	.577	.559
850		.604	.597	.583

Table 31:(Continued)

APPENDIX RR

$$\text{RPM}_s = \text{Flywheel RPM}_n / 2.9166$$

Flywheel RPM _n →	28,000	21,000	14,000
RPM _s →	9,600	7,200	4,800

Table 32:

APPENDIX SS

BEARING AND GEAR
COMPUTER DATA.

BALL AND ROLLER BEARING DISPLACEMENT, LOAD AND LIFE DETERMINATION

NASA COT STUDY INPUT PLANET BEARINGS

7-23 W/ AT 27240 RPM

INPUT DATA FOR SYSTEM NO. 1

BEARINGS

NO. 1

TYPE BALLS/ROLLS

1-1000E 01

1-1000E 01

1-1000E 01

1-1000E 01

1-1000E 01

1-1000E 01

1-1000E 01

1-1000E 01

1-1000E 01

1-1000E 01

1-1000E 01

1-1000E 01

1-1000E 01

1-1000E 01

1-1000E 01

1-1000E 01

1-1000E 01

1-1000E 01

1-1000E 01

1-1000E 01

1-1000E 01

1-1000E 01

1-1000E 01

1-1000E 01

1-1000E 01

1-1000E 01

1-1000E 01

1-1000E 01

1-1000E 01

1-1000E 01

1-1000E 01

1-1000E 01

1-1000E 01

1-1000E 01

1-1000E 01

1-1000E 01

1-1000E 01

1-1000E 01

1-1000E 01

1-1000E 01

1-1000E 01

1-1000E 01

1-1000E 01

1-1000E 01

1-1000E 01

1-1000E 01

1-1000E 01

ELEMENT NO.	UPPER EDGE OF PAIN				JUNCTION CLEARANCE				ROLLING TORQUE				
	INNER	OUTER	INNER	OUTER	INNER	OUTER	INNER	OUTER	RATIO	INNER	OUTER	INNER	OUTER
1	1.9400E-01	1.9720E-01	1.1402E-01	1.3134E-01	0.0	0.0	0.0	0.0	1.7433E-02	8.6277E-04	8.4044E-04	1.1823E-01	1.2061E-01
2	1.9400E-01	1.9720E-01	1.1402E-01	1.3134E-01	0.0	0.0	0.0	0.0	1.7433E-02	8.6277E-04	8.4044E-04	1.1823E-01	1.2061E-01
3	1.9400E-01	1.9720E-01	1.1402E-01	1.3134E-01	0.0	0.0	0.0	0.0	1.7433E-02	8.6277E-04	8.4044E-04	1.1823E-01	1.2061E-01
4	1.9400E-01	1.9720E-01	1.1402E-01	1.3134E-01	0.0	0.0	0.0	0.0	1.7433E-02	8.6277E-04	8.4044E-04	1.1823E-01	1.2061E-01
5	1.9400E-01	1.9720E-01	1.1402E-01	1.3134E-01	0.0	0.0	0.0	0.0	1.7433E-02	8.6277E-04	8.4044E-04	1.1823E-01	1.2061E-01
6	1.9400E-01	1.9720E-01	1.1402E-01	1.3134E-01	0.0	0.0	0.0	0.0	1.7433E-02	8.6277E-04	8.4044E-04	1.1823E-01	1.2061E-01
7	1.9400E-01	1.9720E-01	1.1402E-01	1.3134E-01	0.0	0.0	0.0	0.0	1.7433E-02	8.6277E-04	8.4044E-04	1.1823E-01	1.2061E-01

ELEMENT NO.	MAX. DISTORSION SHEAR				MAXIMUM SHEAR STRESS			
	INNER	OUTER	INNER	OUTER	INNER	OUTER	INNER	OUTER
1	1.6000E-01	1.6000E-01	1.6000E-01	1.6000E-01	1.6000E-01	1.6000E-01	1.6000E-01	1.6000E-01
2	1.6000E-01	1.6000E-01	1.6000E-01	1.6000E-01	1.6000E-01	1.6000E-01	1.6000E-01	1.6000E-01
3	1.6000E-01	1.6000E-01	1.6000E-01	1.6000E-01	1.6000E-01	1.6000E-01	1.6000E-01	1.6000E-01
4	1.6000E-01	1.6000E-01	1.6000E-01	1.6000E-01	1.6000E-01	1.6000E-01	1.6000E-01	1.6000E-01
5	1.6000E-01	1.6000E-01	1.6000E-01	1.6000E-01	1.6000E-01	1.6000E-01	1.6000E-01	1.6000E-01
6	1.6000E-01	1.6000E-01	1.6000E-01	1.6000E-01	1.6000E-01	1.6000E-01	1.6000E-01	1.6000E-01
7	1.6000E-01	1.6000E-01	1.6000E-01	1.6000E-01	1.6000E-01	1.6000E-01	1.6000E-01	1.6000E-01

ELEMENT NO.	UPPER EDGE OF PAIN		JUNCTION CLEARANCE		ROLLING TORQUE	
	INNER	OUTER	INNER	OUTER	INNER	OUTER
1	1.9400E-01	1.9720E-01	1.1402E-01	1.3134E-01	0.0	0.0
2	1.9400E-01	1.9720E-01	1.1402E-01	1.3134E-01	0.0	0.0
3	1.9400E-01	1.9720E-01	1.1402E-01	1.3134E-01	0.0	0.0
4	1.9400E-01	1.9720E-01	1.1402E-01	1.3134E-01	0.0	0.0
5	1.9400E-01	1.9720E-01	1.1402E-01	1.3134E-01	0.0	0.0
6	1.9400E-01	1.9720E-01	1.1402E-01	1.3134E-01	0.0	0.0
7	1.9400E-01	1.9720E-01	1.1402E-01	1.3134E-01	0.0	0.0

BALL AND ROLLER BEARINGS DISPLACEMENT, LOAD AND LIFE DETERMINATION

FROM CUT STUDY HELIX-LEVEL CLUSTER 11-20-77

HEAD CONDITIONS AT 10,000 HP 14,520 RPM

INPUT DATA FOR SYSTEM NO. 1

BEARING NO.	TYPE	NUMBER OF BALLS/ROLLS	PISTON DIA.	RACE CURVATURES	CONTACT ANGLE	INTERNAL CLEARANCE	DISTANCE TO ORIGIN
1	ROLLER	6.0000E 00	4.8000E-01	OUTER 0.0	0.0	3.070E-04	5.0000E-01
2	ROLLER	6.0000E 00	4.8000E-01	INNER 0.0	0.0	3.0000E-04	-2.0000E-01
3	BALL	7.0000E 00	1.4200E 00	5.2000E-01	0.0	3.0000E-04	-2.0000E-01
BEARING NO.	TYPE	EFFECTIVE BALL/TOTAL	BALL/ROLL	MODULUS OF ELASTICITY	POISSON'S RATIO	RACES	COEFFICIENT
1	ROLLER	1.3720E-01	2.8300E-01	2.9000E 07	0.0	0.0	0.0
2	ROLLER	1.3720E-01	2.8300E-01	2.9000E 07	0.0	0.0	0.0
3	BALL	0.0	0.0	2.9000E 07	0.0	0.0	0.0
BEARING NO.	TYPE	SWIN THICKNESS	INITIAL DISPLACEMENTS AT BEARING CENTER	ALONG X	ALONG Y	ALONG Z	ABOUT Y
1	ROLLER	0.0	0.0	0.0	0.0	0.0	0.0
2	ROLLER	0.0	0.0	0.0	0.0	0.0	0.0
3	BALL	0.0	0.0	0.0	0.0	0.0	0.0
BEARING NO.	TYPE	PRELOAD	RADIAL SPRING RATES	ALONG Y	ALONG Z	FATIGUE CONSTANT	VALUE OF LAMBDA
1	ROLLER	0.0	0.0	0.0	0.0	0.0	0.0
2	ROLLER	0.0	0.0	0.0	0.0	0.0	0.0
3	BALL	0.0	0.0	0.0	0.0	0.0	0.0

EXTERNAL LOADS APPLIED TO SHAFT

ALONG X ALONG Y ALONG Z ABOUT Y ABOUT Z

1 1.0710E 01 0.0 0.0 0.0 0.0

2 0.0 0.0 0.0 0.0 0.0 0.0

3 0.0 0.0 0.0 0.0 0.0 0.0

OUTPUT DATA FOR LOAD CASE NO. 1, SYSTEM NO. 1

REACTINGS OF BEARINGS ON SHAFT

ALONG X ALONG Y ALONG Z ABOUT Y ABOUT Z

1 -3.4498E 01 -3.2420E 01 0.0 0.0

2 -2.272E 01 3.769E 01 0.0 0.0

3 -5.0334E-04 1.2337E-03 -0.2033E 00 -1.4430E-02

DISPLACEMENTS OF INNER RACE WITH RESPECT TO OUTER

ALONG X ALONG Y ALONG Z ABOUT Y ABOUT Z

1 -2.2924E-04 -1.2702E-04 0.0 0.0

2 -2.287E-04 1.7685E-04 0.0 0.0

3 -3.539E-04 2.418E-07 9.972E-05 -3.210E-04 -1.1842E-04

PARTIAL NON-LINEAR SPRING RATES OF INDIVIDUAL BEARINGS

BEY/BE BEY/DALZ BEY/DALZ

1 0.0 0.0 0.0

2 0.0 0.0 0.0

3 0.0 0.0 0.0

FATIGUE LIFE (% PERCENT SURVIVAL)

OUTER INNER BEARING

1 2.0720E 05 1.4452E 04 1.3839E 04

2 2.0714E 05 1.4523E 04 1.3736E 04

3 8.327E 01 2.9314E 01 2.8735E 01

RPM OF

OUTER INNER

1 1.6349E 04

2 0.0

3 0.0

STD AND NON STD EXTERNAL HELICAL
BEAMS - MAX BENDING STRESS

2 D P U T B A T A S E 3 I D N
MAGA CVT STUDY INPUT PLANETARY HELICALS

MR. OF SELECTED CENTER DISTANCE MISEPUMER EPW-PINION
PINION BEAR STD NON STD 7.320000 27500.00 1.000000 1.000000 1.000000 1.000000
20 40 1.500000 1.500000 7.320000 27500.00 1.000000 1.000000 1.000000 1.000000
NORMAL PLANE HELIX BACHLAP 7.320000 27500.00 1.000000 1.000000 1.000000 1.000000
PRO B ANGLE BACHLAP 7.320000 27500.00 1.000000 1.000000 1.000000 1.000000
19.733827 21.073794 20.000000 0.0020 0.0000 0.0000 0.250000 0.250000 0.0
BUSHING BLA - RIG N MAX PINION BEAR PINION BEAR
PINION BEAR N ROOT BLA - RIG N PINION BEAR PINION BEAR
1.077777 2.077777 0.000000 1.077777 0.077900 0.077900 0
SAMPLED OR N ROOT FILLET RAD-RIG N MAX UNDERCUT KT KR KM DENSITY
RIGID 0 PINION BEAR PINION BEAR 1.00000 1.00000 1.00000 1.00000
SAMPLED 0 0.02000 0.02000 0.0 0.0 0.0 0.0

20IMP= 0.02238
20IMP= 0.02338
TUP = 0.04482
TUB = 0.02323
RFRIP= 0.02000
RFRIP= 0.02000
MP = 0.09949
MG = 0.08965
JP = 0.03375
YCP = 0.58972
YCG = 0.73386
KTP = 1.58540
KTB = 1.09959
FLR = 0.50770
FLR = 0.00000
SMEP = 0.0
SMLE = 0.0
FCOMP= 1.00000

SURFACE COMPRESSIVE STRESS- 37748.00000 P.S.I.

POWER LESS- 0.03723 MP
PINION LEAD- 5.00100 IN.
BEAR LEAD- 10.00200 IN.
BASE HELIX- 0.09001 IN.
PROFILE CONTACT RATIO- 0.22343 IN.
LOAD SHARING RATIO- 1.53942 IN.
AGMA BENDING STRESS/PINION- 0.00324 P.S.I.
AGMA BENDING STRESS, BEAR- 3003.20219 P.S.I.
AGMA HELICAL FACTOR, CH- 0.00000 P.S.I.

----- INPUT DATA -----

TOOTH GEOMETRY

PMI (PRESSURE ANGLE)

TRANSVERSE PLANE) = 22.49998

CIRCULAR PITCH	=	0.15708	GEAR
DIAMETRAL PITCH	=	20.00000	PERIOD
PITCH DIA		1.00000	2.00000
BASE CIRCLE DIA		0.92388	1.84776
PCSA CONTACT DIA		0.97440	2.10000
LPB CONTACT DIA		1.10000	1.92817
WEAKEST SECTION DIA		0.99350	1.79637
ARC TOOTH THK AT			
OPERATING MP		0.07700	0.07700
CM		1.20576	1.20619
YC		0.38331	0.47814
RP		1.38340	1.49459
J		0.30054	0.34999

BENDING STRESS

PC (MPC) 4917.37 5935.38

BENDING STRESS PERIOD-AT MPC IS LESS

THAN THE ENDURANCE LIMIT OF 175000. PSI - INFINITE LIFE.

BENDING STRESS WEAR -AT MPC IS LESS

THAN THE ENDURANCE LIMIT OF 175000. PSI - INFINITE LIFE.

BENDING STRESS (COMBINED)

PC (MPC) 4953.00 5969.19

SPINAL BEVEL GEAR DIMENSIONS
 PART NO. - 4450 CUT STUDY SUP DRIVER-58BELL NO. 100.004C

NUMBER OF TESTS	PISTON	BEAM	GEOM
19	57	27	2-095
DIAMETRAL PITCH	0.440	13.270	10.470
FACE WIDTH	228.304	0.000	0.119
PRESSURE ANGLE	98.840	1.209	0.038
SHAFT ANGLE		1.541	0.840
TRANSVERSE CONTACT RATIO		1.758	0.837
FACE CONTACT RATIO		10.222	20.240
MODIFIED CONTACT RATIO		1.770	30.320
OUTER CONE DISTANCE		0.134	30.170
NEAR CONE DISTANCE		0.010	30.090
PITCH DIAMETER		0.053	30.000
CIRCULAR PITCH		0.047	30.090
MODULES DEPTH		0.000	30.170
UNSLIT DEPTH		0.000	30.210
CLEARANCE		0.010	30.000
ADDENDUM		0.070	30.000
BEVELS		0.007	30.000
BEVELING ANGLES MODIFIED PER 1977 FORMULAS		0.000	30.000
THEORETICAL CUTTER RADII		0.000	30.000
CUTTER RADIUS		0.000	30.000
CALC. GEAR FINISH. P.C. WIDTH		0.000	30.000
GEAR FINISHING PRINT WIDTH		0.000	30.000
GEAR FINISHING PRINT WIDTH		0.000	30.000
NEAR SLOT WIDTH		0.035	30.000
OUTER SLOT WIDTH		0.035	30.000
INNER SLOT WIDTH		0.035	30.000
FLANKING CUTTER BLANK PRINT		0.020	30.000
STOCK ALLIANCE		-0.000	30.000
MAX. RADII-CUTTER BLANKS		0.018	30.000
MAX. RADII-INTERFERENCE		0.043	30.000
MAX. RADII-INTERFERENCE		0.020	30.000
CUTTER EDGE RADII		0.015	30.000
CALC. CUTTER NUMBER		0	30.000
MAX. NO. BLANKS IN CUTTER		0	30.000
CUTTER BLANKS REMOVED		0	30.000
NEAR ANGULAR FACE - CONCAVE		0.0	30.000
NEAR ANGULAR FACE - CONVEX		0.0	30.000
GEAR ANGULAR FACE - TOTAL		0.0	30.000

OUTSIDE DIAMETER	PISTON	BEAM	GEOM
PITCH APER TO CROWN	1.537		10.470
NEAR CIRCULAR THICKNESS	0.119		0.119
OUTER NORMAL TOP LAND	0.038		0.038
INNER NORMAL TOP LAND	0.038		0.038
PITCH ANGLE	30.470		20.240
FACE ANGLE OF BLANK	30.500		30.320
ROOT ANGLE	30.420		30.170
DEGENERATE ANGLE	0.070		30.090
OUTER SPIRAL ANGLE	30.210		30.210
INNER SPIRAL ANGLE	30.000		30.000
INNER SPIRAL ANGLE	30.000		30.000
HAND OF SPIRAL	RH		
DRIVING MEMBER	DR		
DIRECTION OF ROTATION-DRIVER CU	CU		
OUTER NORMAL BACKLASH	0.003		0.003
TOOTH TAPER	0.003		0.003
CUTTING METHOD	SB		
GEAR TYPE	SB		
FACE WIDTH IN PERCENT OF CONE DISTANCE	5.702		

GEOMETRY FACTOR-STRENGTH-J	0.3299
STRENGTH FACTOR-B	51.020
SIZE FACTOR - NS	0.521
FACTOR	1.0213
STRENGTH BALANCE DESIRED - STRS	0.0731
STRENGTH BALANCE OBTAINED - STRS	13.441
GEOMETRY FACTOR-DURABILITY-I	0.003630
DURABILITY FACTOR-Z	0.4416
GEOMETRY FACTOR-SCORING-S	0.400
SCORING FACTOR - I	0.602016
ROOT LINE FACE WIDTH	1.020
PROFILE SLIDING FACTOR	0.002311
RATIO OF INVOLUTE/OUTER CONE	0.002311
AXIAL FACTOR-DRIVER CU	0.000
AXIAL FACTOR-DRIVER CU	0.894
SEPARATING FACTOR-DRIVER CU	0.758
SEPARATING FACTOR-DRIVER CU	0.645
DUPLICATE SUM OF DEGENERATE ANG	0.070
ROUGHING RADIAL	0.070

STRENGTH FACTOR IS GIVEN IN THE 1977 APPROVED EDITION

SID AND NON SID EXTERNAL MELICAL
GEARS - MAX BENDING STRESS

INPUT DATA SECTION

INNER MELICAL BEARINGS

NO. OF TEETH 20.000000
 PINION GEAR 20
 CENTER DISTANCE 2.349999
 HORSEPOWER 10.799999
 RPM-PINION 14322.00
 KV 1.000000
 KS 1.500000
 MN 1.000000
 NORMAL PLANE MELIX 24.020787
 MAX BACHLASH 0.0030
 FACE WIDTH - MIN PINION 0.500000
 MAX TIP BREAM GEAR 0.0
 MOUTINE DIA - MIN GEAR 0.100000
 PINION GEAR 0.100000
 1.340000 3.420177
 ROST DIA - MIN GEAR 0.100000
 PINION GEAR 0.100000
 1.271777 3.100777
 ROST FILLET RAD-RID MAX UNDERCUT 0
 PINION GEAR 0.0
 MARKED 0.00300 0.00300 0.0
 SHAPED 0.00377
 XIDIM- 0.00007
 TYP - 0.00170
 TMS - 0.07134
 R/WIP- 0.00300
 W/RLD- 0.00300
 WP - 0.12007
 W - 0.12404
 JP - 0.31234
 J - 0.51067
 YCP - 0.51740
 YCS - 0.48171
 WTP - 1.34474
 WTB - 1.07240
 FLW - 0.53100
 FLW - 0.40337
 SWP - 0.0
 SWB - 0.0
 FCMT- 1.10204
 SURFACE COMPRESSIVE STRESS- 44204.67278 P.S.I.
 POWER LOSS- 0.00006 HP.
 PINION LEAD- 9.75377 IN.
 GEAR LEAD- 22.72445 IN.
 MSE MELIX- 0.37971 RAD.
 LENGTH OF LINE OF ACTION- 0.37632 IN.
 PROFILE CONTACT RATIO- 1.50434
 LEAD SHARING RATIO- 0.61270
 AGMA BENDING STRESS-PINION- 3376.02026 P.S.I.
 AGMA BENDING STRESS, GEAR- 2073.56201 P.S.I.
 AGMA MELICAL FACTOR, C1M- 1.179412

SURFACE COMPRESSIVE STRESS- 44204.67278 P.S.I.
 POWER LOSS- 0.00006 HP.
 PINION LEAD- 9.75377 IN.
 GEAR LEAD- 22.72445 IN.
 MSE MELIX- 0.37971 RAD.
 LENGTH OF LINE OF ACTION- 0.37632 IN.
 PROFILE CONTACT RATIO- 1.50434
 LEAD SHARING RATIO- 0.61270
 AGMA BENDING STRESS-PINION- 3376.02026 P.S.I.
 AGMA BENDING STRESS, GEAR- 2073.56201 P.S.I.
 AGMA MELICAL FACTOR, C1M- 1.179412

GEAR HELICAL FACTOR, C_h = 1.39412
 ----- B O T H -----
 180TH ELEMENT

PSI (PRESSURE ANGLE)
 TRANSMISSION PLANE) = 21.78917

CIRCULAR PITCH	=	0.21893	
DIAMETRAL PITCH	=	14.87142	
PITCH DIA		1.41808	3.27000
MATE CIRCLE DIA		1.28973	1.03491
WELD CONTACT DIA		1.32410	1.42420
EW CONTACT DIA		1.34408	1.19722
WEARST SECTION DIA		1.24737	1.15461
ASC TESTIN TIME AT			
OPTIMIZING W		0.18409	0.18300
CA		1.27934	1.27123
VC		0.33333	0.44847
W		1.34474	1.49240
J		0.33201	0.42302

BEARING STRESS
 BC (MPC) 3643.24 3171.78
 BEARING STRESS PINION-AT MPC IS LESS
 THAN THE ENDURANCE LIMIT OF 475000. PSI - INFINITE LIFE.
 BEARING STRESS GEAR -AT MPC IS LESS
 THAN THE ENDURANCE LIMIT OF 475000. PSI - INFINITE LIFE.
 BEARING STRESS (COMBINED)
 BC (MPC) 3624.94 3183.31

081209 END OF FILE

STD AND NON STD EXTERNAL HELICAL

GEARS - MAX BENDING STRESS

I P B T D A T A S E L E C T I O N

ENTIRE PLANETARY GEARS

MR. OF TEETH 20.000000 21.875399 38.000000 9.9639 0.8950 0.500000 0.750000 0.0
 PINION BEAR 40 30 1.750000 1.750000 9.799999 18677.00 1.000000 1.000000 1.000000 1.000000 1.000000 1.000000
 NORMAL PLANE HELIX ANGLE HIN HAZ BACHLASH FACE WIDTH - HIN MAX TIP BREAK
 OUTSIDE DIA - HIN 38.000000 9.9639 0.8950 0.500000 0.750000 0.0 0.0
 PINION BEAR 2.099999 1.599999 1.860000 1.360000 0.877000 0.877000 0
 SAMPLER BE N PINION BEAR ROOT FILLET RAD-HIN MAX UNDERCUT KT KR KM DENSITY
 MESHED SHAPED 0 0.03000 0.03000 0.0 0.0 1.00000 1.00000 1.00000 1.00000 1.00000 1.00000 0.28300

SURFACE COMPRESSIVE STRESS- 36116.89844 P.S.I.
 POWER LOSS- 0.04744 HP.
 PINION LEAD- 10.86281 IN.
 GEAR LEAD- 0.16211 IN.
 BASE HELIX- 0.48912 RAD.
 LENGTH OF LINE OF ACTION- 0.22699 IN.
 PROFILE CONTACT RATIO- 1.34750
 LOAD SHARING RATIO- 0.59700
 AGMA BENDING STRESS-PINION- 2079.16673 P.S.I.
 AGMA BENDING STRESS, GEAR- 1403.96243 P.S.I.
 AGMA HELICAL FACTOR, CH- 1.03983

AGAVE METAL FACTOR, CM- 1-03965

----- OUTPUT DATA -----

TOOTH GEOMETRY
PSE (PRESSURE ANGLE
TRANSVERSE PLANE) = 22.77590

CIRCULAR PITCH	=	0.15798	
AXIAL PITCH	=	20.00000	
PITCH DIA		2.00000	GEAR
BASE CIRCLE DIA		1.84378	1.50000
WELSH CONTACT DIA		1.72442	1.38294
LOW CONTACT DIA		2.10000	1.40000
WELSH SECTION DIA		1.87949	1.42443
ARC TOOTH THK AT OPERATING BP		0.07700	1.37892
CM		1.78839	0.07700
YC		0.47833	1.52230
NY		1.04344	0.44442
J		0.41333	1.42917
BEARING STRESS			0.27343
MC (MPC)		1798.43	1472.43

BEARING STRESS PITCH-AT MPC IS LESS
THAN THE ENDURANCE LIMIT OF 175000. PSE - INFINITE LIFE.
BEARING STRESS GEAR -AT MPC IS LESS
THAN THE ENDURANCE LIMIT OF 175000. PSE - INFINITE LIFE.
BEARING STRESS (COMBINED)
MC (MPC) 1804.54 1485.00

BALL AND ROLLER BEARING DISPLACEMENT, LOAD AND LIFE DETERMINATION

11-20-77

BASE CUT STUDY WITHOUT PLANET BEARINGS

HEAD CONDITIONS AS TO CB HP 30430 RPM

INPUT DATA FOR SYSTEM NO. 1

BEARING NO.	TYPE	NUMBER OF BALLS/ROLLS	DIA.	PITCH DIA.	RACE CURVATURES	CONTACT ANGLE	INTERNAL CLEARANCE	DISTANCE TO ORIGIN
1	ROLLER	4.0000E 00	1.3750E-01	6.8000E-01	OUTER 0.0	0.0	3.0000E-04	5.0000E-01
2	ROLLER	8.0000E 00	1.3750E-01	6.8000E-01	INNER 0.0	0.0	3.0000E-04	-5.0000E-01
3	BALL	7.0000E 00	1.0000E-01	1.4200E 00	5.2000E-01	1.0000E 01	-2.0000E-04	-2.0000E 00
BEARING NO.	TYPE	EFFECTIVE TOTAL BALL/ROLL	MODULUS OF ELASTICITY	POISSON'S RATIO	RACES	COEFFICIENT OF FRICTION		
1	ROLLER	1.5750E-01	1.7720E-01	2.8300E-01	2.9000E 07	2.5000E-01	2.5000E-01	0.0
2	ROLLER	1.5750E-01	1.7720E-01	2.8300E-01	2.9000E 07	2.5000E-01	2.5000E-01	0.0
3	BALL	0.0	0.0	2.8300E-01	2.9000E 07	2.5000E-01	2.5000E-01	7.5000E-02
BEARING NO.	TYPE	PHASE FACTOR	SHIM THICKNESS	INITIAL DISPLACEMENTS AT BEARING CENTER				
1	ROLLER	0.0	0.0	ALONG X 0.0	ALONG Y 0.0	ALONG Z 0.0	ABOUT X 0.0	ABOUT Y 0.0
2	ROLLER	0.0	0.0	ALONG X 0.0	ALONG Y 0.0	ALONG Z 0.0	ABOUT X 0.0	ABOUT Y 0.0
3	BALL	0.0	0.0	ALONG X 0.0	ALONG Y 0.0	ALONG Z 0.0	ABOUT X 0.0	ABOUT Y 0.0
BEARING NO.	TYPE	PRELOAD	AXIAL PRELOAD	RADIAL SPRING RATES	FATIGUE CONSTANT	VALUE OF LAMDBA		
1	ROLLER	0.0	0.0	ALONG Y 0.0	OUTER 4.7500E 04	4.1000E-01	4.1000E-01	0.0
2	ROLLER	0.0	0.0	ALONG Z 0.0	INNER 4.7500E 04	4.1000E-01	4.1000E-01	0.0
3	BALL	0.0	0.0	1.0000E 00	2.1400E 03	0.0	0.0	0.0

LOAD DATA FOR LOAD CASE NO. 1, SYSTEM NO. 1

EXTERNAL LOADS APPLIED TO SHAFT

ALONG X ALONG Y ALONG Z

ALONG X ALONG Y ALONG Z

ALONG X ALONG Y ALONG Z

ALONG X ALONG Y ALONG Z

ALONG X ALONG Y ALONG Z

ALONG X ALONG Y ALONG Z

ALONG X ALONG Y ALONG Z

ALONG X ALONG Y ALONG Z

ALONG X ALONG Y ALONG Z

ALONG X ALONG Y ALONG Z

ALONG X ALONG Y ALONG Z

ALONG X ALONG Y ALONG Z

ALONG X ALONG Y ALONG Z

ALONG X ALONG Y ALONG Z

ALONG X ALONG Y ALONG Z

ALONG X ALONG Y ALONG Z

ALONG X ALONG Y ALONG Z

ALONG X ALONG Y ALONG Z

ALONG X ALONG Y ALONG Z

ALONG X ALONG Y ALONG Z

ALONG X ALONG Y ALONG Z

ALONG X ALONG Y ALONG Z

ALONG X ALONG Y ALONG Z

ALONG X ALONG Y ALONG Z

ALONG X ALONG Y ALONG Z

ALONG X ALONG Y ALONG Z

ALONG X ALONG Y ALONG Z

ALONG X ALONG Y ALONG Z

ALONG X ALONG Y ALONG Z

ALONG X ALONG Y ALONG Z

ALONG X ALONG Y ALONG Z

ALONG X ALONG Y ALONG Z

ALONG X ALONG Y ALONG Z

ALONG X ALONG Y ALONG Z

BEARING NO.	TYPE	REACTIIONS OF BEARINGS ON SHAFT	FRICTION TORQUE	FATIGUE LIFE 100 PERCENT SURVIVAL
1	ROLLER	ALONG X ALONG Y ALONG Z	OUTER 4.1500E 05	INNER 3.2704E 04
2	ROLLER	ALONG X ALONG Y ALONG Z	OUTER 4.1470E 05	INNER 3.2794E 04
3	BALL	ALONG X ALONG Y ALONG Z	OUTER 4.3741E 01	INNER 1.6148E 01
BEARING NO.	TYPE	DISPLACEMENTS OF BEARING WITH RESPECT TO LOAD	DISPLACEMENTS OF FLOATING OUTER RACE	
1	ROLLER	ALONG X ALONG Y ALONG Z	ALONG X ALONG Y ALONG Z	
2	ROLLER	ALONG X ALONG Y ALONG Z	ALONG X ALONG Y ALONG Z	
3	BALL	ALONG X ALONG Y ALONG Z	ALONG X ALONG Y ALONG Z	
BEARING NO.	TYPE	PARALLEL NON-LINEAR SPALLING RATES OF INDIVIDUAL BEARINGS		
1	ROLLER	DFY/DBY DFZ/DBZ	DFY/DBY DFZ/DBZ	
2	ROLLER	DFY/DBY DFZ/DBZ	DFY/DBY DFZ/DBZ	
3	BALL	DFY/DBY DFZ/DBZ	DFY/DBY DFZ/DBZ	

BEARING NO.	TYPE	RPM OF INNER	RPM OF OUTER
1	ROLLER	3.0403E 04	
2	ROLLER		
3	BALL		

2 0.0 0.0 0.0 0.0 0.0 0.0 4.8524E 05 -1.6954E 05 0.0 0.0
 3 0.435E 03 -3.431E 01 -1.7231E 04 -1.8913E 04 -3.4211E 01 3.7876E 02 4.2264E 00 4.8828E-01 9.4215E 04
 B2/2/2 B2/2/2 B2/2/2 B2/2/2 B2/2/2 B2/2/2 B2/2/2 B2/2/2
 1 0.3678E 03 0.0 0.0 0.0 0.0 0.0 0.0 0.0
 2 0.4806E 03 0.0 0.0 0.0 0.0 0.0 0.0 0.0
 3 3.2718E 03 7.4394E 04 5.6608E-01 3.4719E 04 1.6816E 00 3.6201E 04
 DISPLACEMENTS OF REFERENCE LINE AT ORIGIN
 ALONG X ALONG Y ALONG Z ABOUT X ABOUT Y ABOUT Z

6.2342E-04 -1.9462E-04 4.2074E-07 -3.1331E-04 -8.4906E-07
 OUTPUT DATA FOR BEARING NO. 1, LEAD CASE NO. 1, SYSTEM NO. 1

ELEMENT NO.	CONTACT FORCE		OPERATING CONTACT ANGLE		CONTACT AREA LENGTH		CONTACT AREA WIDTH	
	OUTER	INNER	OUTER	INNER	OUTER	INNER	OUTER	INNER
3	1.8808E 02	2.2010E 00	7.8601E-01	0.0	1.5750E-01	1.5750E-01	4.8034E-04	3.5225E-04
4	2.2506E 02	3.1848E 01	3.8339E 01	0.0	1.5750E-01	1.5750E-01	2.3411E-03	1.9454E-03
7	2.7906E 02	1.6448E 01	1.3143E 01	0.0	1.5750E-01	1.5750E-01	1.7128E-03	1.2985E-03
OTHERS	1.3033E 00	1.3033E 00	0.0	0.0	1.5750E-01	0.0	5.1488E-04	0.0
CENTRIFUGAL FORCE	1.1758E 00	1.1758E 00	0.0	0.0	ROLLING VELOCITY	CONTROLLING MEAN COMPRESSIVE STRESS		
MOMENT	1.1758E 00	1.1758E 00	0.0	0.0	INNER	OUTER	INNER	INNER
VELOCITY	1.1758E 00	1.1758E 00	0.0	0.0	8.1346E 04	8.1346E 04	2.1397E 04	1.2479E 04
ROTATIONAL VELOCITY	1.1758E 00	1.1758E 00	0.0	0.0	5.0772E 04	5.0772E 04	7.5764E 04	9.8648E 04
DEPTH	1.1758E 00	1.1758E 00	0.0	0.0	8.1370E 04	8.1370E 04	5.3631E 01	4.4748E 04
MAX. BRINELL	1.1758E 00	1.1758E 00	0.0	0.0	0.0	0.0	1.4097E 04	0.0
MAX. BRINELL SKEW	1.1758E 00	1.1758E 00	0.0	0.0	MAXIMUM SHEAR STRESS	DEPTH TO MAXIMUM SHEAR STRESS		
INNER	1.7014E-04	1.7014E-04	8.8043E-03	8.1472E 03	0.7592E 03	2.6751E-04	1.3846E-04	0.0
OUTER	2.3741E 04	2.3741E 04	4.9139E-04	3.0420E 04	3.2714E 04	9.9831E-04	7.7242E-04	0.0
INNER	1.7014E-04	1.7014E-04	4.2241E-04	2.0058E 04	2.4743E 04	6.7327E-04	5.8727E-04	0.0
OUTER	1.1758E 00	1.1758E 00	0.0	6.1541E 03	0.0	0.0	0.0	0.0

6.2342E-04 -1.9462E-04 4.2074E-07 -3.1331E-04 -8.4906E-07
 OUTPUT DATA FOR BEARING NO. 2, LEAD CASE NO. 1, SYSTEM NO. 1

ELEMENT NO.	CONTACT FORCE		OPERATING CONTACT ANGLE		CONTACT AREA LENGTH		CONTACT AREA WIDTH	
	OUTER	INNER	OUTER	INNER	OUTER	INNER	OUTER	INNER
3	1.8808E 02	2.2010E 00	7.8601E-01	0.0	1.5750E-01	1.5750E-01	4.8034E-04	3.5225E-04
4	2.2506E 02	3.1848E 01	3.8339E 01	0.0	1.5750E-01	1.5750E-01	2.3411E-03	1.9454E-03
7	2.7906E 02	1.6448E 01	1.3143E 01	0.0	1.5750E-01	1.5750E-01	1.7128E-03	1.2985E-03
OTHERS	1.3033E 00	1.3033E 00	0.0	0.0	1.5750E-01	0.0	5.1488E-04	0.0
CENTRIFUGAL FORCE	1.1758E 00	1.1758E 00	0.0	0.0	ROLLING VELOCITY	CONTROLLING MEAN COMPRESSIVE STRESS		
MOMENT	1.1758E 00	1.1758E 00	0.0	0.0	INNER	OUTER	INNER	INNER
VELOCITY	1.1758E 00	1.1758E 00	0.0	0.0	8.1346E 04	8.1346E 04	2.1397E 04	1.2479E 04
ROTATIONAL VELOCITY	1.1758E 00	1.1758E 00	0.0	0.0	5.0772E 04	5.0772E 04	7.5764E 04	9.8648E 04
DEPTH	1.1758E 00	1.1758E 00	0.0	0.0	0.0	0.0	1.4097E 04	0.0
MAX. BRINELL	1.1758E 00	1.1758E 00	0.0	0.0	MAXIMUM SHEAR STRESS	DEPTH TO MAXIMUM SHEAR STRESS		
INNER	1.7014E-04	1.7014E-04	8.8043E-03	3.0420E 04	2.4743E 04	6.7327E-04	5.8727E-04	0.0
OUTER	2.3741E 04	2.3741E 04	4.9139E-04	2.0058E 04	2.4743E 04	6.7327E-04	5.8727E-04	0.0
INNER	1.7014E-04	1.7014E-04	4.2241E-04	2.0058E 04	2.4743E 04	6.7327E-04	5.8727E-04	0.0
OUTER	1.1758E 00	1.1758E 00	0.0	6.1541E 03	0.0	0.0	0.0	0.0

ELEMENT NO.	CONTACT FORCE		CONTACT ANGLE		CONTACT AREA LENGTH		CONTACT AREA WIDTH	
	INNER	OUTER	INNER	OUTER	INNER	OUTER	INNER	OUTER
1	2.5514E 01	1.7315E 01	1.7804E 01	3.4597E-02	3.4691E-02	4.4231E-03	4.8672E-03	
2	2.5622E 01	1.8449E 01	1.7832E 01	3.4667E-02	3.4547E-02	4.4066E-03	4.8739E-03	
3	2.5443E 01	2.1879E 01	2.1783E 01	3.4554E-02	3.4533E-02	4.4159E-03	4.8971E-03	
4	2.6421E 01	2.3204E 01	2.3937E 01	3.4991E-02	3.5087E-02	4.4671E-03	4.9142E-03	
5	2.6422E 01	2.3213E 01	2.3948E 01	3.4993E-02	3.5091E-02	4.4674E-03	4.9155E-03	
6	2.5499E 01	2.1109E 01	2.1803E 01	3.4534E-02	3.4434E-02	4.4153E-03	4.8827E-03	
7	2.5244E 01	1.8485E 01	1.7998E 01	3.4466E-02	3.4544E-02	4.4065E-03	4.8737E-03	
CENTRIFUGAL STRESS								
FORCE								
1	4.9644E-01	3.4274E 04	2.1642E 05	2.0275E 05	2.3187E 05	2.1719E 05	2.2713E 05	
2	4.9724E-01	3.4609E-03	3.4784E 04	2.1643E 05	2.3174E 05	2.1647E 05	2.2824E 05	
3	4.1873E-01	4.3931E-03	1.4301E 04	2.1458E 05	2.3150E 05	2.1710E 05	2.2873E 05	
4	4.1704E-01	4.4233E-03	1.4317E 04	2.1454E 05	2.3150E 05	2.1986E 05	2.3151E 05	
5	4.1207E-01	4.4248E-03	1.4317E 04	2.1454E 05	2.3128E 05	2.1987E 05	2.3152E 05	
6	4.1675E-01	4.3799E-03	1.4302E 04	2.1458E 05	2.3149E 05	2.1711E 05	2.2874E 05	
7	4.9725E-01	3.4632E-03	3.4784E 04	2.1643E 05	2.3174E 05	2.1644E 05	2.2824E 05	
BALL CENTER COORDINATES								
X								
1	2.7502E-04	9.3317E-05	1.1413E 04	1.2799E-02	2.7744E-03	2.9488E 05	1.8329E-01	1.6674E-01
2	3.3898E-04	7.5674E-05	1.2177E 04	1.2918E-02	2.7898E-03	3.1441E 05	1.8972E-01	1.1302E-01
3	4.3013E-04	4.6194E-05	1.3013E 04	1.2943E-02	3.3793E-03	3.5835E 05	1.2454E-01	1.2902E-01
4	5.8337E-04	3.9774E-05	1.5024E 04	1.3597E-02	3.5708E-03	3.9744E 05	1.3882E-01	1.4379E-01
5	4.9389E-04	1.9673E-05	1.5031E 04	1.3597E-02	3.5754E-03	3.5961E 05	1.3888E-01	1.4385E-01
6	4.3061E-04	4.3927E-05	1.3027E 04	1.2943E-02	3.3814E-03	3.5869E 05	1.2448E-01	1.2915E-01
7	3.2744E-04	7.8407E-05	1.2184E 04	1.2817E-02	2.9724E-03	3.1445E 05	1.8933E-01	1.1310E-01
UPPER EDGE OF PAIR								
INNER								
1	3.4727E 01	3.2729E 01	2.1099E 00	-1.4013E 04	0.0	0.0	0.0	0.0
2	3.4724E 01	3.4694E 01	2.1099E 00	-3.3028E-01	0.0	0.0	0.0	0.0
3	4.0472E 01	4.1247E 01	1.8044E 00	2.3197E 00	0.0	0.0	0.0	0.0
4	4.2839E 01	4.3437E 01	1.5492E 00	4.2212E 00	0.0	0.0	0.0	0.0
5	4.0512E 01	4.1248E 01	1.7028E 00	4.2283E 00	0.0	0.0	0.0	0.0
6	3.7803E 01	3.8511E 01	1.8759E-01	-3.3192E-01	0.0	0.0	0.0	0.0
MAX. SHEAR STRESS								
INNER								
1	8.1197E 01	8.3428E 04	1.0724E-03	-1.0466E 05	-1.1004E 05	1.4812E-03	1.5594E-03	
2	8.0824E 01	8.3303E 04	1.0081E-03	-1.0081E 05	-1.0432E 05	1.4749E-03	1.5548E-03	
MAX. SHEAR STRESS								
OUTER								
1	8.1197E 01	8.3428E 04	1.0724E-03	-1.0466E 05	-1.1004E 05	1.4812E-03	1.5594E-03	
2	8.0824E 01	8.3303E 04	1.0081E-03	-1.0081E 05	-1.0432E 05	1.4749E-03	1.5548E-03	
MAX. SHEAR STRESS								
RATIO								
1	4.9223E-02	9.2745E-04	9.2745E-04	9.2745E-04	9.2745E-04	9.2745E-04	9.2745E-04	
2	5.2548E-02	9.1161E-04	9.1161E-04	9.1161E-04	9.1161E-04	9.1161E-04	9.1161E-04	
3	6.4774E-02	9.2272E-04	9.2272E-04	9.2272E-04	9.2272E-04	9.2272E-04	9.2272E-04	
4	6.4994E-02	9.8100E-04	9.8100E-04	9.8100E-04	9.8100E-04	9.8100E-04	9.8100E-04	
5	5.9727E-02	9.2324E-04	9.2324E-04	9.2324E-04	9.2324E-04	9.2324E-04	9.2324E-04	
6	5.2583E-02	9.1149E-04	9.1149E-04	9.1149E-04	9.1149E-04	9.1149E-04	9.1149E-04	
MAXIMUM SHEAR STRESS								
INNER								
1	1.4812E-03	1.5594E-03	1.4812E-03	1.5594E-03	1.4812E-03	1.5594E-03	1.4812E-03	1.5594E-03
2	1.4749E-03	1.5548E-03	1.4749E-03	1.5548E-03	1.4749E-03	1.5548E-03	1.4749E-03	1.5548E-03

1	0.0000E 00	0.0000E 00	0.0000E 00	0.0000E 00	0.0000E 00	0.0000E 00	0.0000E 00	0.0000E 00
2	0.1000E 04	0.5479E 04	1.0907E-03	1.0114E-03	-1.0461E 05	-1.0985E 05	1.2702E-03	1.5596E-03
3	0.2100E 04	0.4304E 04	1.1032E-03	1.0208E-03	-1.0573E 05	-1.1110E 05	1.0981E-03	1.5402E-03
4	0.3200E 04	0.4322E 04	1.1036E-03	1.0208E-03	-1.0594E 05	-1.1121E 05	1.0982E-03	1.5393E-03
5	0.4300E 04	0.5404E 04	1.0907E-03	1.0113E-03	-1.0461E 05	-1.0984E 05	1.2703E-03	1.5400E-03
6	0.5400E 04	0.5303E 04	1.0003E-03	1.0002E-03	-1.0432E 05	-1.0962E 05	1.2749E-03	1.5547E-03

ELEMENT VECTOR
 NO. ATTITUDE
 1 1.4890E 01
 2 1.7271E 01
 3 1.9720E 01
 4 2.1711E 01
 5 2.1719E 01
 6 1.9740E 01
 7 1.7294E 01

23

APPENDIX TT

SYMBOLS

<u>SYMBOL</u>	<u>DESCRIPTION</u>
\propto	proportional
Δ	measure of change
μ	Traction Coefficient or Micro(1×10^{-6})
∞	Infinity
$^{\circ}$	Centigrade
Cs	Cone Speed
CVT	Continuously Variable Transmission
EV	Electric Vehicle
F	Force
f	Frequency
F_t	Feet
G	Gate
Hr	Hours
HP	Horsepower
Hz	Hertz (Cycles/Seconds)
I/O	Input to Output Buffer Circuit
θ	Angle (Degrees)
J	Joules
K	Kilowatts
k	1×10^3
Lb	Pounds
Kg	Kilograms
M	Meters or Mill (1×10^{-3})

APPENDIX TT

SYMBOLS (CONTINUED)

<u>SYMBOL</u>	<u>DESCRIPTION</u>
MPU	Microprocessor Unit
N	Newtons
n	Nano (1×10^{-9})
OTC	Optimized Traction Control
P	Pressure
PCV	Pressure Control Valve
PT	Pressure Transducer
TPC	Traction Pressure Control
R _C	Rockwell Hardness Scale "C"
R _C	Roller/Cone Ratio
ROM	Read Only Memory
RPM or W	Revolutions Per Minute
R _s	Roller Speed
Sp or u	Slip
T	Torque
t	Time
T _f	Traction Force
S _d	Speed
V	Velocity or Volts
V _C	Surface Velocity of Cone
V _R	Surface Velocity of Roller
W _n	Normal Load